This is to certify that the

dissertation entitled

MUTATIONAL ANALYSIS OF PHOTOSYSTEM 1 IN
THE CYANOBACTERIUM SYNECHOCYSTIS SP. PCC 6803

presented by

Jianping Yu

has been accepted towards fulfillment
of the requirements for

Ph.D. degree in Botany & Plant Pathology

Kenneth Keegstra

Kenneth Keegstra

Major professor

Date January 23, 1997

MUTATIONAL ANALYSIS OF PHOTOSYSTEM I IN THE CYANOBACTERIUM SYNECHOCYSTIS SP. PCC 6803

By

Jianping Yu

A DISSERTATION

Submitted to
Michigan State University
in partial fulfillment of the requirements
for the degree of

DOCTOR OF PHILOSOPHY

Department of Botany and Plant Pathology

1997

ABSTRACT

MUTATIONAL ANALYSIS OF PHOTOSYSTEM I IN THE CYANOBACTERIUM SYNECHOCYSTIS SP. PCC 6803

By

Jianping Yu

The focus of this study is an investigation of the assembly, structure and function of photosystem I (PSI) in the unicellular cyanobacterium *Synechocystis* sp. PCC 6803. *Synechocystis* sp. PCC 6803 is an excellent organism for the study of PSI because its genome has been completely sequenced and it is readily transformable. It also has an active homologous recombination system, and a photosynthetic apparatus much like that of higher plants. Furthermore, it may be grown heterotrophically. The PsaA and PsaB subunits of the PSI complexes form a heterodimer that contains the primary electron donor P700, and the electron carriers A_0, A_1, and F_X. The PsaC subunit provides ligands for two [4Fe-4S] clusters, denoted F_A and F_B. When the gene for PsaC was inactivated and PsaC was absent, subunits PsaD and PsaE did not accumulate in thylakoid membranes, whereas PsaA and PsaB did accumulate and electrons could move between P700 and F_X. A set of site-directed PsaC mutants was made in which a cysteine ligand to F_A (C51) or F_B (C14) was substituted by aspartate, serine, or alanine. All mutant strains were unable to grow photoautotrophically or mixotrophically (in the presence of glucose) under white light at an intensity of 22 μmol m^{-2} s^{-1}. Photoautotrophic and mixotrophic growth may be rescued by red light. Mixotrophic growth may also be rescued by addition of a specific inhibitor of PSII, DCMU, to the growth medium. Mutant

cells grown under light-activated-heterotrophic-growth (LAHG) conditions showed lower capacity of whole-chain oxygen evolution than did wild-type cells. Thylakoids from all these mutants have lower or undetectable levels of PsaC, PsaD, and PsaE, and lower PSI capacity. EPR and optical spectroscopic studies showed that the electron transfer efficiency of PSI complex is also decreased by the mutations, and that mixed-ligand [4Fe-4S] clusters that formed at the mutated sites are capable of accepting electrons. Spontaneous pseudorevertants of primary PSI mutant strains have been isolated and genetically characterized. Suppressor mutations in some pseudorevertants have been localized by functional complementation and sequencing.

ACKNOWLEDGMENTS

I wish to express my deepest gratitude to those people who have shared their precious time, knowledge, experience, and enthusiasm with me in the process of completing this project. I am pleased to have had the opportunity to exchange ideas and techniques with my collaborators at University of Nebraska: Dr. Yean-Sung Jung, Dr. Ilya Vassiliev, and Dr. John Golbeck. I am indebted to Dr. Lawrence Smart for sharing his techniques and helping me to start this project. I have been very fortunate to have had the enthusiastic support and encouragement of my advisory committee, Dr. Kenneth Keegstra, Dr. Barbara Sears, Dr. C. Peter Wolk, and Dr. Charles Yocum. Equally supportive have been past and present members in the McIntosh lab, especially Dr. Neil Bowlby, Dr. Carrie Hiser, Dr. Rudiger Schulz, Dr. Denis Maxwell, Yong Wang, and Roxy Nickels. I must give a great deal of credit for the success of this project to Dr. Lee McIntosh, who has given unending support and guidance. Finally, I would like to thank my wife Yali Li for her loving understanding and support, and our son Shian who has given me so much pride and fun.

TABLE OF CONTENTS

LIST OF TABLES

Table **Page**

LIST OF FIGURES

Figure **Page**

LIST OF SYMBOLS AND ABBREVIATIONS

A_0	the first electron acceptor in PSI, a chlorophyll
A_1	the secondary electron acceptor in PS I, a phylloquinone
ATP	adenosine 5'-triphosphate
chl	chlorophyll
COX	cytochrome oxidase
cyt	cytochrome
DCBQ	2,6-dichloro-*p*-benzoquinone
DCMU	3-(3,4-dichlorophenyl)-1,1-dimethyl-urea, diuron
DCIP	2,6-dichlorophenol-indophenol
DM	*n*-dodecyl β-D-maltoside
EPR or ESR	electron paramagnetic resonance or electron spin resonance
F_A	[4Fe-4S] center A in PSI
F_B	[4Fe-4S] center B in PSI
Fd	ferredoxin
F_X	[4Fe-4S] center X in PSI
Gm	gentamycin
kb	kilobases or kilobase pairs
kDa	kilodalton
Km	kanamycin
LAHG	light-activated heterotrophic growth
LHC	light harvesting complex
Mb	million basepairs
NADPH, $NADP^+$	nicotinamide adenine dinucleotide phosphate, reduced and oxidized
P_{680}, P700	the primary electron donor in PSII and PS I, respectively. Chlorophyll *a* dimers
PAGE	polyacrylamide gel electrophoresis

PBS	phycobilisome
PCC	Pasteur Culture Collection
PCR	polymerase chain reaction
PSI, PSII	photosystem I or II
SDS	sodium dodecyl sulfate
wt	wild type
ΔA_{820}	photoinduced absorbance change at 820 nm
τ	life time of exponential decay component

Chapter 1

INTRODUCTION

PHOTOSYNTHESIS

Light is of fundamental importance for life on earth. Through photosynthesis, light ultimately provides the sole source of energy for the growth and development of almost all life. Photosynthesis, a series of chemical reactions used by plants, algae, and some bacteria to convert light energy into chemical energy, dramatically affects the earth and its atmosphere. This series of chemical reactions is responsible for generating the O_2 that we breathe and for fixing CO_2 into organic compounds.

Plants, algae, and cyanobacteria perform oxygenic photosynthesis, evolving O_2 from the light-driven oxidation of water and transferring electrons through a linear series of carriers, eventually yielding reducing equivalents, in addition to performing cyclic photophosphorylation. Anoxigenic photosynthesis is characterized by cyclic electron flow through a single reaction center, driving ATP synthesis but not the generation of reducing equivalents. Anoxigenic photosynthesis is performed by species of bacteria and the reaction center has been best characterized structurally in the purple bacteria *Rhodobacter sphaeroides* and *Rhodopseudomonas viridis* (Deisenhofer *et al.*, 1985; Allen *et al.*, 1987).

Oxygenic photosynthesis (recently reviewed by Nugent, 1996) involves the light-driven flow of electrons from water to reduce nicotinamide adenine dinucleotide

phosphate ($NADP^+$) to NADPH, used as reductant for many anabolic reactions. The electron transport process is accomplished by three thylakoid membrane-bound, multi-subunit protein complexes: photosystem II (PSII), the cytochrome b_6f (Cyt b_6f) complex, and photosystem I (PSI). As electrons are transferred by certain carriers, a proton gradient is generated across the thylakoid membrane. This gradient is released by the flow of protons through the ATP synthase (also called the coupling factor), driving ATP synthesis (Figure 1.1). ATP and NADPH act as substrates for carbon fixation and sugar synthesis, amino acid synthesis, fatty acid synthesis, and other anabolic reactions. In plants and algae, the thylakoids and many of the enzymes involved in biosynthetic processes are compartmentalized within the chloroplasts.

The basic requirements for the light-dependent photosynthetic reactions are: light capture, charge separation, and stabilization of charge separation. To use energy efficiently, the charge separation must be quickly stabilized by a series of oxidation-reduction reactions between spatially separate electron carriers. The initial step is the capture of energy from light by antenna pigments on protein complexes such as PSI, PSII, LHCI, LHCII and phycobilisomes. This energy migrates to a special reaction center chlorophyll dimer, which in PSII is termed P_{680}. The energy captured by P_{680} excites an electron, which is transferred to a pheophytin, which in turn reduces a bound plastoquinone molecule called Q_A. Q_A reduces a second quinone, Q_B, which unlike Q_A functions as a two-electron accepter (Figure 1.1). On the donor side of PSII, P_{680}^+ oxidizes a tyrosine residue TyrZ, which in turn oxidizes a cluster of four manganese atoms. The tetrad of Mn atoms accumulates oxidizing equivalents in a series of oxidation states or S-states, and finally oxidizes water and releases oxygen (Barry *et al.*, 1994).

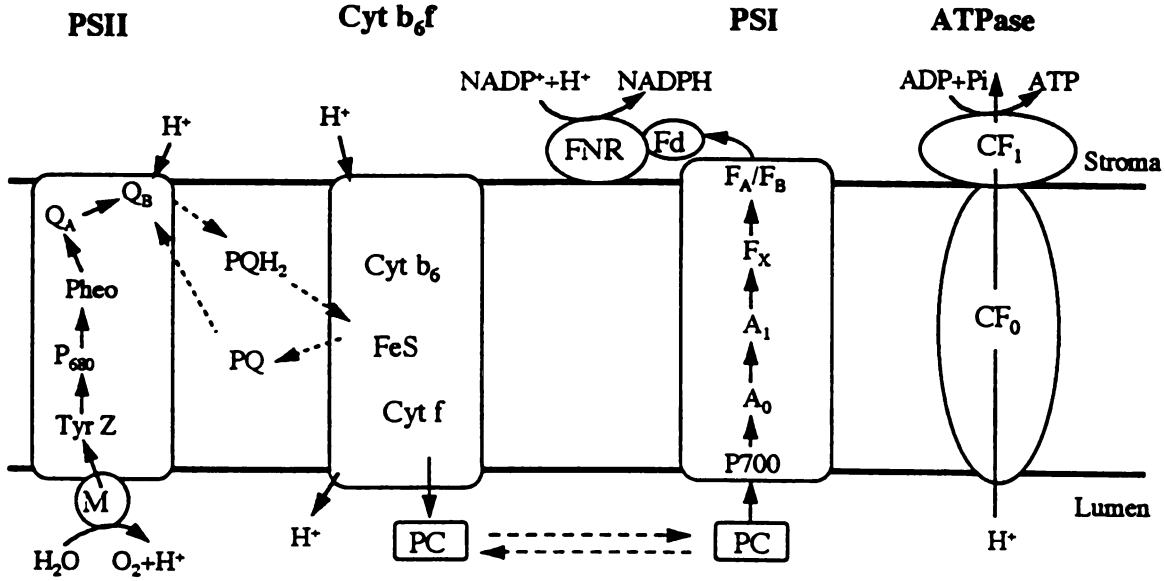

Figure 1.1. Scheme for electron transport from water to $NADP^+$. CF_1 and CF_0, major coupling factor components; M, the manganese containing component involved in the reduction of water and the release of oxygen; TyrZ, a tyrosine residue and the first electron donor to $P680^+$; P680, PSII reaction center Chl *a*; Pheo, pheophytin; Q_A and Q_B, first and second quinone electron acceptors, respectively; PQ, plastoquinone; PQH_2, plastoquinol; Fe-S, Rieske iron-sulfur center; Cyt *f*, cytochrome *f*; Cyt b_6, cytochrome b_6; PC, plastocyanin; P700, PSI reaction center Chl *a*; A_0 and A_1, primary and secondary PSI electron acceptors, respectively; F_X, F_A and F_B, iron-sulfur centers; Fd, ferredoxin; FNR, ferredoxin-NADP oxidoreductase. Solid lines indicate electron and proton transfers, dashed lines indicate component diffusion.

The electrons on Q_B are carried to the Rieske Fe-S center in the Cyt b_6f complex by a mobile pool of plastoquinone (PQ) molecules which shuttle between PSII and the Cyt b_6f complex. Concomitantly with transferring electrons to the Rieske center, PQ transfers protons from the stromal to the lumenal side of the thylakoid (Figure 1.1). Cyt f donates single electron to the second mobile carrier of electron transport, plastocyanin, which may be replaced by cytochrome c_6 in cyanobacteria. The Cyt b_6f complex is shared between photosynthesis and respiration in the cyanobacteria (Kallas, 1994). Plastocyanin or cytochrome c_6 donates electrons to P700, the reaction center chlorophyll pair in PSI.

The antenna of PSI captures the second photon of light needed to complete reduction of $NADP^+$ and transfers the energy to P700, creating P700*, the strongest reductant in a biological system (≈-1.2V) (Vos and van Gorkom, 1988). P700 passes an electron to a series of electron carriers in PSI, which then donate electrons to ferredoxin (Figure 1.1). In cyanobacteria, flavodoxin can substitute for ferredoxin under conditions of iron-limitation (Ho and Krogmann, 1982). Ferredoxin then reduces $NADP^+$ to NADPH, a reaction catalyzed by the ferredoxin:$NADP^+$ oxidoreductase (Ho and Krogmann, 1982). The detailed nature of the electron carriers in PSI will be discussed below. PSI is also capable of catalyzing cyclic electron flow, in which electrons are returned to the cytochrome complex to cycle back to P700 (Kallas, 1994). This process does not reduce $NADP^+$, but does cause formation of a proton gradient for ATP synthesis.

PHOTOSYSTEM I

PSI components

PSI is a heteromultimeric pigment-protein complex that functions as a light-driven plastocyanin-ferredoxin oxidoreductase (Figure 1.2). It contains polypeptides and cofactors that are required for light absorption, charge separation and stabilization. PSI consists of at least 11 different proteins in cyanobacteria and 13 in chloroplasts (Chitnis, 1996). All PSI proteins are believed to be present as one copy per P700 reaction center. They vary considerably in their molecular weights, hydrophobicities, and locations with respect to the lipid bilayer. In addition to proteins, the PSI complex contains approximately 100 Chl *a* molecules, several β-carotenes, two phyloquinone molecules, and three [4Fe-4S] clusters. The cofactors of PSI are bound to the PsaA, PsaB, and PsaC proteins. The remaining subunits of PSI do not bind any redox centers. Trimers of PSI have been observed by electron microscopy of the photosynthetic membranes of cyanobacteria and are considered to be the functional units *in vivo* (Boekema *et al.*, 1994).

In plants and green algae, PSI is localized in the non-appressed regions of the thylakoid membrane, where it is surrounded by a pigment- protein light harvesting complex (LHCI). LHCI functions as an antenna complex, harvesting light energy and funneling it to the PSI reaction center (Preiss *et al.*, 1993). LHCI contains hydrophobic apoproteins with apparent molecular masses of 11 to 24 kD that bind Chl *a*, Chl *b*, violaxanthin, and lutein. Such separate, membrane-embedded, PSI-specific LHCs have not been found in cyanobacteria. However, phycobilisomes serve as additional antennae for PSI in cyanobacteria, although they primarily transfers excitation energy to PSII (Fujita *et al*, 1994).

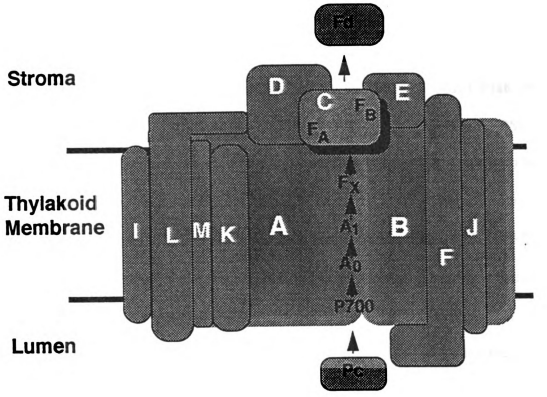

Figure 1.2. A model for the organization of PSI subunits and electron transfer components. PSI subunits PsaA, PsaB, etc, are indicated using letters A, B, etc. PC, plastocyanin; P700, PSI reaction center Chl *a* dimer; A_0 and A_1, primary and secondary electron acceptors, respectively; F_X, F_A and F_B, iron-sulfur centers; Fd, ferredoxin. Arrowheads indicate electron transfers.

In the past 10 years, multi-disciplinary research efforts have led to characterization of the components, the electron transfer reactions, and the structure of PSI. Detailed recent reviews of the structure and function of PSI have been published and provide the reader with a valuable compilation of the current state of understanding of PSI (Chitnis, 1996; Golbeck, 1994).

The primary structures of individual PSI proteins and the overall mechanism of PSI function are remarkably conserved among cyanobacteria, green algae, and plants. The PsaA (83.0 kDa for *Synechocystis* sp. PCC 6803) and PsaB (82.4 kDa) proteins form the photoreactive core of PSI. Three peripheral proteins PsaC (8.9 kDa), PsaD (15.6 kDa), and PsaE (8.0 kDa) and five integral membrane proteins PsaL (16.6 kDa), PsaK (8.5 kDa), PsaF (15.7 kDa), PsaI (4.3 kDa), and PsaJ (4.4 kDa) are present in the PSI complexes from the cyanobacteria, green algae, and plants. PsaM (3.4 kDa) had been detected in the cyanobacterial PSI but has yet to be shown in the PSI preparations from eukaryotes. In contrast, PsaG (10-10.8 kDa, in higher plants), PsaH (10.2-111 kDa), and PsaN (9 kDa) have been shown only in the PSI preparation from green algae and plants. Genes for all known subunits of PSI have been cloned from several plants, algae, and cyanobacteria. These genes are designated as *psaX*, where X is assigned in the order of discovery. The protein subunits of eukaryotic PSI are encoded in both chloroplast and nuclear genomes; the *psaA*, *psaB*, *psaC*, *psaI*, and *psaJ* genes are localized on the chloroplast DNA, and the others are present in the nucleus. The nuclear-encoded PSI proteins are synthesized as precursors with amino-terminal transit peptides and are imported posttranslationally into chloroplasts.

Functions of some PSI proteins have been studied by biochemical approaches. In

recent years, many researchers have also used molecular genetic strategies, or "reverse genetics", to decipher structure-function relations in PSI. The cyanobacteria *Synechocystis* sp. PCC 6803, *Synechococcus* sp. PCC 7002, *Anabaena variabilis* ATCC 29413, and the green alga *Chlamydomonas reinhardtti* have been the most popular and versatile model systems to generate PSI mutants.

PsaA, PsaB, and PsaC: Binding to redox centers and cofactors. In the late 1980s, Golbeck and colleagues developed resolution-reconstitution assays to identify the PSI proteins that bind redox centers. Treatment with chaotropic agents (urea, NaBr, NaI, NaSCN, and $NaClO_4$), followed by sucrose density ultracentrifugation, was used to prepare a PsaA-PsaB core lacking peripheral subunits, including PsaC (Golbeck *et al.*, 1988b). Such core complexes contain all pigments in the intact PSI and are capable of charge separation and electron transfer to F_X. F_A and F_B can be reconstituted in purified PsaC and subsequently assembled on a PsaA-PsaB core (Golbeck *et al.*, 1988a). These analyses demonstrated that PsaA, PsaB, and PsaC bind all electron transfer centers of PSI. Biochemical evidence for the function of PsaA, PsaB, and PsaC has been corroborated by the phenotypes of cyanobacterial and algal mutants. Inactivation of psaA or psaB results in the absence of PSI in the mutant thylakoids, showing that these subunits cannot form homodimers and that the presence of the PsaA-PsaB heterodimer is essential for the assembly of the complex (Smart *et al.*, 1991; Smart *et al.*, 1993a). Vigorous site-directed mutagenesis of the PSI core has been focused on identifying the residues that bind different cofactors. Conserved cysteinyl residues have been proposed to function as F_X ligands (Golbeck and Bryant, 1991). As an experimental proof, the replacement of these residues affects F_X and drastically reduces accumulation of PSI in the membranes (Smart

et al., 1993b; Vassiliev *et al*, 1995). The results also demonstrate that F_X is essential for stable assembly of the PSI core (Smart *et al.*, 1993b).

The absence of PsaC has different effects on the assembly of the core complex in different organisms. The PSI core is unstable in the PsaC-less mutant of *C. reinhardtii* (Takahashi *et al.*, 1991) but is assembled and functional in charge separation in *A. variabilis* (Mannan *et al.*, 1991). Conserved cysteinyl residues of PsaC have been proposed to function as ligands for F_A and F_B. A combination of site-directed mutagenesis and *in vitro* reconstitution has been used to test the proposal. Mutant PsaC expressed in *E. coli* was reconstituted with a biochemical preparation of a PSI core. These experiments showed that Cys 21, 48, 51, and 54 in PsaC provide ligands to the F_A cluster, whereas Cys 11, 14, 17, and 58 are ligated to the F_B cluster (Zhao *et al.*, 1992). Similar mutations of ligands to F_A and F_B were introduced into *A. variabilis in vivo*, and the mutant strains were shown to grow under photoautotrophic conditions (Mannan *et al.*, 1996).

Interaction with soluble electron acceptors: PsaC, PsaD, PsaE, PsaM, and PsaF.

Formation of the PSI-ferredoxin (Fd) complex precedes electron transfer; the rate constants for complex formation depend on ionic strength, suggesting that there are electrostatic interactions between Fd and PSI. Fd accepts electrons from the F_A and F_B clusters of PsaC, implying that Fd and PsaC contact each other. The major obstacle in the association between PsaC and Fd is the unfavorable electrostatic interactions; both proteins have strong electro-negative surfaces at physiological pH. Therefore, docking proteins are required to facilitate the interaction by providing amino acid clusters of opposite charges. Numerous recent studies involving biochemical reconstitutions,

chemical cross-linking, and subunit-deficient mutants have revealed crucial roles of PsaD and PsaE in the docking of Fd (reviewed in Chitnis *et al.*, 1995). Thus, PsaC, PsaD, and PsaE form the reducing site of PSI, on which Fd can dock and accept electrons. On the oxidizing side, PsaF may form a docking site for plastocyanin (Fafah *et al.*, 1995). In addition to the linear electron transfer that results in NADP+ photoreduction, PSI also participates in cyclic electron flow. Characterization of cyanobacterial mutant strains has shown that PsaE and PsaM may be involved in cyclic electron flow around PSI (Yu *et al.*, 1993).

Role in PSI organization and its interaction with LHCI. Some PSI subunits, such as PsaL, are essential components of the trimeric quaternary structure of PSI, which has been demonstrated in the photosynthetic membranes of cyanobacteria (Boekema *et al.*, 1994). Trimers of PSI cannot be obtained from cyanobacterial mutants that lack PsaL (Chitnis, *et al.*, 1995). Recent characterization of PsaI- and PsaJ-less mutants of *Synechocystis* sp. PCC 6803 indicates that these polypeptides assist in the correct organization of PsaL and PsaF, respectively, presumably by stabilizing their transmembrane domains in the lipid bilayer (Xu *et al.*, 1995).

Electron transfer reactions

The PsaA and PsaB proteins of PSI bind the electron transfer components P700, A_0, A_1, and F_X. The reaction center chl dimer, P700, is the site of the primary photochemical charge separation in PSI. It is named by the wavelength at the peak of the oxidized-minus-reduced difference spectrum (Kok, 1956). When a photon is absorbed by a PSI antenna pigment and the energy from the photon is transferred to P700, P700 is

raised to an excited state, P700*, then donates an electron to A_0 and forms the cation $P700^+$, which is detectable by EPR spectroscopy. $P700^+$ is reduced by plastocyanin or in cyanobacteria, by cyt c_6.

P700 has been assigned to PSI crystal structure as a Chl *a* dimer (Fromme *et al.*, 1996). Two chl molecules have been assigned to the spectroscopically characterized 'primary' electron accepter A_0. Two additional monomeric 'accessory' chlorophylls were found between P700 and A_0; their function remains to be determined. Because of the quasi-symmetrical arrangement, it was not possible to identify either one of the chlorophyll molecules as the primary accepter, A_0, that is active in electron transport (Fromme *et al.*, 1996).

A_0 has been characterized best by time-resolved optical spectroscopy, in which the flash-induced absorption changes of P700 are measured under highly reducing conditions, and by flash-induced difference spectra. A_0 is identified as a chl *a* molecule (Mathis, *et al.*, 1988). PSI contains two phylloquinone molecules, either one or both of which serves as A_1. The next intermediate acceptor is the [4Fe-4S] cluster F_X. The subsequent path of electrons through the [4Fe-4S] clusters F_A and F_B remains an unresolved area in the electron transfer pathway in PSI (Jung *et al.*, 1995). The electrons may travel in a series: F_X to $F_{B/A}$ to $F_{A/B}$ to Fd. Alternatively, the electrons from F_X may be transferred to F_A or F_B and then one or both of these reduced clusters can donate electrons to Fd. The proposed locations of these redox centers in the X-ray crystallographic structure are at different distances from F_X, thus implying a serial flow of electrons between F_B and F_A (Krauss *et al.*, 1993). Selective inactivation of F_B with mercurial such as $HgCl_2$ indicates that photoreduction of F_A is independent of F_B (Jung *et al.*, 1995). Therefore, F_B may be

functionally and spatially more distant from F_X than is F_A.

The electron from F_A or F_B is used to reduce Fd, and the electron lost by P700 is regained by oxidizing plastocyanin. Thus, the PSI complex interacts with soluble electron carrier proteins on both sides of the thylakoid membrane. The interprotein electron transfer on the reducing side of PSI is a complex process. It involves several different PSI-Fd complexes and three different first-order components with half lives of approximately 500 ns, 13-20 μs, and 100-123 μs (Setif and Bottin, 1995). The 500-ns phase corresponds to electron transfer from F_A or F_B to Fd. When grown under iron-deficient conditions, cyanobacteria contain flavodoxin as an additional electron acceptor from PSI. The structural requirements for efficient electron transfer to *Anabaena* Fd and flavodoxin are highly dependent on the reaction partner (Navarro *et al.*, 1995).

On the oxidizing side of PSI, the interaction between plastocyanin and PSI involves a fast phase with a half life of 12 to 14 μs and second slower phase with a half life of 200 μs (Haehnel *et al.*, 1994). The fast rate can be attributed to the association of plastocyanin close to P700, whereas the slower phase may represent a distant plastocyanin population. In cyanobacteria and green algae, Cyt c_6, a second electron donor, is synthesized during growth in copper-depleted medium. Recently, interaction of PSI with plastocyanin or Cyt c_6 proteins from diverse organisms was studied by laser flash absorption spectroscopy (Hervas *et al.*, 1995). PSI reduction by plastocyanin or Cyt shows varying kinetics depending on the organism from which the photosystem and metalloproteins are isolated. These findings suggest that PSI was able to first optimize its interaction with positively charged Cyt and that the evolutionary replacement of the ancestral Cyt by plastocyanin, as well as the appearance of the fast kinetic phase in the

plastocyanin/PSI system of higher plants, involved structural modifications in both the donor protein and PSI (Hervas *et al.*, 1995).

PSI structure

Major advances have been made in the past few years in understanding the structure of PSI. Electron microscopic studies have provided valuable information concerning the global shape and size of PSI complexes (Boekema *et al.*, 1994), X-ray crystallography has permitted a more detailed knowledge of secondary and tertiary structural elements in PSI (Krauss *et al.*, 1993; Schubert *et al.*, 1995), and biochemical studies have revealed some details of PSI topography and subunit interactions. On the basis of the electron density maps, a structural model for trimeric PSI from *Synechococcus elongatus* was initially proposed at a resolution of 6 Å (Krauss *et al.*, 1993). From new data, many aspects of this model were later refined to 4.5 Å resolution (Schubert *et al.*, 1995).

The crystal analysis of PSI has indicated the location of the [4Fe-4S] clusters F_X, F_A, and F_B, 86 Chl molecules, 29 transmembrane α helices, and 4 α-helices that are parallel to the plane of the membrane. A monomer of PSI consists of a "catalytic domain" and a smaller "connecting domain" that links monomers to form a trimer. The connecting domain does not extend significantly beyond the lipid bilayer and contains three transmembrane helices which may belong to PsaL and PsaI. The catalytic domain contains all cofactors and protrudes 15 and 35 Å into the lumen and stroma, respectively (Chitnis, 1996).

Because of the high electron density, the three iron-sulfur centers of PSI are clearly

identified in the crystal structure of PSI. They form an obtuse-angled triangle oriented roughly perpendicular to the plane of the membrane. F_X is located at the edge of the membrane plane. From the top view of PSI, F_X is at the center of the PSI complex. The other two clusters are located 15.4 and 22.2 Å from F_X, respectively. The F_A-F_B axis is tilted 54° from the membrane perpendicular axis. Two α-helices are present close to F_A and F_B, thus resembling two iron-sulfur centers of the soluble Fd from *Peptostreptococcus asaccharolyticus* (formerly known as *Peptococcus aerogenes*), which has sequence similarity to PsaC. However, an unambiguous assignment of F_A and F_B to the respective clusters is not yet possible.

A striking feature of the proposed PSI structure is the arrangement of helices around the electron transfer chain. The framework of the inner core of PSI consists of 10 helices of PsaA and PsaB that resemble similar helices of the L and M subunits of the bacterial reaction center. These tilted transmembrane helices, along with four additional helices parallel to the membrane plane, make a cage for coordination and protection of the electron transfer chain.

The proposed arrangement of the antenna Chl *a* in PSI is different from that seen in the bacterial LHC or in LHCII of higher plants (Schubert *et al.*, 1995). Located 8 to 15 Å from each other, Chl a molecules are positioned along the wall of an oval bowl with the bottom oriented toward the luminal side. This wall may function as a storage device for rapid delocalization of an excited state.

GENETIC MANIPULATION OF PSI IN A MODEL ORGANISM *SYNECHOCYSTIS* SP. PCC 6803

Molecular biology offers the researcher the ability to alter an element of a biological system in order to learn more about that element in the normal system. *Synechocystis* sp. PCC 6803 is an excellent genetic system for the study of oxygenic photosynthesis. It is a unicellular cyanobacterium that is naturally competent, and thus is readily transformable. It has an active homologous recombination mechanism, making gene replacement by double recombination a straightforward technique (Williams, 1988). There does not appear to be an active restriction or modification system in this strain that can digest transforming DNA (Williams, 1988). Of great importance is that this strain may be grown photoheterotrophically (with DCMU and glucose) (Williams, 1988) or heterotrophically, under light-activated heterotrophic growth conditions (LAHG), complete darkness except for 5 min of light every 24 h, and in the presence of glucose (Anderson and McIntosh, 1991). Growth under these conditions eliminates the selective advantage conferred by the expression of wild-type photosynthesis genes, allowing for complete segregation of mutations (Smart *et al.*, 1991). This strain has approximately 8-10 copies of its chromosome per cell (Williams, 1988); thus in order to obtain a homozygous strain, segregation is crucial.

The entire 3.57 Mb genome of *Synechocystis* sp. PCC 6803 has recently been sequenced (Kaneko *et al.*, 1996). Availability of the sequences will undoubtedly simplify genetic studies in this model organism. Inactivation of individual subunits has led to identification of the function of some subunits in the assembly of, stability of, and electron transport in PSI (Smart *et al.*, 1991). Site-directed mutagenesis has been used to study

the structure-function relationships of particularly interesting regions such as ligands to F_X and the electronic environment near F_X (Smart *et al.*, 1993b).

FOCUS OF THIS STUDY

The body of the work presented in this thesis addresses the development and utilization of the cyanobacterium *Synechocystis* sp. PCC 6803 as a system for the study of PSI assembly, structure and function. Two *psaC* genes, *psaC1* and *psaC2*, have been reported in *Synechocystis* sp. PCC 6803. The initial stage of the project was the inactivation of the *psaC2* gene, in order to find out which gene codes for the PsaC subunit. This stage included the analysis of the assembly of the PSI complex and of electron transport in the absence of PsaC. Mutations were introduced at the proposed cysteine ligands to F_A and F_B. Analysis of these mutants gives us insight into the assembly of PSI complex and the efficiency of electron transfer, as well as into the functions and properties of iron-sulfur clusters with alternate ligands. Since the PsaC mutants were unable to grow photoautotrophically under white light and their mixotrophic growth was inhibited by white light of moderate intensity, spontaneous pseudorevertants were isolated to gain insight of the structure of PSI complex and to study its function in cyanobacterial metabolism .

REFERENCES

Allen JP, Feher G, Yeats TO, Komiya H and Rees DC (1987) Structure of the reaction center from *Rhodobacter sphaeroides* R-26: the cofactors. *Proc. Natl. Acad. Sci. USA* **84**: 5730-5734

Anderson SL, McIntosh L: Light-activated heterotrophic growth of the cyanobacterium *Synechocystis* sp. strain PCC 6803: a blue-light-requiring process. *J Bacteriol* **173**: 2761-2767 (1991).

Barry BA, Boerner RJ, and de Paula JC (1994) The use of cyanobacteria in the study of the structure and function of photosystem II. In: The molecular biology of cyanobacteria. Bryant DA, ed. Kluwer Academic Publishers, pp.217-257

Boekema EJ, Boonstra AF, Dekker JP, and Rogner M (1994) Electron microscopic structural analysis of photosystem I, photosystem II, and the cytochrome *b6/f* complex from green plants and cyanobacteria. *J Bioenerg Biomembr* **26**: 17-29

Chitnis PR, Xu Q, Chitnis VP, and Nechushtai R (1995) Function and organization of photosystem I polypeptides. *Photosynth Res* **44**: 23-40

Chitnis PR (1996) Photosystem I. *Plant Physiology* **111**: 661-669

Deisenhofer J, Epp O, Miki K, Huber R, and Michel H (1985) Structure of the protein subunits in the photosynthetic reaction centre of *Rhodopseudomonas viridis* at 3 Å resolution. *Nature* **318**: 618-624

Farah J, Rappaport F, Choquet Y, Joliot P, and Rochaix JD (1995) Isolation of a *psaF*-deficient mutant of *Chlamydomonas reinhardtii*: efficient interaction of plastocyanin with the photosystem I reaction center is mediated by the PsaF subunit. *EMBO J* **14**: 4976-4984

Fromme P, Witt HT, Schubert W-D, Klukas O, Saenger W, and Krauß N (1996) Structure of photosystem I at 4.5 Å resolution : a short review including evolutionary aspects. *Biochim Biophys Acta* **1275**: 76-83

Fujita Y, Murakami A, Aizawa K (1994) Short-term and long-term adaptation of the photosynthetic apparatus: homeostatic properties of thylakoids. In: The molecular biology of cyanobacteria. Bryant DA, ed. Kluwer Academic Publishers, pp. 677-692

Golbeck JH (1994) Photosystem I in cyanobacteria. In: The molecular biology of cyanobacteria. Bryant DA, ed. Kluwer Academic Publishers, pp. 319-360

Golbeck JH and Bryant (1991) Photosystem I. *Curr. Topics Bioenerg.* **16**: 83-177

Golbeck JH, Mehari T, Parrett K, Ikegami I (1988a) Reconstitution of the photosystem I complex from the P700 and F_X-containing reaction center core protein and F_A/F_B polypeptide. *FEBS Lett* **240**: 9-14

Golbeck JH, Parrett K, Mehari T, Jones KL, Brand JJ (1988b) Isolation of the intact photosystem I reaction center core containing P700 and iron-sulfur center F_X. *FEBS Lett* **228**: 268-272

Haehnel W, Jansen T, Gause K, Klosgen RB, Stahl B, Michel D, Huvermann B, Karas M, Herrmann R (1994) Electron transfer from plastocyanin to photosystem I. *EMBO J* **13**: 1028-1038

Hervas M, Navarro JA, Diaz A, Bottin H, de la Rosa MA (1995) Laser-flash kinetic analysis of the fast electron transfer from plastocyanin and cytochrome c_6 to photosystem I. Experimental evidence on the evolution of the reaction mechanism. *Biochemistry* **34**: 11321-11326

Ho KK and Krogmann DW (1982) Photosynthesis. In The Biology of Cyanobacteria, Carr NG and Whitton BA, eds. Los Angeles: University of California Press, pp.191-214

Jung Y-S, Yu L, Golbeck JH (1995) Reconstitution of iron-sulfur center F_B results in complete restoration of $NADP^+$ photoreduction in Hg-treated photosystem I complexes from *Synechococcus* sp. PCC 6301. *Photosynth Res* **46**: 249-255

Kallas T (1994) The cytochrome b_6f complex. In: The molecular biology of cyanobacteria. Bryant DA, ed. Kluwer Academic Publishers, pp. 259-317

Kaneko T, Sato S, Kotani H, Tanaka A, Asamizu E, Nakamura Y, Miyajima N, Hirosawa M, Sugiura M, Sasamoto S, Kimura T, Hosouch T, Matsuno A, Muraki A, Nakazaki N, Naruo K, Okumura S, Shimpo S, Takeuchi C, Wada T, Watanabe A, Yamada M, Tasuda M, and Tabata S (1996) Sequence analysis of the genome of the unicellular cyanobacterium *Synechocystis* sp. strain PCC 6803. II. Sequence determination of the entire genome and assignment of potential protein-coding regions. *DNA research* **3**: 109-136

Kok B(1956) On the reversible absorption change at 705 mμ in photosynthetic organisms. *Biochim. Biophys. Acta* **22**: 399-401

Krauß N, Hinrichs W, Witt I, Fromme P, Pritzkow W, Dauter Z, Betzel C, Wilson KS, Witt HT, and Saenger W (1993) Three-dimensional structure of system I of photosynthesis at 6 Å resolution. *Nature* **361**: 326-331

Mannan RM, He W-Z, Metzger S, Whitmarsh J, Malkin R, and Pakrasi HB (1996) Active photosynthesis in cyanobacterial mutants with directed modifications in the ligands for two iron-sulfur clusters in the PsaC protein of photosystem I. *EMBO J* **15**: 1826-1833

Mannan RM, Whitmarsh J, Nyman P, and Pakrasi HB (1991) Directed mutagenesis of an iron-sulfur protein of the photosystem I complex in the filamentous cyanobacterium *Anabaena variabilis* ATCC 29413. *Proc Natl Acad Sci USA* **88**:10168-10172

Mathis P, Ikegami I and Setif P (1988) Nanosecond flash studies of the absorption spectrum of the photosystem I primary acceptor A_0. *Photosynth Res* **16**: 203-210

Navarro JA, Hevas M, Genzor CG, Cheddar G, Fillat MF, de la Rosa MA, Gomez-Moreno C, Cheng H, Xia B, Chae YK, Yan H, Wong B, Straus NA, Markley JL, Hurley JK, Tollin G (1995) Site-specific mutagenesis demonstrates that the structural requirements for efficient electron transfer in *Anabaena* ferredoxin and flavodoxin are highly dependent on the reaction partner: kinetic studies with photosystem I, ferredoxin:$NADP^+$ reductase, and cytochrome *c*. *Arch Biochem Biophys* **321**: 229-238

Nugent JH (1996) Oxygenic photosynthesis. Electron transfer in photosystem I and photosystem II. *Eur J Biochem* **237**: 519-531

Preiss S, Peter GF, Anandan S, and Thornber JP (1993) The multiple pigment-proteins of the photosystem I antenna. *Photochem Photobiol* **57**: 152-157

Setif PQ, and Bottin H (1995) Laser flash absorption spectroscopy study of ferredoxin reduction by photosystem I: spectral and kinetic evidence for several photosystem I-ferredoxin complexes. *Biochemistry* **34**: 9059-9070

Schubert WD, Klukas O, Krauss N, Saenger W, Fromme P, Witt HT (1995) Present state of the crystal structure analysis of photosystem I at 4.5 Å resolution. In Mathis P, ed, Photosynthesis: From Light to Biosphere, Vol II. Kluwer Academic, Dordrecht, The Netherlands, pp 3-10

Smart LB, Anderson SL, and McIntosh L (1991) Targeted genetic inactivation of the photosystem I reaction center in the cyanobacterium *Synechocystis* sp PCC 6803. *EMBO J* **10**:3289-3296

Smart LB, and McIntosh L (1993a) Genetic inactivation of the *psaB* gene in *Synechocystis* sp PCC 6803 disrupts assembly of photosystem I. *Plant Mol Biol* **21**: 177-180

Smart LB, Warren PV, Golbeck JH, and McIntosh L (1993b) Mutational analysis of the structure and biogenesis of the photosystem I reaction center in the cyanobacterium *Synechocystis* sp PCC 6803. *Proc Natl Acad Sci USA* **90**: 1132-1136

Takahashi Y, Goldschmidt-Clermont M, Soen SY, Franzen, and Rochaix JD (1991) Directed chloroplast transformation in *Chlamydomonas reinhardtii:* insertional inactivation of the *psaC* gene encoding the iron sulfur protein destabilizes photosystem I. *EMBO J* **10**: 2033-2040

Vassiliev IR, Jung YS, Smart LB, Schulz R, McIntosh L, and Golbeck JH (1995) A mixed-ligand iron-sulfur cluster ($C556S_{PsaB}$ or $C565S_{PsaB}$) in the F_X-binding site leads to a decreased quantum efficiency of electron transfer in photosystem I. *Biophys J* **69**: 1544-1553

Vos MH and van Gorkom HJ (1988) Thermodynamics of electron transport in photosystem I studied by electric field-stimulated charge recombination. *Biochim. Biophys. Acta* **934**: 293-302

Williams JGK (1988) Construction of specific mutations in photosystem II photosynthetic reaction center by genetic engineering methods in *Synechocystis* 6803. *Meth Enzymol* **167**: 766-778

Xu Q, Chitnis PR (1995) Organization of photosystem I polypeptides. Identification of PsaB domains that may interact with PsaD. *Plant Physiol* **108**: 1067-1075

Yu L, Zhao J, Mühlenhoff, Bryant DA, and Golbeck JH (1993) PsaE is required for *in vivo* cyclic electron flow around photosystem I in the cyanobacterium *Synechococcus* sp. PCC 7002. *Plant Physiol* **103**: 171-180

Zhao J, Li N, Warren PV, Golbeck JH, and Bryant DA (1992) Site-directed conversion of a cysteine to aspartate leads to the assembly of a [3Fe-4S] cluster in PsaC of photosystem I. The photoreduction of F_A is independent of F_B. *Biochemistry* **31**:5093-5099

Chapter 2

ABSENCE OF PsaC SUBUNIT ALLOWS ASSEMBLY OF PHOTOSYSTEM I CORE BUT PREVENTS THE BINDING OF PsaD and PsaE IN *SYNECHOCYSTIS* SP. PCC 6803

Published in modified form as Jianping Yu, Lawrence B. Smart, Yean-Sung Jung, John Golbeck and Lee McIntosh. *Plant Molecular Biology* vol. 29, pp. 331-342 (1995).

Introduction

Photosystem I (PSI) is a multi-subunit, thylakoid membrane-bound pigment-protein complex that catalyzes the light-dependent transfer of electrons from plastocyanin or cytochrome c_6 to ferredoxin or flavodoxin. Purified PSI typically contains at least eleven polypeptides, approximately 100 chlorophyll a molecules, a pair of phylloquinones, and three [4Fe-4S] clusters. The PSI core consists of a heterodimer of homologous 83 and 82 kDa reaction center polypeptides, encoded by the *psaA* and *psaB* genes, respectively. This complex is responsible for binding the electron donor P700 and the acceptors A_0, A_1, and F_X (Golbeck, 1992). The terminal PSI electron acceptors F_A and F_B, both [4Fe-4S] clusters, are associated with a single 8.9 kDa polypeptide encoded by the *psaC* gene (Høj *et al.*, 1987; Oh-oka *et al.*, 1988). The 15.5 kDa PsaD subunit is proposed to be a ferredoxin-binding subunit (Zilber and Malkin, 1988) and is required for stable binding of the PsaC to the reaction center

core in reconstitution experiments (Li *et al.*, 1991b). The 8 kDa PsaE subunit is suggested to stimulate the reduction of soluble electron acceptors such as ferredoxin and /or flavodoxin, and is also suggested to be associated with cyclic electron transport around PSI (Yu *et al.*, 1993). The 15.7 kDa PsaF subunit is proposed to be a plastocyanin-binding subunit (Wynn and Malkin, 1988), and the 16.6 kDa PsaL subunit is proposed to play a role in PSI trimmer formation (Chitnis *et al.*, 1993). The cyanobacterial PSI complex contains at least 4 additional polypeptides of unknown function (Golbeck, 1994; Henry *et al.*, 1990).

We are employing site-directed mutagenesis to understand the protein architecture responsible for electron flow in the PSI reaction center. This genetic manipulation is most readily accomplished using the unicellular cyanobacterium *Synechocystis* sp. PCC 6803, since it has a photosynthetic apparatus much like that of plants, is easily transformed, has an active homologous recombination system, can use bacterial drug resistance genes, and may be grown heterotrophically (Anderson and McIntosh, 1991a). A number of mutants have been made in PsaA and PsaB proteins. Analysis of these mutants has provided new insights into the identity and function of F_X (Smart *et al.*, 1993; Warren *et al.*, 1993).

The nucleotide and the protein sequences of several *psaC* genes and PsaC proteins of cyanobacteria, algae and plants are known (Golbeck, 1992). The *psaC* gene is located in the chloroplast genome in eukaryotes. The mature PsaC protein has 80 amino acids, is highly acidic, and has two regions of the CXXCXXCXXXCP binding motif characteristic of 8Fe-8S proteins. The PsaC amino acid sequence is highly conserved among cyanobacteria (>90% identical) and higher plants (>95% identical) (Golbeck, 1992), and the differences are usually conservative.

The *psaC* gene has been previously inactivated in a cyanobacterium, *Anabaena*

variabilis sp. ATCC 29413 (Mannan *et al.*, 1991), and in the alga *Chlamydomonas reinhardtii* (Takahashi *et al.*, 1991). In *Anabaena variabilis* 29413, the loss of PsaC prevented autotrophic growth and caused the cells to be light-sensitive, but it did not significantly alter stable assembly of the PSI reaction center; further study showed that PsaD and PsaE were absent in isolated thylakoid membranes (Mannan *et al.*, 1994). However, in *Chlamydomonas*, inactivation of *psaC* prevented stable accumulation of the PSI reaction center proteins and of seven additional peripheral PSI polypeptides.

Unlike other cyanobacteria, two different *psaC* genes have been reported in *Synechocystis* 6803: one (*psaC1*) (Anderson and McIntosh, 1991b) with a deduced amino acid sequence identical to that of tobacco, and another (*psaC2*) (Steinmüller, 1992) with a deduced amino acid sequence similar to those reported for other cyanobacteria. Specific transcripts for *psaC1* were not detected (Anderson and McIntosh, 1991b). In contrast, the *psaC2* gene is transcribed into an abundant mRNA of about 450 nucleotides (Steinmüller, 1992). Two questions arise: which gene encodes PsaC protein and what is the role of PsaC in assembly and function of PSI? We describe here the inactivation of the *psaC2* gene and characterization of the resulting mutant strain in *Synechocystis* 6803.

Materials and methods

Materials

Chemicals and antibiotics used were obtained from Sigma Chemical Co. (St. Louis, MO) or Research Organics (Cleveland, OH). Restriction endonucleases and other enzymes were purchased from New England Biolabs (Beverly, MA). Radioactive isotope ([α-^{32}P]dATP and [γ^{32} P]ATP) was purchased from Amersham (Arlington Heights, IL),

nitrocellulose membrane from Schleicher and Schuell (Keene, NH), and Bacto-agar from Difco (Detroit, MI).

Strains and growth conditions

A glucose-tolerant strain of the cyanobacterium *Synechocystis* sp. PCC 6803 (Williams, 1988) was used in this study. Cells were grown in liquid BG-11 medium with 5 mM glucose or on BG-11 with 5 mM glucose and 1.5% purified Bacto-agar under LAHG conditions, as previously described (Anderson and McIntosh, 1991a). Transformation of *Synechocystis* 6803 was performed essentially as described (Williams, 1988). The mutant strain CDK25 was isolated and maintained in medium containing 5 mg/l kanamycin sulfate. For analysis of mutants, cells were grown in carboys containing 15 l of medium, were harvested using a SS34 continuous flow rotor (DuPont Sorvall, Wilmington, DE), and were frozen at -70 °C in BG-11 with 15% v/v glycerol.

Nucleic acid manipulations

All nucleic acid manipulations were performed using standard procedures (Sambrook *et al.*, 1989), unless otherwise stated. Plasmid p61-2.4, containing the *psaC2* gene, was a kind gift from Klaus Steinmüller (Universität Düsseldorf, Düsseldorf, Germany). Genomic DNA was isolated from *Synechocystis* 6803 essentially as described (Williams, 1988), fractionated by agarose gel electrophoresis, and transferred to nitrocellulose. RNA isolation and conditions for hybridization were previously described (Smart *et al.*, 1991). Synthetic oligonucleotides designed to recognize both *psaC1* and *psaC2* sequences (CGCAGTATGGGTCTAGCTTA) or to recognize *psaC2* specifically (using a probe of two mixed sequences,

A=GGCTTGCCCCCTCGATGTT and B=CCGAGTTTATTTGGGTGCCGAA) were end-labeled and used as probes. Plasmid pSLA4-1 (Anderson and McIntosh, 1991b), consisting of pUC119 containing a 202bp Sau3A1-Taq1 fragment of *psaC1*, was random primer-labeled (Feinberg *et al.*, 1983) and used as a *psaC1*-specific probe.

psaC Interposon mutagenesis

A 2.4 kilobase pair (Kb) *Sal* I fragment containing *psaC2* gene from *Synechocystis* 6803 (Steinmüller, 1992), in pSP65 (plasmid p61-2.4), was digested with *Xba*I and the resulting single-stranded DNA overhangs were digested briefly with mung bean nuclease. A 1.25-Kb *Hinc*II fragment, encoding an aminoglycoside 3' phosphotransferase from *Tn903* and conferring resistance to kanamycin(km) (Oka *et al.*, 1981), was purified from pUC4k (Vieira and Messing, 1982) and ligated into the blunt *Xba*I site of p61-2.4. The product was transformed into *Escherichia coli* XL1-Blue (Stratagene, La Jolla, CA), and km-resistant (Km^R) colonies were recovered. The resulting plasmid, p61-2.4k, had lost the *Xba*I site and the *Hinc*II sites flanking the Km^R cassette. A restriction map of the construct from p61-2.4k is shown in figure 2.1.

Transformation of Synechocystis *6803 and selection conditions*

Synechocystis 6803 that had been maintained under LAHG conditions for two subcultures was transformed with the plasmid p61-2.4k. Selection for Km^R colonies was performed under LAHG conditions. Single Km^R colonies were streaked to at least five serial transfers to obtain full segregation of the mutation. Km^R colony CDK25 was analyzed further.

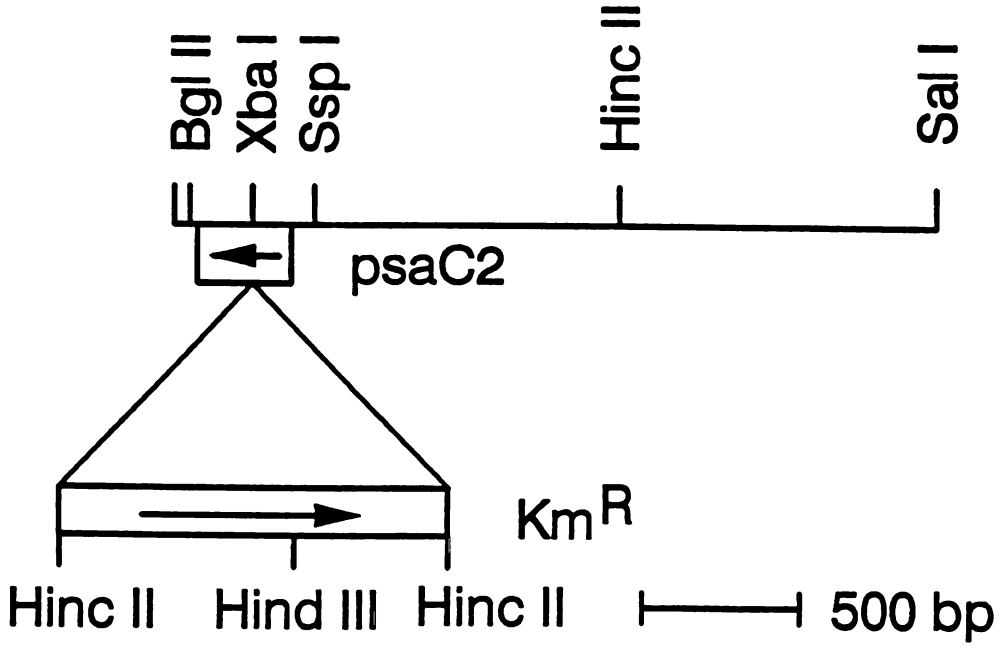

Figure 2.1. Partial restriction map of the plasmid p61-2.4k2. The plasmid was used for inactivation of *psaC2*. Cloned *Synechocystis* 6803 DNA in p61-2.4k2 is indicated as a line (insert from p61-2.4, a gift from K. Steinmüller), The *psaC2* gene reading frame and the Km^R gene cassette from Tn*903* are indicated as boxes. The arrows indicate the direction of transcription. The Km^R gene cassette was inserted at the *Xba*I site.

Membrane isolation and analysis

Thylakoid membranes were isolated and SDS-PAGE and immunoblotting were performed as described (Smart *et al.*, 1991). To resolve the PsaA/B proteins, 10% SDS-PAGE gels were used; 17% gels were used to resolve PsaC, PsaD, PsaE and PsaF. D2 protein in photosystem II was resolved with 17% gel to serve as a control. Protein assays were performed using the method of Lowry *et al.* (Lowry *et al.*, 1951). Equal amounts of protein (150 μg) were loaded in each lane. Antibody to PsaA/B proteins from *Synechococcus* was raised in rabbits as previously described (Henry *et al.*, 1990). Also raised in rabbits were antibodies to PsaC or PsaD protein purified from strains of *Escherichia coli* expressing, respectively, the *psaC* gene from *Synechococcus* sp. PCC 7002 or the *psaD* gene from *Nostoc* sp. PCC 8009 (Li *et al.*, 1991a). Antibodies against PsaE and PsaF are gifts from Dr. Parag Chitnis and were raised in rabbit immunized with PsaE and PsaF purified from *Synechocystis* sp. PCC 6803. Antibodies to the D2 polypeptide from spinach were raised as previously described (Vermaas *et al.*, 1988). Chlorophyll was extracted with methanol and quantified using published extinction coefficients (Lichtenthaler, 1987).

Thylakoid membrane preparations for EPR and optical measurements

Thylakoid membranes were isolated from *Synechocystis* sp. PCC 6803 using a modification of the procedure described by Noren *et al.* (Noren *et al.*, 1991). The cells were broken in six cycles of a prechilled bead-beater (Biospec Products, OK) in buffer containing 20 mM Tris, pH 7.2, 0.8 M sucrose, and protease inhibitor; one cycle consists of a 30-s "on phase" and a 15-min "off phase". The membranes were pelleted by centrifugation in 40 mM $CaCl_2$ and washed with Tris, pH 8.3, 20 mM $CaCl_2$ and 20 mM $MgCl_2$. The thylakoid

membranes were resuspended in buffer containing 50 mM Tris, pH 8.3, frozen in liquid nitrogen, and stored at -80°C.

In vitro reconstitution

In vitro reconstitution was performed as described (Li *et al.*, 1991b), using thylakoid membrane from CDK25 and PsaC from *Synechococcus* sp. PCC 7002 and PsaD from *Nostoc* sp. PCC 8009. Both PsaC and PsaD were overexpressed by *E. coli* (Li *et al.*, 1991b).

Electron paramagnetic resonance spectroscopy

Electron paramagnetic resonance (EPR) studies were performed with a Bruker ESC-106 X-band spectrometer. Cryogenic temperatures were maintained with an Oxford liquid helium cryostat and an Oxford ITC4 temperature controller. Microwave frequency was sampled during run-time with a Hewlett-Packard 5340A frequency counter. The field was calibrated using the position of the "g" = 2.0025 resonance derived from the $P700^+$ cation. Sample temperature was monitored by a calibrated thermocouple situated beneath the 3-mm i.d. quartz sample tube and referenced to liquid nitrogen. Actinic illumination of the sample was provided by a 150-W xenon arc source (Oriel) filtered through 5 cm of water and passed through a heat-absorbing filter to remove the near-IR wavelengths. Sample contained 1.8 mg/ml Chl, 1.7 mM sodium ascorbate, and 0.033 mM DPIP in 50 mM Tris, pH 8.3.

Flash-induced absorption change

Flash-induced absorption changes in the millisecond time range were determined at 698 nm with a laboratory-built, single-beam spectrometer described previously (Parrett *et al.*,

1989). Actinic illumination was provided by a 5-μs xenon flash (PTI Model 610, London, ON). The absorption transient was captured with a Biomation Model 8100 digitizer interfaced to a Macintosh IIci computer for signal averaging, data storage, and data manipulation. The cuvette contained thylakoid membranes at 8.75 μg/ml Chl, 1.7 mM sodium ascorbate, 0.033 mM DPIP in 50 mM Tris, pH 8.3. The point-by-point spectrum was determined between 400 and 500 nm at a chlorophyll concentration of 10 μg/ml.

Results

Southern and Northern analysis

Southern blots of *Eco*RI digests of genomic DNA from CDK25 were probed with a synthetic oligonucleotide designed to be specific for *psaC2* (C2 probe; Fig. 2.2A), and to recognize both *psaC1* and *psaC2* (C1/C2 probe; Fig. 2.2B); or probed with pSLA4-1 (Anderson and McIntosh, 1991b) which was pUC119 containing a 202bp *Sau*3A1-*Taq*1 fragment of *psaC1* (C1 probe; Fig. 2.2C). In all the digests of CDK25 DNA, no wild-type copies of the *psaC2* genes were detected (Fig. 2.2A), and the *psaC1* gene was found unchanged in CDK25, as in wild-type cells. (Fig. 2.2C). The C2 probe hybridized to a 10.2-Kb *Eco*RI fragment of CDK25 DNA, rather than to the 9.0 Kb wild-type fragment, confirming the insertion of the Km^R gene into *psaC2*. The C1 probe hybridized to a 3.3-Kb *Eco*RI fragment or to both CDK25 and wild-type DNA, confirming that the *psaC1* gene was not interrupted in CDK25. These results are further supported by C1/C2 probe hybridization. In CDK25, insertion of the Km^R cassette caused premature termination of *psaC2* transcription, and its transcripts were not detectable using a synthetic oligonucleotide probe designed to be specific for *psaC2* mRNA. In contrast, a 450-bp message was detected in the

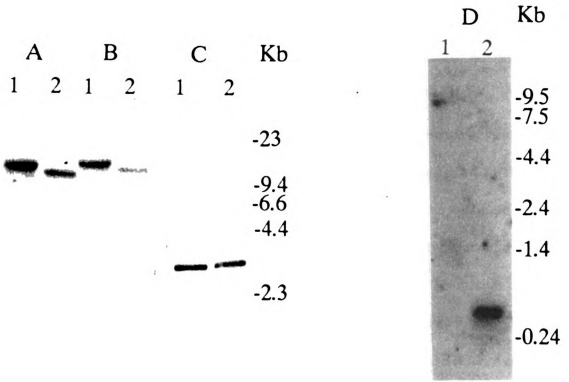

Figure 2.2. Southern and Northern analysis of CDK25.
Panels A--C: Southern blot analysis of CDK25 (lane 1) and wt-6803 (lane 2) genomic DNA. Each lane contains 5 µg DNA digested by *Eco*RI. The same blot was hybridized with synthetic oligonucleotide probe designed to be specific for *psaC2* (panel A) and to recognize both *psaC1* and *psaC2* (panel B). Another blot was hybridized with pSLA4-1 which was pUC119 containing a 202 bp *Sau*3A1-*Taq*1 fragment of *psaC1* (panel C). Panel D: Northern blot analysis with CDK25 (lane 1) and wt-6803 (lane 2) RNA. Synthetic oligonucleotide probe designed to be specific for *psaC2* mRNA was used. CDK25 RNA was isolated from LAHG grown cells. Wt-6803 RNA was isolated from mixotrophically grown cells. Each lane contains 120 µg RNA.

wild type by the same probe (Fig. 2.2D). Expression of *psaC1* was not detected when the same blot was reprobed with oligonucleotide probe designed to be specific for *psaC1* mRNA (data not shown).

Growth characteristics

The growth of CDK25 was indistinguishable from that of wild-type cells under LAHG conditions (data not shown). However, after several attempts, CDK25 would not divide under continuous illumination of 20 μmol m^{-2} s^{-1}, our standard conditions for growth of wild-type *Synechocystis* 6803 (Jansson *et al.*, 1987), in both the presence and absence of glucose in the medium. Under mixotrophic conditions with a light intensity of 5 μmol m^{-2} s^{-1}, CDK25 cells were able to grow, with a doubling time (15 hours) close to that of the wild-type strain (20 hours), although CDK25 started log phase one day later than the wild type, and did not reach the maximum cell density of the wild type (Figure 2.3). However, in the absence of glucose in the medium, CDK25 would not divide under the same light conditions. The results indicated that CDK25 is a photosynthesis-deficient mutant and its growth is more susceptible to photoinhibition than is that of wild type. Shen *et al.* (Shen *et al.*, 1993) recently reported a PSI deletion strain of *Synechocystis* 6803 that was also sensitive to higher light intensity (50 μmol m^{-2} s^{-1}) but was able to grow under photoheterotrophic conditions at 5 μmol m^{-2} s^{-1} (doubling time ≈ 28 hours). A major difference between CDK25 and the PSI deletion strain appears to be that the PSI deletion strain needed about four weeks to go through transition from LAHG condition to continuous light condition, but CDK25 liquid culture needed only one day to grow into log phase during the transition (Fig. 2.3). Moreover, the wild-type strain grew into log phase in the first day of the transition (Fig. 2.3). Our data do not seem to agree

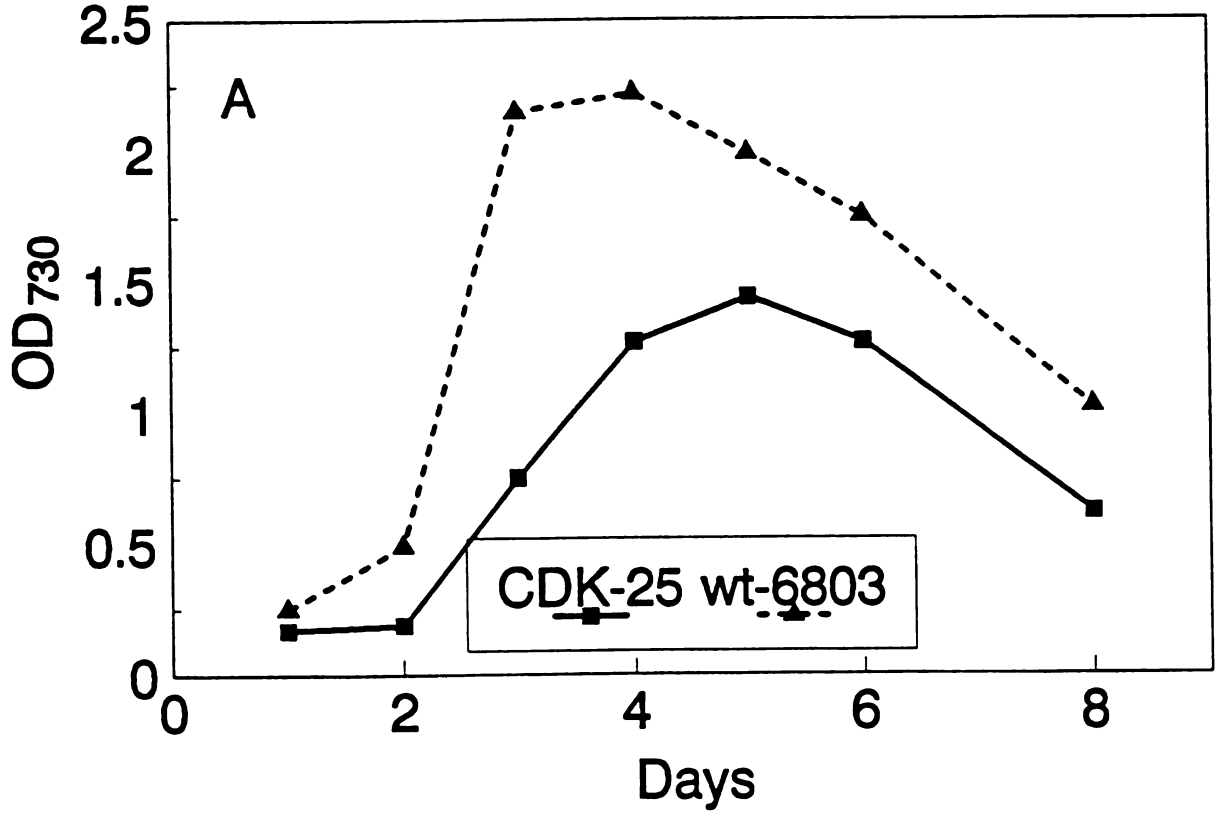

Figure 2.3. Growth of CDK25 and wt-6803 under mixotrophic conditions. Light intensity: 5 $\mu mol\, m^{-2} s^{-1}$. Medium: BG11 + Glucose 5 mM. Kanamycin was added to CDK25 growth medium at 5 mg/l. Starting OD_{730} for both strains were 0.08.

with the speculation (Shen *et al.*, 1993) that under LAHG and continuous dim-light conditions the cells employ dramatically different metabolic pathways, and specific metabolites accumulated to deal with dark growth may be poisonous to cells under continuous dim-light conditions.

Detection of proteins by antibodies

Thylakoid proteins from wild-type and CDK25 cells grown under LAHG conditions were separated by SDS-PAGE, transferred to nitrocellulose, and probed with antibodies raised to PSI proteins and to the D2 protein of PSII (Fig. 2.4). Antibodies raised to *Synechococcus* 7002 PsaC cross-reacted to protein of ≈9 kDa in wild-type sample, but not in CDK25 (panel A). Similarly, antibodies raised to *Nostoc* 8009 PsaD cross-reacted to protein of ≈16 kDa in wild-type sample, but not in CDK25 (panel B); antibodies raised to *Synechocystis* 6803 PsaE reacted to protein of ≈9kDa in the wild-type sample, but not in CDK25. Antibodies raised to *Synechococcus* PsaA/B cross-reacted to adjacent bands with apparent molecular mass of 60-65 kDa in both wild-type and CDK25 samples. This anomalous behavior of the P700-apoproteins in SDS-PAGE, migration at a lower molecular weight than the predicted 83 kDa, has been observed previously and is probably due to the hydrophobic nature of these proteins (Fish *et al.*, 1985). Antibodies raised to *Synechocystis* 6803 PsaF reacted to protein of ≈16kDa in both wild-type and CDK25 samples. Antibodies raised to spinach D2 polypeptide cross-reacted to protein of ≈34 kDa in both wild-type and CDK25 samples, which indicates the assembly of photosystem II is not interrupted in this photosystem I mutant.

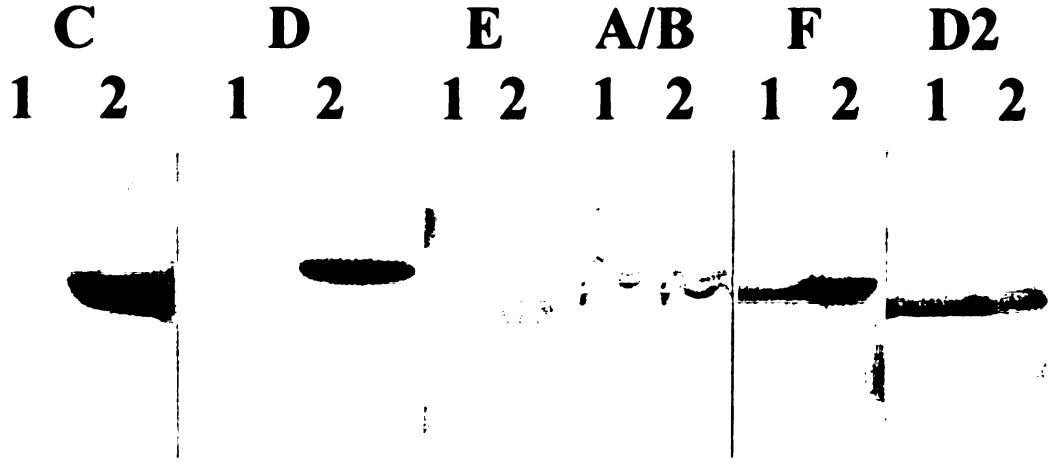

Figure 2.4. Western blot analysis of CDK25. Thylakoid membranes were isolated from LAHG grown cells. SDS-PAGE and immunoblotting were performed as described (Smart *et al.*, 1991). To resolve the PsaA/B proteins, 10% SDS-PAGE gels were used; 17% gels were used to resolve PsaC, PsaD, PsaE and PsaF. D2 protein in photosystem II was resolved with 17% gel to serve as a control. Lane 1: CDK25; lane 2: wt-6803. Protein assays were performed using the method of (Lowry *et al.*, 1951). Equal amounts of protein (150 μg) were loaded in each lane. Antibodies used were against PsaC, PsaD, PsaE, PsaF, PsaA/B and D2.

EPR spectral characterization of CDK25 thylakoid membranes

Figure 2.5a shows a low temperature EPR spectrum of the CDK25 thylakoid membranes after freezing during illumination. The presence of resonances at $g = 2.079$ (partly obscured by the $P700^+$ radical), 1.903 and 1.784, the broad linewidths, and the requirement for high microwave powers and low temperatures are diagnostic of iron-sulfur center F_X. As shown in figure 2.6a, there is no evidence for the presence of iron-sulfur centers F_A or F_B in the CDK25 membranes (Fig. 2.6a). The F_X spectrum differs only slightly from that when PsaC, PsaD and PsaE are removed from a dodecyl maltoside *Synechococcus* sp. PCC 6301 complex using chaotropic agents (Figure 2.5b). Within the limits imposed by the signal to noise ratio, the highfield resonance appears somewhat broader in the CKD25 mutant, and the midfield resonance a $g = 1.903$ in the CDK25 membranes is located upfield at $g = 1.885$ in the P700-$F_X$core. This difference may be species related, or it may be due to the presence of detergents or secondary action of the chaotropic agents. When the CDK25 membranes are frozen in darkness, the resonances at $g = 2.079$, 1.903 and 1.784 appear during illumination and disappear in subsequent darkness, indicating complete reversibility of the signal. This behavior is diagnostic of low temperature electron transfer between P700 and F_X. There are no other signals that can be attributed to F_A or F_B; however, the resonances are about 70% as intense as when the sample is frozen during illumination (data not shown).

When PsaC from *Synechococcus* sp. PCC 7002 and PsaD from *Nostoc* sp. PCC 8009 are added to the thylakoid membranes, resonances at $g = 2.046$, 1.936, 1.922 and 1.880 appear when the sample is illuminated during freezing to 15 K (Figure 2.6b). The resonance at 3440 G is present in all reconstituted PS I complexes, and is probably not derived from either F_A or F_B. The Rieske iron-sulfur center is present at $g = 1.922$, but one or more of the

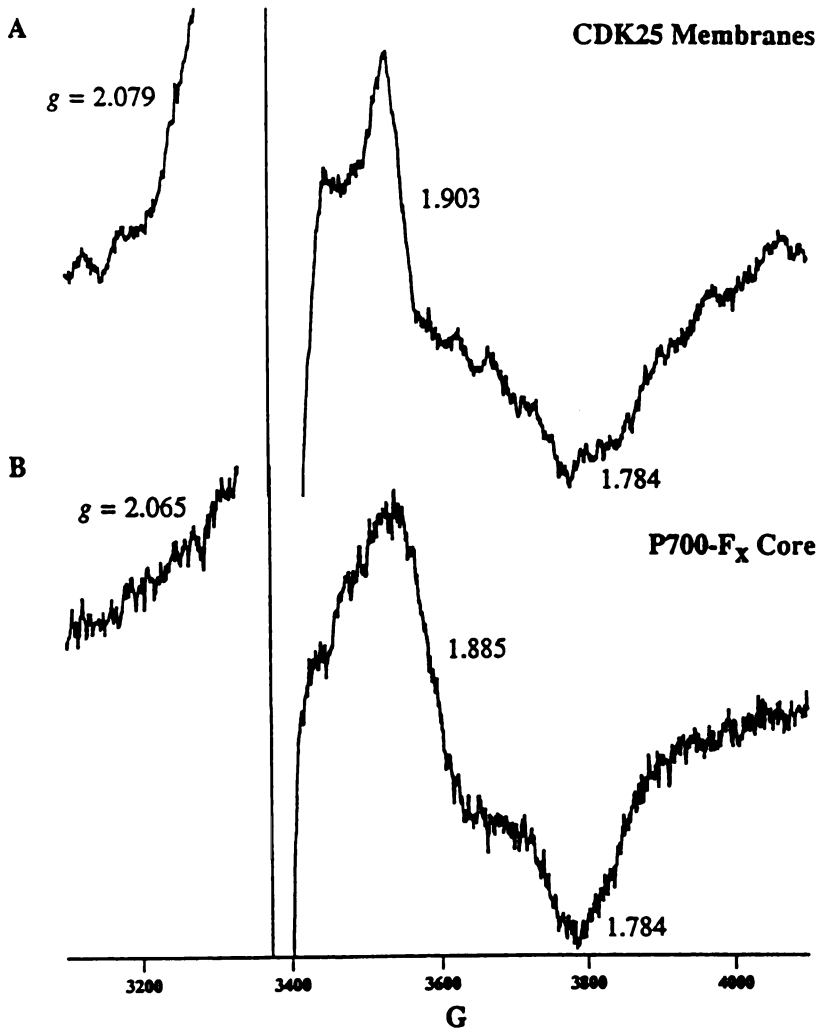

Figure 2.5. EPR spectra for F_X.
2.5a) Electron paramagnetic resonance (EPR) spectrum of the thylakoid membrane of CDK25 under conditions optimal for observing iron-sulfur centers F_X. The sample contained 1.7 mM ascorbate and 0.033 mM DPIP in 50 mM Tris, pH 8.3. The spectrum shown is the difference between a dark frozen sample and one that was frozen during illumination.
2.5b) Electron paramagnetic resonance spectrum of the dodecyl-maloside P700-F_X core isolated from *Synechococcus* sp. PCC 6301. Spectrometer conditions: microwave power, 40 mW; microwave frequency, 9.151 GHz; receiver gain, 2.0×10^4; modulation amplitude, 32 G at 100 kHz, magnetic field, 3600 G with scan width of 1000 G. The temperature was 9 K; the Chl concentration was 200 μg/ml.

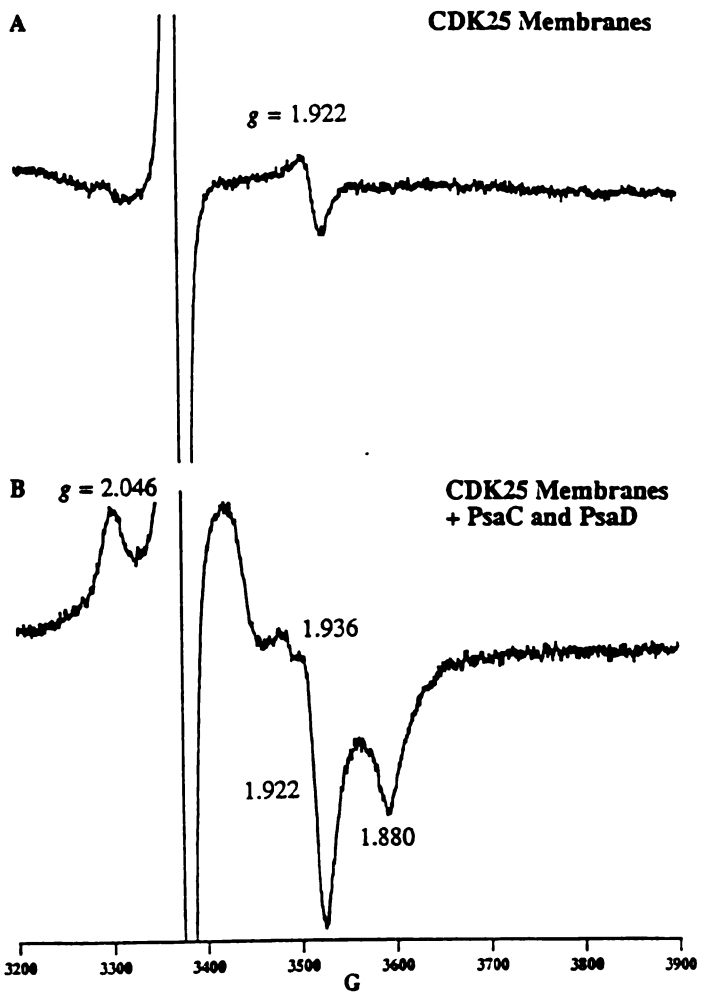

Figure 2.6. EPR spectra for F_A and F_B.
2.6a) Electron paramagnetic resonance (EPR) spectrum of the thylakoid membrane of CDK25 under conditions optimal for observing iron-sulfur centers F_A and F_B. The sample contained 1.7 mM ascorbate and 0.033mM DPIP in 50mM Tris, pH8.3. The spectrum shown is the difference between a dark frozen sample and one that was frozen during illumination. 2.6b) EPR spectrum after the addition of recombinant PsaC from *Synechococcus* sp. PCC 7002 and PsaD from *Nostoc* sp. PCC 8009 to the whole thylakoid membrane of CDK25. The resonances at g= 2.046, 1.936.(1.922), and 1.880 are characteristic of an interaction-type spectrum of F_A^- and F_B^-. Spectrometer conditions: microwave power, 20 mW; microwave frequency, 9.128 GHz; receiver gain, 2.0×10^4; modulation amplitude, 10 G at 100 kHz, magnetic field, 3400 G with scan width of 1000 G. The temperature was 15 K; the Chl concentration was 700 μg/ml Chl. The large derivative-shaped resonance at 3525 G (g = 1.92) is the midfield peak of the Rieske iron-sulfur center.

of the midfield resonances of the F_A^-/F_B^- interaction spectrum also contributes in this region. With the single qualification that the midfield resonances are obscured by the Rieske center, these signals are characteristic of an interaction spectrum of F_A^- and F_B^-. As expected, the F_X spectrum can be observed in the PsaC/PsaD-reconstituted membranes only when F_A and F_B are prereduced prior to illumination. These data indicate that the *in vitro* reconstitution leads to a PS I complex with photochemical properties that are nearly identical to that of the wild-type.

Optical characterization of thylakoid membrane of CDK25

Figure 2.7 shows the flash-induced absorption transient at 698 nm in thylakoid membranes isolated from the CDK25 mutant (solid line) and the theoretical fit (dashed line). The decay of the $P700^+$ transient is biphasic; the two kinetic phases have half-time of 310 μs and 1.048 ms representing 29% and 54% of the total absorption change, respectively (the remaining 17% is a function of the concentration of DPIP). Previously, we reported monophasic decay with a half-time of 1.2 ms in the $P700^+F_X^-$ backreaction from a P700-F_X core isolated from *Synechococcus* sp. PCC 6301 (Parrett *et al.*, 1989). On reexamining these data, we found that the $P700^+$ transient also fits better to two exponentials, with half-times similar to that reported in the CDK25 mutant above. The presence of the two kinetic phases in the P700-F_X core is therefore not a result of damage caused by the use of chaotropic agents. As a consequence, there may be several kinetic components to the backreaction from F_X^-; however, the origin of the heterogeneity is unknown.

The inset shows the point-by-point differences in spectra of the electron donor and acceptor in the CDK25 mutant from 400 to 500 nm. We measured the absorption change at

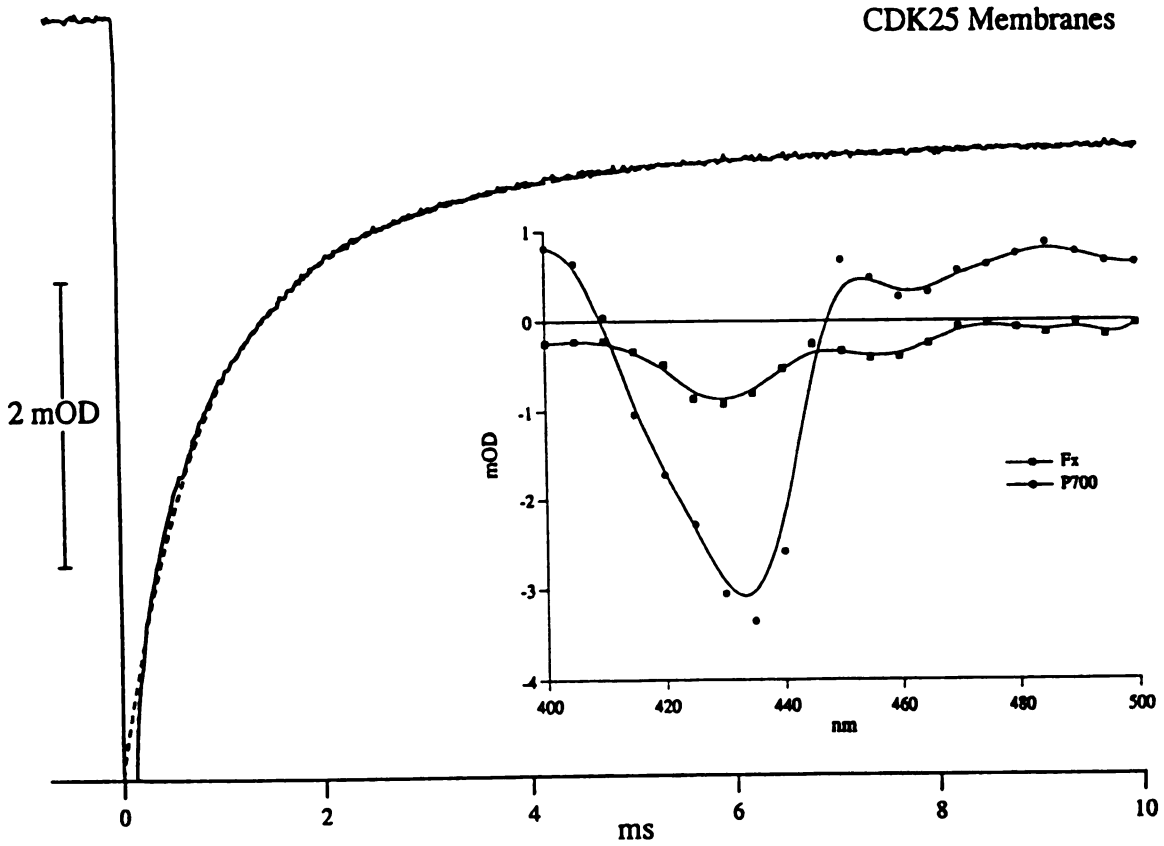

Figure 2.7. Optical spectroscopy for CDK25.

Flash-induced absorption change at 698 nm in thylakoid membranes of CDK25. The measurement was performed at 8.75 μg/ml Chl in 50 mM Tris, pH 8.3, containing 1.7 mM ascorbate and 0.033 mM DPIP. The dashed line represents the curve-fit to a biexponential decay. The deviation between experimental and fit points immediately after the flash represents the settling time of the amplifier due to the use of filtering with a 10 kHz high frequency rolloff.

Inset: Point-by-point difference spectrum of P700/P700$^+$ and F_X/F_X^- in CDK25 thylakoid membranes. The difference spectrum for P700/P700$^+$ (open circles) was obtained on a sample containing 0.033 mM DPIP, 1.7 mM ascorbate and 450 mM methyl viologen. The difference spectrum for F_X/F_X^- (open squares) was obtained by subtracting the absorption change in a sample containing 0.033 mM DPIP, 1.7 mM ascorbate and 450 mM methyl viologen from one lacking methyl viologen. The measurements were performed at 10 μg/ml Chl in 50 mM Tris, pH 8.3.

a single wavelength to obtain the composite absorption change for $P700^+ F_X^-$, then added methyl viologen to obtain only the $P700^+$ absorption change. The difference between the two samples is the absorption change due to the electron acceptor. The negative-going absorption change from 400 to 500 nm, with the broad peak at 430 nm is characteristic of the weak charge-transfer bands of an iron-sulfur cluster. The two kinetic phases show the same spectrum from 400 to 500 nm, hence, only the composite is shown. In sum, the kinetics and the spectral properties are compatible with the identity of the room temperature electron acceptor as F_X.

The addition of recombinant PsaC from *Synechococcus* sp. PCC 7002 and recombinant PsaD from *Nostoc* sp. PCC 8009 to CDK25 thylakoid membrane leads to the replacement of the 1.2 ms backreaction with a long-lived kinetic transient (not shown). The decay of this transient shows a dominant phase with a half-time of about 30 ms, and the minority phase with a half-time that depends on the concentration of DPIP. The 30 ms transient is characteristic of the $P700^+[F_A/F_B]^-$ backreaction, and indicates that the room temperature electron flow is re-established to the terminal iron-sulfur clusters by the addition of PsaC and PsaD.

In summary, the EPR and optical spectral characterizations clearly show that the terminal electron acceptor in CDK25 is iron-sulfur center F_X. This agrees with the molecular and biochemical data, which indicate that the mutant lacks PsaC, and as a consequence, F_A and F_B. The data show that an intact F_X cluster is able to form and function in *Synechocystis* sp. PCC 6803 in the absence of the PsaC and PsaD.

Discussion

Assembly of the PSI core (PsaA-PsaB dimer) is independent of PsaC, PsaD and PsaE subunits in Synechocystis 6803

In this study we inactivated the *psaC2* gene by inserting a Km^R cassette into its coding region, thus creating a PsaC deletion mutant in *Synechocystis* 6803. The mutant CDK25 lacked the PsaC, PsaD and PsaE subunits in the thylakoid membrane, and thus lacked the F_A and F_B iron-sulfur clusters. However, the PsaA/PsaB dimer assembled in thylakoid membranes in the absence of PsaC; and primary electron donor P700 and electron carriers A_0, A_1, and F_X inserted and were functional in the PsaC-PsaD-PsaE minus photosystem I complex. Evidence supporting this finding includes (a) the presence of PsaA/B polypeptides detected through immunoblot analysis (Fig 2.4), (b) EPR and time-resolved optical spectroscopic data showing formation of $P700^+$ and F_X^- (Fig 2.5), and (c) *in vitro* reconstitution of CDK25 thylakoid membrane with PsaC and PsaD proteins restores near wild-type PSI EPR signals (Fig 2.6). PsaF was also present in CDK25 thylakoid membranes, suggesting its incorporation into PSI is also independent of PsaC, PsaD, and PsaE. It was observed in an *in vitro* reconstitution experiment that PsaD and PsaE did not bind to the PSI core in the absence of the PsaC holoprotein (Li *et al.*, 1991a). Assembly of PsaA/B dimer in the absence of PsaC was also reported in another cyanobacterium, *Anabaena variabilis* (Mannan *et al.*, 1991), in which it was also found that the PsaC is necessary for the stable association of the PsaD and PsaE in PSI complex (Mannan *et al.*, 1994). But in green alga *Chlamydomonas reinhardtii*, inactivation of the *psaC* gene prevented stable assembly of all other PSI subunits into the thylakoid membrane (Takahashi *et al.*, 1991). The contrasting results between cyanobacteria and green alga suggest an intrinsic difference in subunit interaction and PSI biogenesis in

these different organisms.

Assembly of PsaD and PsaE into the PSI complex is dependent on PsaC

When PsaC was absent in *Synechocystis* 6803, the PsaD and PsaE subunit could not stably assemble into the thylakoid membrane, even though PsaA/B and PsaF subunits did so. PsaD is proposed to be located at the cytoplasmic side of the PSI complex, functions to bind ferredoxin, and is required for stable binding of PsaC to the reaction center core in *in vitro* reconstitution experiments (Li *et al.*, 1991b). In the presence of PsaC, reconstitution experiments also showed that the PsaD and PsaE proteins rebind to the PSI core, but there is little or no rebinding of either PsaD or PsaE in the absence of the F_A/F_B iron-sulfur clusters (Li *et al.*, 1991b). These results indicate that binding of PsaD and PsaE to the PSI core is mediated by PsaC. A reasonable speculation might be that the binding of PsaC induced a conformational change in PsaA/B, thus providing the binding sites for PsaD and PsaE.

psaC1

Two different *psaC* genes have been reported in *Synechocystis* 6803. In this study we demonstrate that the *psaC2* gene encodes the PsaC subunit in PSI. When *psaC2* is inactivated, no PsaC polypeptide is found in the thylakoid membrane, which shows that the *psaC1* does not encode a PsaC protein. Moreover, the protein it encodes, if any, cannot substitute PsaC function. We did not find any transcription from *psaC1* (data not shown). However, efforts to inactivate *psaC1* were not successful (Anderson and McIntosh, unpublished results).

The deduced amino acid sequence of *psaC1* more closely resembles PsaC sequences of higher plants than of cyanobacteria. It is identical to the tobacco PsaC sequence. At the

nucleotide level, the *psaC1* sequence is 93% identical to the tobacco sequence (Anderson and McIntosh, 1991b), but only 75% to *psaC2* (Steinmüller, 1992). The *psaC1* flanking sequences resemble *ndhD* and *ndhE* sequences, respectively, of higher plants, and the gene organization is conserved relative to that in chloroplast genomes. It is possible that the *psaC1* gene and its flanking regions were derived from a transformation of *Synechocystis* 6803 with higher plant chloroplast DNA, before the strain was isolated (Steinmüller, 1992). Our results are consistent with this speculation, and further suggest the *psaC1* is a pseudogene in the *Synechocystis* 6803 genome. Why this sequence is maintained in the cyanobacterial genome remains unknown.

Acknowledgments

I thank L. Smart for helping me start this work. The EPR and optical spectrocopy was performed by Y.-S. Jung in J. Golbeck lab. I thank N. Bowlby for helpful advice. Gift of antibodies from J. Guikema, P. Chitnis, and W. Vermaas is appreciated. I also wish to thank K. Steinmüller for the generous gift of *psaC2* and helpful discussions.

References

Anderson SL, McIntosh L (1991a) Light-activated heterotrophic growth of the cyanobacterium *Synechocystis* sp. strain PCC 6803: a blue-light-requiring process. *J Bacteriol* **173**: 2761-2767 .

Anderson SL, McIntosh L (1991b) Partial conservation of the 5'*ndhE-psaC-ndhD* 3' gene arrangement of chloroplasts in the cyanobacterium *Synechocystis* sp. PCC 6803: implications for NDH-D function in cyanobacteria and chloroplasts. *Plant Mol Biol* **16**: 497-499.

Chitnis VP, Xu Q, YU L, Golbeck JH, Nakamoto H, Xie DL, and Chitnis PR (1993) Targeted inactivation of the gene *psaL* encoding a subunit of photosystem I of the cyanobacterium *Synechocystis* sp PCC 6803. *J Biol Chem* **268**: 11678-1168.

Feinberg AP and Vogelstein B (1983) A technique for radiolabelling DNA restriction endonuclease fragments to high specific activity. *Anal Biochem* **132**: 6-13.

Fish LE, Kück U, and Bogorad L (1985) Two partially homologous adjacent light-inducible maize chloroplast genes encoding polypeptides of the P700 chlorophyll *a*-protein complex of photosystem I. *J Biol Chem* **260**: 1413-1421.

Golbeck JH (1992) Structure and function of photosystem I. *Annu Rev Plant Physiol Plant Mol Biol* **43**: 293-324.

Golbeck JH (1994) Photosystem I in Cyanobacteria. In Bryant DA (ed), The Molecular Biology of Cyanobacteria. Kluwer Academic Publishers, Dordrecht, Netherlands. pp. 179-220.

Henry RL, Li M, and Guikema JA (1990) A comparison of the PSI polypeptide organization on soybean and the cyanobacterium, *Anacystis nidulans.* In Baltscheffsky M(ed), Current Research in Photosynthesis, Vol. II. Kluwer Academic Publishers, Dordrecht, Netherlands. pp.567-570.

Høj PB, Svendsen I, Scheller HV, and Møller BR (1987) Identification of a chloroplast-encoded 9-kDa polypeptide as a 2[4Fe-4S] protein carrying centers A and B of photosystem I. *J Biol Chem* **262**: 12676-12684.

Jansson C, Debus RJ, Osiewacz HD, Gurevitz M, and McIntosh L (1987) Construction of an obligate photoheterotrophic mutant of the cyanobacterium *Synechocystis* 6803. *Plant Physiol* **85**: 1021-1025.

Li N, Warren PV, Golbeck JH, Frank G, Zuber H, and Bryant DA (1991a) Polypeptide composition of the photosystem I complex and the photosystem I core protein from *Synechococcus* sp. PCC 6301. *Biochim Biophys Acta* **1059**: 215-225.

Li N, Zhao J, Warren PV, Warden JT, Bryant DA, and Golbeck JH (1991b) PsaD is required for the stable binding of PsaC to the photosystem I core protein of *Synechococcus* sp. PCC 6301. *Biochemistry* **30**: 7863-7872.

Lichtenthaler HK (1987) Chlorophylls and carotenoids: pigments of photosynthetic biomembranes. *Methods Enzymol* **148**: 350-382.

Lowry OH, Rosebrough NJ, Farr AL, and Randall RJ (1951) Protein measurement with the folin phenol reagent. *J Biol Chem* **193**: 265-275.

Mannan RM, Pakrasi HB, and Sonoike K (1994) The PsaC protein is necessary for the stable association of the PsaD, PsaE, and PsaL proteins in the photosystem I complex: analysis of a cyanobacterial mutant strain. *Arch Biochem Biophys* **315**: 68-73.

Mannan RM, Whitmarsh J, Nyman P, and Pakrasi HB (1991) Directed mutagenesis of an iron-sulfur protein of the photosystem I complex in the filamentous cyanobacterium *Anabaena variabilis* ATCC 29413. *Proc Natl Acad Sci USA* **88**:10168-10172.

Noren GH, Boerner RJ, and Barry BA (1991) EPR characterization of an oxygen-evolving photosystem II preparation from the transformable cyanobacterium *Synechocystis* 6803. *Biochemistry* **30**: 3943-3950.

Oh-oka H, Takahashi Y, Kuriyama K, Saeki K, and Matsubara H (1988) The protein responsible for center A/B in spinach photosystem I: isolation with iron-sulfur cluster(s) and complete sequence analysis. *J Biochem* **103**: 962-968.

Oka A, Sugisaki H, and Takanami M (1981) Nucleotide sequence of the kanamycin resistance transposon *Tn*903. *J Mol Biol* **174**: 217-226.

Parrett KG, Mehari T, Warren PV, and Golbeck JH (1989) Purification and properties of the intact P700 and F_X-containing photosystem I core protein. *Biochim Biophys Acta* **973**: 324-332.

Sambrook J, Fritsch EF, and Maniatis T (1989) Molecular Cloning: A Laboratory Manual. Cold Spring Harbor, New York: Cold Spring Harbor Laboratory Press.

Shen G, Boussiba S, and Vermaas WFJ (1993) *Synechocystis* sp PCC 6803 strains lacking photosystem I and phycobilisome function. *Plant Cell* **5**: 1853-1863.

Smart LB, Anderson SL, and McIntosh L (1991) Targeted genetic inactivation of the photosystem I reaction center in the cyanobacterium *Synechocystis* sp PCC 6803. *EMBO J* **10**:3289-3296.

Smart LB, Warren PV, Golbeck JH, and McIntosh L (1993) Mutational analysis of the structure and biogenesis of the photosystem I reaction center in the cyanobacterium

Synechocystis sp PCC 6803. *Proc Natl Acad Sci USA* **90**: 1132-1136.

Steinmüller K (1992) Identification of a second *psaC* gene in the cyanobacterium *Synechocystis* sp PCC 6803. *Plant Mol Biol* **20**: 997-1001.

Takahashi Y, Goldschmidt-Clermont M, Soen SY, Franzen, and Rochaix JD (1991) Directed chloroplast transformation in *Chlamydomonas reinhardtii:* insertional inactivation of the *psaC* gene encoding the iron sulfur protein destabilizes photosystem I. *EMBO J* **10**: 2033-2040.

Vermaas WFJ, Ikeuchi M, and Inoue Y (1988) Protein composition of the photosystem II core complex in genetically engineered mutants of the cyanobacterium *Synechocystis* sp PCC 6803. *Photosynth Res* **17**: 97-113.

Vieira J and Messing J (1982) The pUC plasmids, an M13mp7-derived system for insertion mutagenesis and sequencing with synthetic universal primers. *Gene* **19**: 259-268.

Warren PV, Smart LB, McIntosh L, and Golbeck JH (1993) Site-directed conversion of cysteine-565 to serine in PsaB of photosystem I results in the assembly of [3Fe-4S] and [4Fe-4S] clusters in F_X. A mixed-ligand [4Fe-4S] cluster is capable of electron transfer to F_A and F_B. *Biochemistry* **32**: 4411-4419.

Williams JGK (1988) Construction of specific mutations in photosystem II photosynthetic reaction center by genetic engineering methods in *Synechocystis* 6803. *Methods Enzymol* **167**: 766-778.

Wynn RM and Malkin R (1988) Interaction of plastocyanin with photosystem I: a chemical cross-linking study of the polypeptide that binds plastocyanin. *Biochemistry* **27**: 5863-5869.

Yu L, Zhao J, Mühlenhoff, Bryant DA, and Golbeck JH (1993b) PsaE is required for *in vivo* cyclic electron flow around photosystem I in the cyanobacterium *Synechococcus* sp. PCC 7002. *Plant Physiol* **103**: 171-180.

Zilber AL and Malkin R (1988) Ferredoxin cross-links to a 22kD subunit of photosystem I. *Plant Physiol* **88**: 810-814.

Chapter 3

STRAINS OF *SYNECHOCYSTIS* SP. PCC 6803 WITH ALTERED PsaC. I. MUTATIONS INCORPORATED IN THE CYSTEINE LIGANDS OF THE TWO [4FE-4S] CLUSTERS F_A AND F_B OF PHOTOSYSTEM I

A modified form is in press (JBC) as Jianping Yu, Ilya R. Vassiliev, Yean-Sung Jung, John H. Golbeck and Lee McIntosh

Introduction

Photosystem I (PS I) functions as a plastocyanin:ferredoxin oxidoreductase in the thylakoid membranes of chloroplasts. In cyanobacteria, cytochrome c_6 and flavodoxin serve as alternate donors and acceptors under conditions of low copper and low iron. The PS I complex contains the photosynthetic pigments, the primary donor P700, and five electron transfer centers (A_0, A_1, F_X, F_A, and F_B) that are bound to the PsaA, PsaB, and PsaC proteins. In cyanobacteria, the PS I complex contains at least eight other polypeptides (Chitnis *et al.*, 1995). The cofactors of PS I participate in electron transport across the membrane, oxidizing plastocyanin and reducing ferredoxin according to the following sequence: plastocyanin (Cu) or cytochrome c_6 (heme) → P700 (Chl *a* dimer) →A_0(Chl *a*)→A_1 (phylloquinone)→ F_X (a [4Fe-4S] cluster)→ F_A or F_B ([4Fe-4S] clusters)→ ferredoxin ([2Fe-2S] cluster) or flavodoxin (flavin).

The PsaC subunit, encoded by the *psaC* gene, provides the ligands for two [4Fe-4S] clusters, F_A and F_B. Previous studies showed that the introduction of aspartic acid in position 14 (C14D) and in position 51 (C51D) led to the introduction of [3Fe-4S]

and mixed-ligand [4Fe-4S] clusters in the modified F_B and F_A sites, respectively, of *Escherichia coli*-expressed PsaC proteins (Yu L. *et al.*, 1993). However, when the mutant PsaC proteins were rebound to P700-F_X cores, only mixed-ligand [4Fe-4S] iron-sulfur clusters were found in the modified sites of the reconstituted C14D-PS I (Yu *et al.*, 1995a) and C51D-PS I (Yu *et al.*, 1995b) complexes. In both mutant PS I complexes, electrons could be transferred to the mixed-ligand iron-sulfur cluster at 15 K, and room temperature $NADP^+$ photoreduction was supported at rates similar to the wild-type.

The formation of mixed-ligand [4Fe-4S] clusters with altered spectral and redox properties *in vitro* provided a rationale for probing the functions of F_A and F_B *in vivo*. The ability to support [4Fe-4S] clusters which are able to transfer electrons at both 15 K and 298 K suggests that the putative oxygen-ligated iron-sulfur clusters should be functional in living organisms. The step taken in this work is to move mutations in these ligands into a genetic system such as *Synechocystis* sp. PCC 6803 and to study the *in vivo* consequences on growth and electron transfer. Unlike other cyanobacteria, two different *psaC* genes have been reported in *Synechocystis* sp. PCC 6803. One (*psaC*1) (Anderson and McIntosh, 1991a) has a deduced amino acid sequence identical to that of tobacco, while the other (*psaC2*) (Steinmüller, 1992) has a deduced amino acid sequence similar to those reported for other cyanobacteria. The *psaC1* gene is not involved in PS I, nor can it substitute for *psaC2* when the latter is insertionally inactivated. The amino acid sequence of *Synechocystis* sp. PCC 6803 PsaC matched that predicted from *psaC2* (J. Golbeck, personal communication). Insertional inactivation of *psaC2* prevented the formation of PsaC, thus demonstrating that this gene encodes the PS I-bound polypeptide. Further work showed that the PsaC polypeptide is necessary for stable assembly of PsaD and PsaE into PS I complex *in vivo*, and that PsaC, PsaD and PsaE are not needed for assembly of PsaA/PsaB dimer and electron transport from P700 to F_X (Chapter 2). In this chapter the term *psaC* refers to the gene *psaC2*.

Site-directed mutagenesis and transformation of *Synechocystis* sp. PCC 6803 has

been used successfully in the study of PS I biogenesis and function (Smart *et al.*, 1993; Warren *et al.*, 1993). In the work presented here, a set of strains with mutations in PsaC has been created in which a cysteine ligand to F_A and/or F_B is substituted by aspartate, serine or alanine in positions 14 and/or 51 as shown in figure 3.1. The genetic, physiological, and biochemical characterization of the PS I mutants will be presented. Chapte 4 will describe the EPR and optical kinetic properties of the mixed-ligand F_A and F_B clusters in site-modified PS I complexes.

Materials and Methods

Strains and Growth Conditions

Experiments were performed using a glucose-tolerant strain of *Synechocystis* sp. PCC 6803, which was acclimated for growth on solid medium in the dark. Except for tests for photoautotrophic and mixotrophic growth, cells were grown at 30°C under light-activated heterotrophic growth (LAHG) conditions, as previously described (Anderson and McIntosh, 1991b). Antibiotics were added in the following concentrations: kanamycin (Km), 5 mg/liter; gentamicin (Gm), 1mg/liter. Transformations were performed essentially as described (Williams, 1988), except in the case of strain ΔC-RCPT, which was carefully maintained in dim light (5 μmol m^{-2} s^{-1} during 2 hour incubation) throughout the procedure, since it is light-sensitive (its mixotrophic growth in the presence of glucose is inhibited at white light greater than 10 μmol m^{-2} s^{-1}). Tests for photoautotrophic and mixotrophic growth were performed using solid media with or without supplemental glucose in a chamber providing continuous light. Cool white fluorescent bulbs made by General Electric were used. The light intensity was varied by covering plates with layers of cheese cloth and were monitored using a L1-185A photometer (LICOR, Lincoln, NE). Large cultures were grown in carboys (15 l) under LAHG conditions and were bubbled with air.

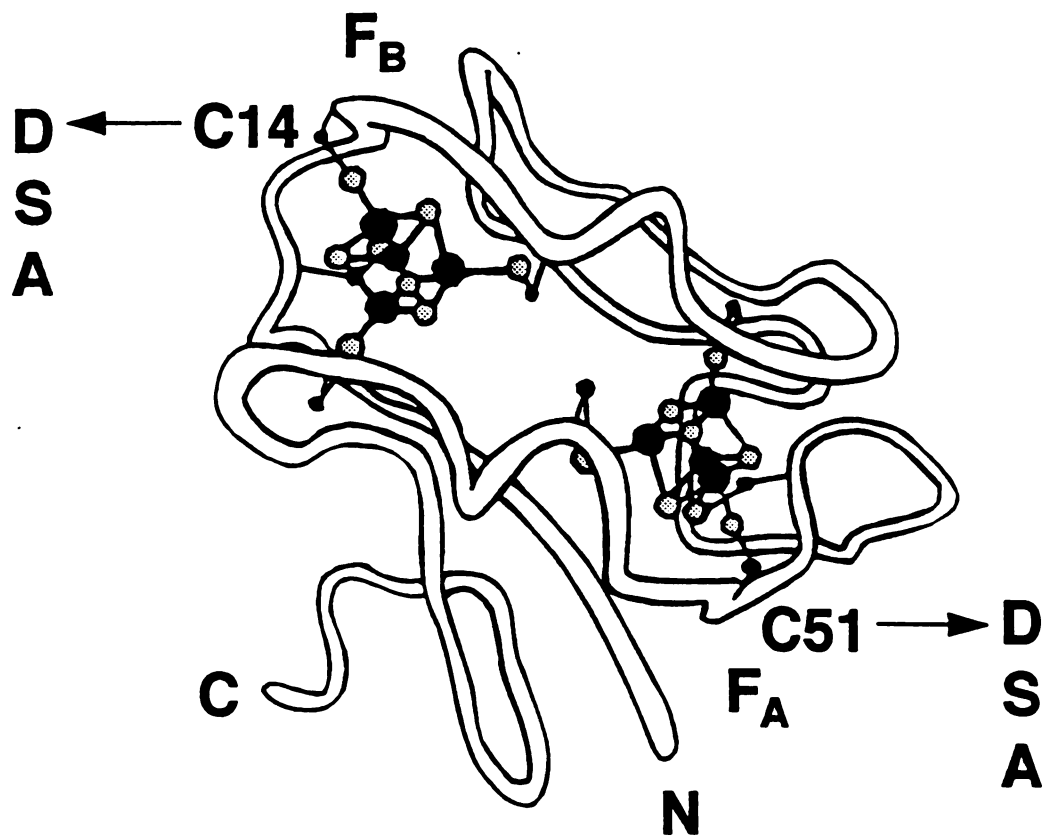

Figure 3.1. Predicted structure of PsaC. Based on its sequence similarity with bacterial ferredoxin, showing identity of FA and FB relative to their cysteine ligands C51 and C14, which were changed to aspartate, serine, or alanine in this work. Modified from Golbeck (1994)

DNA Manipulations

Nucleic acids were manipulated using standard methodology (Sambrook *et al.*, 1989), unless otherwise stated. Site-directed mutagenesis was performed using an oligonucleotide-directed *in vitro* mutagenesis kit as directed by the manufacturer (Amersham, Arlington Heights, IL). For amplification of psaC gene from cyanobacterial strains, cells picked from a medium-size colony or equivalent amount of cells collected from liquid culture were washed once with water and used as template. Amplification products were purified using a PCR purification kit (Promega Corporation, Madison, WI). Procedure for preparation of cyanobacterial DNA was adapted from Ohad and Hirschberg (1992), with two "loopfuls" of cells scraped from plates or cells from 10 ml liquid culture being used to extract DNA.

Transformation of Synechocystis *6803 and Selection Conditions*

Synechocystis sp. PCC 6803 that had been maintained under LAHG conditions for at least two subcultures (cells were subcultured once a week) was transformed with plasmids containing resistance genes to kanamycin or gentamycin. Selection for antibiotic-resistant colonies was performed under LAHG conditions. Resistant colonies were restreaked to single colonies with at least five serial transfers to obtain full segregation of the mutation, as verified by restriction enzyme analysis of PCR products, direct sequencing of PCR products, Southern hybridizations, and growth tests.

Western Blot Analysis of Thylakoid Membrane Proteins

Thylakoid membranes were isolated and SDS-PAGE and immunoblotting were performed as described (Smart and McIntosh, 1991). To resolve the PsaA/PsaB proteins, 10% SDS-PAGE gels were used; 17% gels were used to resolve PsaC, PsaD, PsaE and PsaF. D2 protein in Photosystem II (PS II) was resolved with 17% gel to serve as a control. Protein assays were performed using the method of Lowry *et al.* (1951). Equal

amounts of protein (150 μg) was loaded in each lane for thylakoid preparations and equal amounts of chlorophyll (4 μg) were loaded in each lane for PS I complexes. Rabbit antiserum to PsaC or PsaD were raised using protein purified from strains of *E. coli* expressing, respectively, the *psaC* gene from *Synechococcus* sp. PCC 7002 or the *psaD* gene from *Nostoc* sp. PCC 8009 (Li *et al.*, 1991b). Antibodies against PsaA/B proteins from *Synechococcus* were raised in rabbits as previously described (Henry *et al.*, 1992). Antibodies against PsaE and PsaF (gifts from Dr. Parag Chitnis, Kansas State University) were raised in rabbits immunized with PsaE and PsaF purified from *Synechocystis* sp. PCC 6803. Rabbit antibodies to the D2 polypeptide from spinach (gifts from Dr. Wim Vermaas, Arizona State University) were raised as described (Vermaas *et al.*, 1988). Chlorophyll was extracted with methanol and quantified using published extinction coefficients (Lichtenthaler, 1987).

Oxygen Evolution

LAHG-grown cells were washed once in 40 mM HEPES buffer, pH 7.0 and cells containing 10 μg Chl were resuspended in 1 ml of the same buffer and illuminated by saturating light at 25°C. Rates of oxygen evolution were determined with a Rank-type oxygen electrode unit. Whole-chain electron transport was measured in the presence of 10 mM $NaHCO_3$. PS II electron transport was measured in the presence of 1 mM 2,6-dichloro-*p*-benzoquinone.

Membrane Isolation and Purification of PS I Complex

Thylakoid membranes from *Synechocystis* sp. PCC 6803 were isolated using a modification of the procedure described in Yu *et al.* (1995). The cells were suspended in 0.8 M sucrose, 50 mM HEPES buffer, pH 7.8 and pelleted by centrifugation. The cells were washed twice and suspended in the same buffer containing 0.8 M sucrose and protease inhibitors. The cells were broken in 10 cycles of a pre-chilled bead-beater

(Biospec Products, Bartelsville, OK); one cycle consisted of a 45 sec 'on phase' and a 10 min 'off phase'. The cell solution was removed from the beads by vacuum suction and centrifuged at r_{av} of 5,000 x g to remove unbroken cells. Thylakoid membranes in the supernatant was then pelleted by ultracentrifugation at 100,000 x g with repetitive washing. The thylakoid membranes were suspended in 50 mM Tris, pH 8.3, frozen in liquid nitrogen, and stored at -95°C. *n*-Dodecyl ß-D-maltoside-PS I (DM-PS I) complexes were isolated using the protocol described in Chitnis and Chitnis (1993) with minor modifications. The membranes were solubilized in 1% *n*-dodecyl ß-D-maltoside (DM, Calbiochem, La Jolla, CA) at 4°C for 1 h at the Chl concentration of 0.5 mg ml^{-1}. DM-PS I complexes were isolated from the lower green zone of PS I trimers which appeared after centrifugation of the solubilized membrane suspension loaded in a sucrose density gradient (0.1 M to 1.0 M sucrose) for 24 h at 4°C. In the alanine and double aspartate mutants, a mixture of PS I monomers and trimers was used because it was difficult to completely separate the lower and the upper bands. The problem is that PsaL is easily lost in the presence of 1% DM at 0.4 mg Chl/ml due to the absence of PsaD (Mannan *et al.*, 1991). Even though the lower part of the broad band containing mostly PS I trimers was used (containing <10% of the total Chl), there was nonetheless some contamination by PS I monomers. Isolated PS I complexes were dialyzed in 50 mM Tris, pH 8.3, resuspended with the same buffer containing 15% glycerol and 0.03% DM, frozen as small aliquots in the liquid nitrogen, and stored at -95°C.

Steady State Reductase Activity

The steady state reductase activities of PS I complexes were measured according to Jung *et al.* (1995). The absorbance kinetics were measured using a Cary 219 spectrophotometer with the photomultiplier shielded by appropriate narrow band and interference filters. The sample was illuminated from both sides using two banks of high intensity, LEDs emitting at ca. 660 nm (LS1, Hansatech Ltd.). The light intensity was

saturating at the chlorophyll concentration used.

Rates of flavodoxin photoreduction were measured in a 1.3-ml volume using 15 μM flavodoxin and DM-PS I at 5 μg ml^{-1} of Chl in 50 mM Tricine, pH 8.0, 50 mM $MgCl_2$, 15 μM cytochrome c_6 from *Spirulina maxima*, 6 mM sodium ascorbate, 0.05% DM. The measurement was made by monitoring the rate of change in the absorption of flavodoxin at 467 nm.

Rates of flavodoxin-mediated $NADP^+$ photoreduction were measured in a 1.3-ml volume using 15 μM flavodoxin and 0.8 μM spinach ferredoxin:$NADP^+$ oxidoreductase (FNR, Sigma), and DM-PS I at 5 μg ml^{-1} of chlorophyll in 50 mM Tricine, pH 8.0, 10 mM $MgCl_2$, 15 μM cytochrome c_6 from *Spirulina maxima*, 6 mM sodium ascorbate, 0.05% DM, 0.5 mM $NADP^+$, 0.1% ß-mercaptoethanol. Rates of ferredoxin-mediated $NADP^+$ photoreduction were measured in a 1.3-ml volume using 5 μM spinach ferredoxin and 0.8 μM spinach ferredoxin:$NADP^+$ oxidoreductase (FNR, Sigma), and DM-PS I at 5 μg ml^{-1} of chlorophyll in 50 mM Tricine, pH 8.0, 10 mM $MgCl_2$, 15 μM cytochrome c_6 from *Spirulina maxima*, 6 mM sodium ascorbate, 0.05% DM, 0.5 mM $NADP^+$, 0.1% ß-mercaptoethanol. The flavodoxin was purified from the a strain of *E. coli* containing the gene by DEAE-Sepharose CL 6B and Sephadex G-75 (both, Sigma) (Mühlenhoff *et al.*, 1996a and 1996b). $NADP^+$ reduction were measured by monitoring the rate of change in the absorption of NADPH at 340 nm.

Time-Resolved Optical Absorption Spectroscopy

Transient absorbance changes of P_{700} at 820 nm (ΔA_{820}) were measured from the microseconds to tens-of-seconds time domain with a laboratory-built double-beam spectrometer as described in Vassiliev *et al.* (1995) upon excitation with a frequency-doubled Nd-YAG laser with a flash energy of 250 mJ. The decay transients were fitted to 'sum of several exponentials with baseline' using the Marquardt algorithm in Igor Pro. The user-defined fit function enabled a fit up to 7 exponentials with all amplitudes and rate

constants set free during the fit. In most cases the fit comprised a baseline component accounting for long-term phases and/or possible drift of signal zero during long time scale acquisition. The quality of the fit was estimated using standard techniques including analyses of the residuals plots and comparison of the chi-square values and standard errors of the fit parameters between different fits. Using this approach, the PS I backreactions can be compared visually on a log time scale, and the ratio between the different pathways that contribute to the backreactions with $P700^+$ can be estimated on the right abscissa.

Results

Genetic Characteristics of the PS I Mutants

Construction and Characterization of ΔC-RCPT

To allow rapid segregation of mutations in the *psaC* gene, a recipient strain of *Synechocystis* sp. PCC 6803 was engineered with the *psaC* coding region deleted and replaced by a kanamycin resistant (Km^R) cassette (Fig. 3.2A). PCR-amplified *psaC* upstream (454bp) and downstream (208bp) flanking regions, with linker sequences for *BamH*I and *EcoR*I at either end, were cloned into pUC118 (Vierra and Messing, 1982). A Km^R cassette excised from pUC4K (Taylor and Rose, 1988) using *EcoR*I, was inserted into the *EcoR*I site that separated the upstream and downstream flanking regions to form the plasmid pUC118-ΔC. Glucose-tolerant but otherwise wild-type *Synechocystis* sp. PCC 6803 was transformed with pUC118-ΔC, and Km^R colonies were selected under LAHG conditions and were genetically verified by Southern hybridization using a 1.5-kb *EcoR*I-*Nco*I fragment containing *psaC* as probe, and by PCR. Complete segregation of the deletion mutation was confirmed (data not shown).

psaC *Mutagenesis and Genetic Characterization of the Mutants*

Plasmids for site-directed mutagenesis were constructed *in vitro* and manipulated in *E. coli*. A 1.5-kb *EcoR*I-*Nco*I fragment containing *psaC* was cut out of the plasmid

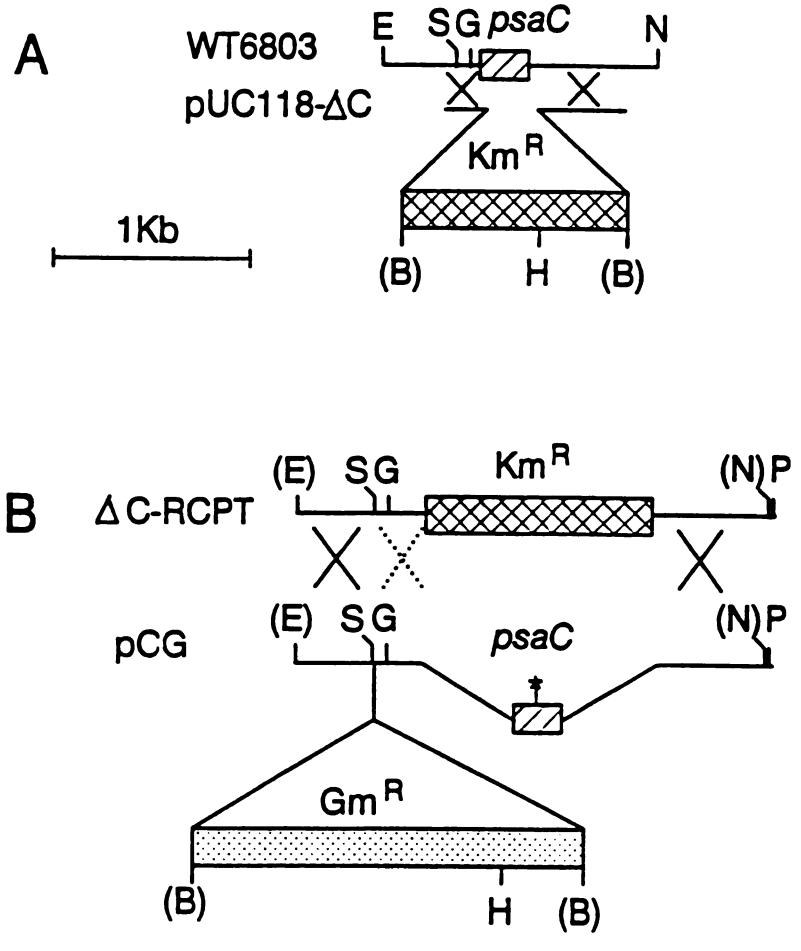

Figure 3.2. PsaC Mutagenesis strategy. (A) Creation of a ΔC-RCPT. (B) Introduction of *psaC* mutations. See text for details. Restriction sites: B, *Bam*HI; E, *Eco*RI; G, *Bgl* II; H, *Hind* III; N, *Nco*I; P, *Pst*I; S, *Bbs* I. Restriction sites in parenthesis on a plasmid have been inactivated.

p6.1S3.5I (Steinmüller, 1992) and cloned into pUC119 (Vierra and Messing, 1982) at the *Sma*I site to create plasmid pC. A 2.0-kb gentamicin resistance (Gm^R) cassette, cut with *BamH*I from pUC119-gen (Smart *et al.*, 1994) was inserted at the *Bbs*I site downstream of *psaC* gene on pC to create plasmid pCG. Single-stranded DNA of pC was used as template for site-directed mutagenesis. Oligonucleotides were designed to effect the desired changes in the coding sequence, while also destroying an endonuclease restriction site (*Rsa*I for the C14 site and *Bbv*I for the C51 site). The resulting change in digestion pattern serves as an effective and simple means of screening for the desired mutation. After verification of the mutations on pC using restriction mapping and DNA sequencing, a 953-bp *Bgl*II-*Pst*I fragment containing the *psaC* mutation was excised from pC and ligated with a 5.7-kb partial digestion product from pCG devoid of the corresponding fragment to form pCG with a mutated *psaC* gene. The mutated pCG plasmids were checked by restriction mapping and DNA sequencing to verify the presence of the desired mutations and of the proper sequences. Taking advantage of an *Xba*I site between the C14 site and the C51 site, pCG with a double mutation C14D/C51D was created by ligating a 758-bp *Xba*I-*Xba*I fragment from pCG with a single mutation C14D and a 5.9-kb *Xba*I-*Xba*I fragment from pCG with a single mutation C51D. Plasmid pCG with wild type *psaC* and its mutated variants (shown as an asterisk on *psaC*) were then used to transform the strain ΔC-RCPT (Fig. 3.2B). Gm^R colonies were selected under LAHG conditions and were genetically characterized by three different methods: (i) Southern hybridization of genomic DNA using a 1.5-kb *Eco*RI-*Nco*I fragment containing *psaC* as probe; (ii) restriction mapping and direct DNA sequencing of PCR product amplified from single colonies; and (iii) growth in the presence of kanamycin. Gene replacement by double crossover and complete segregation of all the mutations was confirmed (data not shown).

Physiological Characterization of the PS I Mutants

Growth Analysis of the Mutants

As shown in Table 3.1, all of the PsaC mutants were unable to grow autotrophically under light intensities ranging from 2.2 to 22 μmol m^{-2} s^{-1}. They were able to grow mixotrophically under 2.2 μmol m^{-2} s^{-1} but not under 22 μmol m^{-2} s^{-1}. In addition, C51D and C14S were tested and found unable to grow photoautotrophically or mixotrophically under white light of 60 μmol m^{-2} s^{-1}. All PsaC mutants showed similar growth rates to wild-type when growing under LAHG or mixotrophically under 2.2 μmol m^{-2} s^{-1}. These results show that the mutants are deficient in photosynthesis, that they are light-sensitive and that their mixotrophic growth is inhibited by moderate light intensity of 22 μmol m^{-2} s^{-1}. The likely source of light inhibition is the overreduction of the electron transfer chain between PSII and PSI by PSII activity. This hypothesis arises from the following results: (1) C51D and C14S were found to grow photoheterotrophically under 22 μmol m^{-2} s^{-1} white light in the presence of 10 mM DCMU, a PS II inhibitor; (2) C51D and C14S were found to grow mixotrophically when 22 or 60 μmol m^{-2} s^{-1} of white light was filtered by a red plastic sheet; and (3) C51D grows photoautotrophically when 60 μmol m^{-2} s^{-1} of white light was filtered by a red plastic sheet. The hypothesis is also supported by a previous study of cyanobacterial PS I-less mutants (Shen *et al.*, 1993), where light inhibition of mixotrophic growth is relieved by genetic inactivation of phycobilisomes. Transformation of C14S and C51D with wild-type *psaC* DNA restored photoautotrophic growth and relieved light inhibition under mixotrophic conditions, demonstrating that the only lesion in these mutants is in *psaC* (data not shown).

Oxygen Evolution of the Mutant Cells

Whole-chain electron transport ($H_2O \rightarrow CO_2$) and PS II electron transport ($H_2O \rightarrow$ 2,6-dichloro-*p*-benzoquinone) were measured using LAHG-grown cells. As shown in Table 3.1, there was essentially no O_2 evolution in ΔC-RCPT indicating that consistent

Table 3.1. Physiological characterization of the PsaC mutants.

	WT Gm^R	ΔC-RCPT	C51D	C51S	C51A	C14D	C14S	C14A	C14D C51D
Photoautotrophic growth (2.2-22 μmol m^{-2} s^{-1})	+	-	-	-	-	-	-	-	-
Mixotrophic growth (2.2 μmol m^{-2} s^{-1})	+	+	+	+	+	+	+	+	+
Mixotrophic growth (22 μmol m^{-2} s^{-1})	+	-	-	-	-	-	-	-	-
Whole-chain O_2 evolution H_2O- CO_2 ; μmolO_2 mgChl^{-1} Hr^{-1}	430± 165	3 ± 18	341± 126	101± 56	39 ± 27	118± 62	141± 61	33 ± 15	30 ± 18
PSII O_2 evolution H_2O- DCBQ; μmolO_2 mgChl^{-1} Hr^{-1}	292± 75	312± 63	553± 253	326± 39	484± 124	368± 80	455± 44	409± 117	370± 68
PS I electron transport cyt c_6 - flavodoxin μmol flavodoxin mgChl^{-1} Hr^{-1}	900	40	460	480	60	510	480	40	60
PS I electron transport cyt c_6 - flavodoxin- $NADP^+$ μmol$NADP^+$ mgChl^{-1} Hr^{-1}	930	70	700	670	170	700	730	200	170
PSI electron transport cyt c_6 - ferredoxin - $NADP^+$ μmol$NADP^+$ mgChl^{-1} Hr^{-1}	820	40	540	430	50	480	380	50	70
Single turnover efficiency (%) ΔA_{820} , $P700^+$ $[F_A/F_B]^-$	80	0	28	21	0	41	32	0	0

Growth tests: BG11 plates supplemented with appropriate antibiotic and glucose, when applicable, were incubated at 30°C. +: growth; -: no growth in 50 days.
O_2 evolution: LAHG-grown cells containing 10 microgram Chl were resuspended in 1ml 40 mM HEPES buffer, pH 7.0 and illuminated by saturating light at 25°C. Rates of oxygen evolution were determined with a Rank type oxygen electrode unit. Whole-chain electron transport was measured in the presence of 10 mM $NaHCO_3$. PS II electron transport was measured in the presence of 1 mM 2,6-dichloro-p-benzoquinone.
PS I-mediated substrate reduction: See text for measurement conditions.
Efficiency of electron donation from P700 to F_A/F_B is shown as the % backreaction with a lifetime ≥ 7 ms.

with previous observations (Yu *et al.*, 1995), PsaC is required for whole-chain photosynthetic electron transport. Compared to the wild type control, all the PsaC mutants had lowered whole-chainO_2 evolution rates to varying degrees, with Asp and Ser mutants showing the highest rates, and Ala mutants and the double Asp mutant showing the lowest rates. However, all the mutants including ΔC-RCPT showed near-wild-type-levels of PS II O_2 evolution rates, indicating that electron transport in PS II was not affected in the short term in the mutants. The lower PSII rates compared to whole chain rates suggest the PSII capacity measurement conditions were not optimal, and DCBQ may not work in cyanobacterial cells as well as in chloroplasts.

Rates of $NADP^+$ Photoreduction

Table 3.1 shows rates of flavodoxin reduction and ferredoxin- and flavodoxin-mediated $NADP^+$ photoreduction for DM-PS I complexes isolated from the wild-type and mutant strains. The wild type PS I complex supports high rates of reductase activity: 800 to 900 μmol $mgChl^{-1}$ Hr^{-1}. The ΔC-RCPT mutant (which lacks PsaC, PsaD, and PsaE) photoreduces flavodoxin at a rate of 40 μmol $mgChl^{-1}$ Hr^{-1} and photoreduces flavodoxin and ferredoxin-mediated $NADP^+$ at rates of 70 and 40 μmol $mgChl^{-1}$ Hr^{-1}. The C14D-PS I and C51D-PS I complexes show lower levels of reductase activity compared to the wild type PS I complex: 460 to 510 μmol $mgChl^{-1}$ Hr^{-1} for flavodoxin reduction, 700 μmol $mgChl^{-1}$ Hr^{-1} for flavodoxin-mediated $NADP^+$ photoreduction and 480 to 540 μmol $mgChl^{-1}$ Hr^{-1} for ferredoxin-mediated $NADP^+$ photoreduction. Both the C14S-PS I and C51S-PS I complexes show nearly the same level of reductase activity as the aspartate mutants. However, the C14A-PS I, C51A-PS I and C14D/C51D-PS I complexes supported minimal rates of PS I reductase activities similar to those for the ΔC-RCPT complex.

Biochemical Characterization of the PS I Mutants

PS I Subunit Composition in the Mutants

Immunoblotting of thylakoid membrane proteins was performed on an equal protein basis, and PS I complexes on an equal chlorophyll basis, using antibodies against the proteins PsaA/B, PsaC, PsaD, PsaE, and PsaF. Antibody against the D2 protein in PS II, which should not vary significantly in the PS I mutants, was used to make sure similar amout of protein was loaded in each lane. Compared to wild-type thylakoid membranes, the levels of PsaC, PsaD, and PsaE were lowered to varying degrees in all mutants (Fig. 3.3). The Asp and Ser mutants demonstrated moderately low levels of these proteins, while Ala mutants and the double Asp mutant did not contain detectable amounts of these three subunits. All mutants contained near-wild-type levels of PsaF and PsaA/PsaB in all samples (Fig. 3.3). It is difficult to quantitate PsaA/PsaB with immunoblots (Smart *et al.*, 1993) or by Elisa (Golbeck, unpublished); however, it is assumed that the levels of PsaA/PsaB in the PsaC mutant thylakoids are similar to that in wild-type since it has been demonstrated that assembly of the PsaA/PsaB dimer does not require PsaC, PsaD or PsaE (Chapter 2; Mannan *et al.*, 1991).

In all mutants the levels of PsaC, PsaD, and PsaE appeared to be closely related, an observation that is consistent with the finding that the stable binding of PsaD and PsaE to PS I complex is dependent on the presence of PsaC (Yu *et al.*, 1995; Li *et al.*, 1991a). The levels of PsaA/B and PsaF are representative of the amounts of PS I in thylakoids (Golbeck and Bryant, 1991). The levels of PsaC, PsaD, and PsaE represent the amounts of these three subunits bound on PS I core to form a complete PS I complex. These results show that the amount of complete PS I complexes is lower to varying degrees in all the mutants compared to the wild type. In thylakoids from the Asp and Ser mutants, a minor portion of PS I contains PsaC, PsaD, and PsaE bound to form a complete PS I complex, while the majority of PS I cores are lacking these

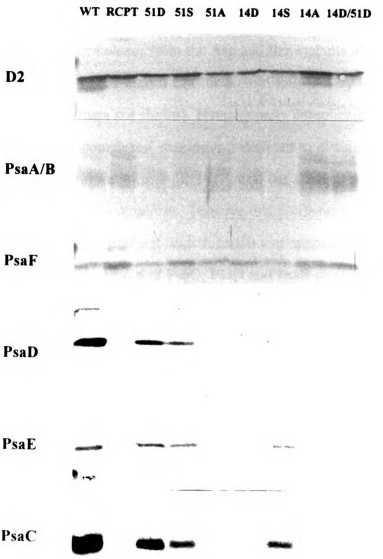

Figure 3.3. Western blots of thylakoid membranes of PsaC mutants. Thylakoid membrane preparations containing 150 microgram protein was loaded in each lane.

subunits (it is difficult to specify the precise amount from the Western blots and efforts to do this by Elisa techniques were unsuccessful). In thylakoids from Ala mutants and the double Asp mutant, no complete PS I complexes are found. To our knowledge this is the first report that the population of PS I complexes is found to be heterogeneous *in vivo* as a result of mutagenesis.

Heterogeneous PS I populations, assayed by immunoblot analysis, were also observed for purified PS I complexes from the Asp and Ser mutants after solubilizing the membranes with 1% DM at 1 mg/ml Chl for 20 min followed by a single sucrose density centrifugation step (data not shown). Heterogeneity complicates functional analysis of the mutant PS I complexes, making it is difficult to distinguish between (i) inefficient electron transfer from A_1 to F_X to F_A/F_B and (ii) a mixed population of P700-F_X cores and P700-F_A/F_B complexes. To solve this problem, a purification procedure with sucrose density gradient centrifugation was adopted to separate the PS I core subpopulation (i.e. those devoid of PsaC, PsaD and PsaE proteins) from the integral PS I complex. The separation principle is based on the finding that at high ratios of DM to Chl, PsaL is readily lost in PS I complexes which lack PsaC, PsaD and PsaE (Mannan *et al.*, 1991). On the other hand, the PsaL-less P700-F_X core was shown to be present in the upper, monomeric band, while the intact PS I complex is present in the lower, trimeric band (Chitnis and Chitnis, 1993). As the result nearly homogeneous PS I holocomplexes, as analyzed by immunobloting, were isolated from the Asp and Ser mutants. Compared to wild-type PS I complexes, all the mutants had similar levels of PsaB and PsaF (data not shown); and the single Asp and Ser mutants had similar levels of PsaC, while the Ala mutants and the double Asp mutant had no detectable levels of PsaC (Fig 3.4).

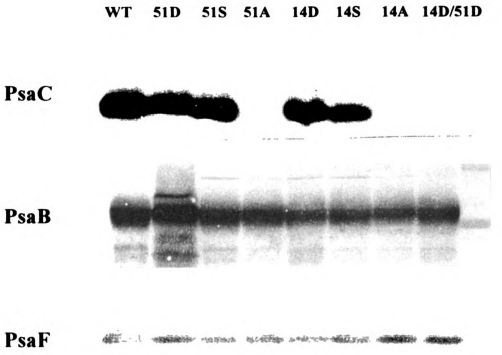

Figure 3.4. Western blots of purified mutant PSI complexes. PS I particles containing 4 microgram chlorophyll was loaded in each lane.

Single Turnover Flash Studies of Mutant PS I Complexes

The effects of different ligand substitutions on $P700^+$ re-reduction kinetics were determined in homogeneous DM-PS I complexes after a single turnover, saturating flash. In wild-type PS I complexes, the vast majority of the backreaction is derived from $[F_A/F_B]^-$. As shown in Fig. 3.5A, 60% of the recombination kinetics are derived from the 25-ms and 112-ms components attributed to $P700^+$ $[F_A/F_B]^-$ recombination. An additional 26% are derived from slower phases with lifetimes of 221 ms and 2.2 s, leading to an 86% efficient electron transfer to F_A/F_B. The slowest kinetic phases are due to exogenous donors undergoing redox reactions with $P700^{+\cdot}$ and come about in reaction centers where $[F_A/F_B]^-$ has become oxidized by exogenous electron acceptors in the medium. The sum contribution of earlier acceptors, including F_X^- and A_1^-, is 14% of the total absorption change.

The major contribution to the absorbance change in the *Synechocystis* sp. PCC 6803 PS I complex with chemically reduced terminal iron-sulfur clusters and in the P700-F_X PS I core isolated by urea treatment of the PS I complex is brought about by the components with life times of ca. 400 μs and 1.5 ms, which result from back reaction of $P700^+$ and F_X^- (Vassiliev *et al.*, 1995). The faster components with life times of ca. 10 μs and 100 μs appearing in these preparations may result from recombination of $P700^+$ and A_1^- (Brettel and Golbeck, 1995) in a fraction of centers which either have a lower quantum efficiency of electron transfer between A_1 and F_X due to some changes of F_X microenvironment or have have the F_X cluster missing or chemically reduced. There is also evidence that decay of the Chl triplets formed upon laser flash excitation in the antenna may contribute to ΔA decay in the tens-of-μs time domain.

The kinetics of the C14D/C51D-PS I (Fig. 3.5B), C14A-PS I (Fig. 3.5C), and C51A-PS I (Fig. 3.5D) complexes are similar to those for the P700-F_X PS I core isolated by urea treatment of the PS I complex (data not shown; see Vassiliev *et al.*,

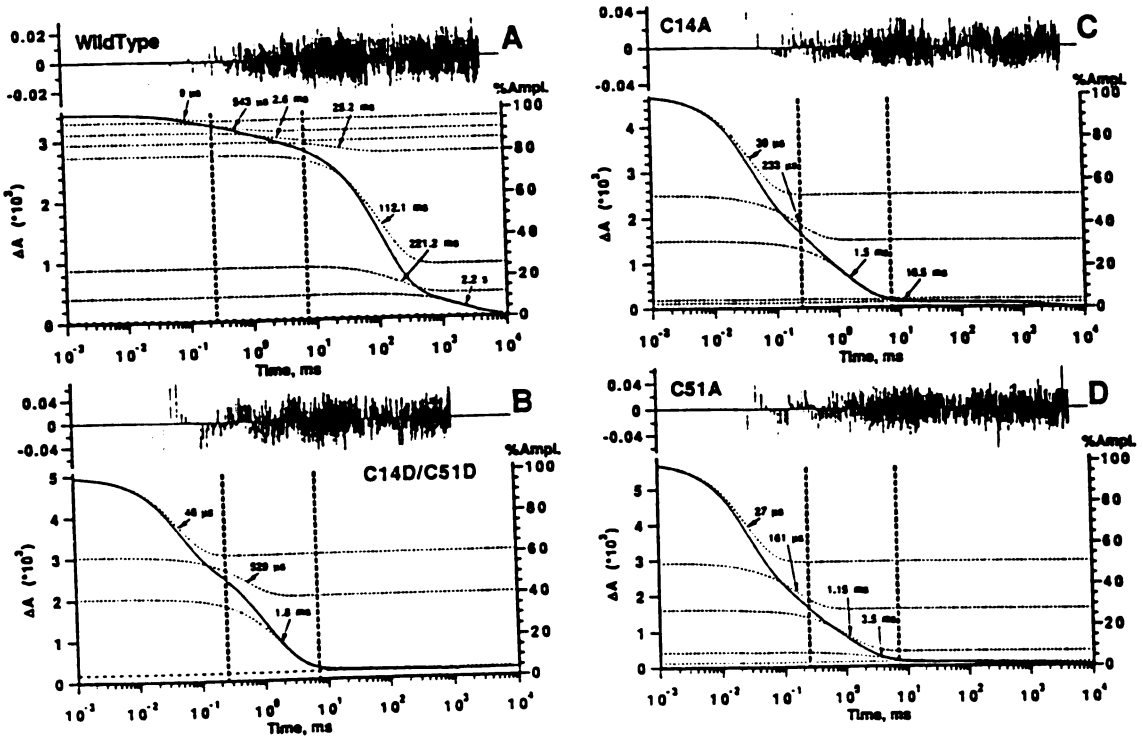

Figure 3.5. Kinetics of ΔA_{820} absorbance changes (I). (A) Wild-type PS I Complex, (B)C14D/C51D-PS I Complex, (C) C14A-PS I Complex, (D) C51A-PS I Complex. The wild-type and mutant PS I complexes were isolated from membranes with ß-D-dodecyl maltoside. The reaction media is 25 mM Tris buffer, pH 8.3 with 0.03% DM, 10 mM sodium ascorbate and 4 μM DCPIP; the chlorophyll concentration is 50 μg ml^{-1}. Each trace (dots) is an average of 16 measurements taken at 50 s intervals. The multiexponential fit is overlaid as a solid line; residuals of the fit shown at the top of the graph. The major individual exponential components are shown as dashed lines, with the percent on the right ordinate, and with offsets equivalent to the relative contribution of the component. The vertical dotted bars separate the time domains in which most of the backreactions of A_1 (left), F_X (middle) and F_A/F_B (right) correspondingly occur.

1995). The majority of the backreaction kinetics for all three mutant complexes is derived from tens-of-μs to ms decay phases, with little or no measurable backreaction in the tens-to-hundreds of ms timescale. Since the PsaC protein is missing in these mutants (Fig. 3.3), and therefore the F_A and F_B clusters, which govern the tens-of-ms decay kinetics are lacking, this is the expected result. The larger ΔA in these three mutants, which is due to a significant μs component, may be derived from additional absorption changes from the decay of Chl triplets in the antenna bed. The optical kinetic data are in agreement with the steady-state rate data (Table 3.1) in which no significant $NADP^+$ reduction occurs in the absence of F_A and F_B.

The kinetics of the C14D-PS I, C14S-PS I, C51D-PS I and C51S-PS I complexes are mixed 'core- and 'complex-type, with each mutant showing a slightly different fractions of the backreaction derived from tens-of-μs to ms decay phases. The C14D-PS I complex has the largest and the C51S-PS I mutant has the smallest, percentage of electrons which arrive at F_A/F_B. The $[F_A/F_B]^-$ backreaction in C14D-PS I (Fig. 3.6A) has lifetime components of 33 ms and 335 ms which contribute 26% to the total absorption change; an additional 15% is contributed by the slower donation to $P700^+$ by external donors, leading to a 41% efficient transfer to F_A/F_B. The remainder of the backreaction occurs from components with lifetimes of 712 μs (19%) and 2.4 ms (20%) derived from F_X, and 19% occurs from a component with a lifetime of 45 μs. The $[F_A/F_B]^-$ backreaction in C51D-PS I (Fig. 3.6B) has lifetimes of 9 ms and 106 ms which contribute 15% to the total absorption change; an additional 13% is contributed by the slower donation to $P700^+$ by external donors, leading to a 28% efficient electron transfer to F_A/F_B. The remainder of the backreaction occurs from components with lifetimes of 206 μs (20%) and 1.0 ms (12%) derived from F_X, and over 39% occurs from a component with a lifetime of 34 μs.

The C14S-PS I complex shows relatively similar kinetic behavior to the above two mutants. The $[F_A/F_B]^-$ backreaction in C14S-PS I (Fig. 3.6C) has lifetime

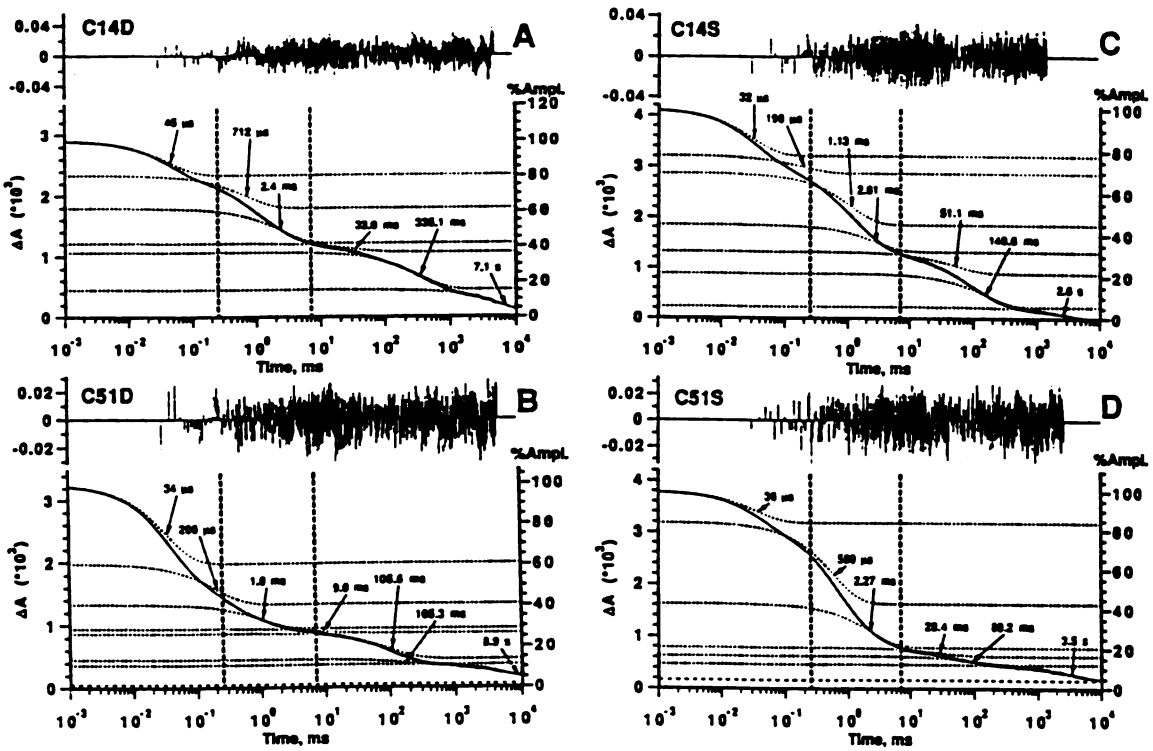

Figure 3.6. Kinetics of ΔA_{820} absorbance changes (II). (A) C14D-PS I Complex, (B) C51D-PS I Complex, (C) C14S-PS I Complex, (D) C51S-PS I Complex. The wild-type and mutant PS I complexes were isolated from membranes with ß-D-dodecyl maltoside. The reaction media is 25 mM Tris buffer, pH 8.3 with 0.03% DM, 10 mM sodium ascorbate and 4 μM DCPIP; the chlorophyll concentration is 50 μg ml^{-1}. Each trace (dots) is an average of 16 measurements taken at 50 s intervals. The multiexponential fit is overlaid as a solid line; residuals of the fit shown at the top of the graph. The major individual exponential components are shown as dashed lines, with the percent on the right ordinate, and with offsets equivalent to the relative contribution of the component. The vertical dotted bars separate the time domains in which most of the backreactions of A_1 (left), F_X (middle) and F_A/F_B (right) correspondingly occur.

components of 51 ms and 148 ms which contribute 26% to the total absorption change; an additional 6% is contributed by the slower donation to $P700^+$ by external donors, leading to a 32% efficient transfer to F_A/F_B. The remainder of the backreaction occurs from components with lifetimes of 1.13 μs (25%) and 2.81 ms (13%) derived from F_X, and over 31% occurs from components with lifetimes of 32 and 198 μs. The $[F_A/F_B]^-$ backreaction in C51S-PS I (Fig. 3.6D) has lifetime components of 28 and 89 ms which contribute only 9% to the total absorption change; an additional 12% is contributed by the slower donation to $P700^+$ by external donors, leading to a 21% efficient electron transfer to F_A/F_B. The remainder of the backreaction occurs from components with lifetimes of 580 μs (41%) and 2.3 ms (22%) derived from F_X, and only 16% occurs from a component with a lifetime of 36 μs.

Discussion

Multiple site-specific mutations to individual cysteine ligands for each of the two PS I [4Fe-4S] centers F_A and F_B were used to produce seven mutant strains of PsaC in *Synechocystis* sp. PCC 6803. Cysteines 14 and 51 were changed to alanine (C14A, C51A), aspartic acid (C14D, C51D) and serine (C14S, C51S), and the results were compared with *in vitro* reconstitution studies (Yu *et al.*, 1995a and 1995b; Jung *et al.*, 1996). In each instance, the PsaC mutant strains could not grow under standard photoautotrophic growth conditions, but could grow mixotrophically under weak light, indicating a light-sensitive lesion in PS I that had become limiting for growth. The characteristics of these separate lines were dependent on the specific ligand substitution for the cysteines in two separable ways. First, some of the mutations resulted in PS I reaction centers where stable incorporation of PsaC was precluded by the specific mutation. These strains included the substitutions C51A, C14A and the double aspartate substitution C14D/C51D. Second, some of the mutations resulted in PS I reaction centers incorporating lower-than-wild-type levels of PsaC. These strains included the

substitutions C51D, C51S, C14D, and C14S. In spite of the heterogeneity of PS I found in the membranes, near-homogeneous PS I complexes with bound PsaC, PsaD and PsaE as judged by protein blotting were isolated from these four mutant strains by detergent fractionation.

These results vary from those recently published for two mutant strains constructed in *Anabaena variabilis* ATCC 29413 (Mannan *et al.*, 1996). In *A. variabilis*, the C13D and C50D mutants (the same functional cysteines in mutants C14D and C51D in *Synechocystis* sp. PCC 6803), grew photoautotrophically, and electron transport rates, measured using ascorbate/DCPIP as a donor, were similar to the wild-type. Although species-specific differences may be invoked to account for these differences, the discrepancy deserves further investigation.

PsaC Mutations and PS I Biogenesis.

The biogenesis and redox properties of membrane complexes containing bound iron-sulfur complexes is dependent upon the associated protein structure; however, protein structure can also be modified by incorporation of mutations to ligands of iron-sulfur clusters (Martin *et al.*, 1990). The *in vivo* experiments with *Synechocystis* sp. PCC 6803 demonstrate that some mutations give rise to altered forms of PsaC which are not stable in the PS I complex or not associated with thylakoids: C51A, C14A and the double mutant C14D/C51D. In these cases little PsaC is seen in thylakoid membranes and none is detected in purified PS I complexes (Fig. 3.3 and 3.4).

The Ala mutants, which contain an $-CH_2$ side group, are not capable of providing a ligand to an iron in the modified site of the cluster. These substitutions are only capable of supporting [3Fe-4S] clusters (Mehari *et al.*, 1995). The implication is that PsaC proteins containing [3Fe-4S] clusters are unable to bind to P700-F_X cores. We suspect that PsaC hosting a [4Fe-4S] cluster and a [3Fe-4S] cluster, as has been found in the unbound PsaC mutants C14D, C51D, C14S and C51S (Yu *et al.*, 1993;

Mehari *et al.*, 1995) has a structure sufficiently different from that of wild type PsaC to preclude its incorporation into PS I. The single substitutions with either aspartic acid (C14D, C51D) or serine (C14S, C51S) lead to lower-than-wild-type levels of PsaC incorporation into PS I complexes in thylakoids (Fig. 3.3). The Asp and Ser mutants, which contain carboxylate and hydroxy side groups respectively, are potentially capable of providing an oxygen ligand to an iron in the modified site of the cluster. These substitutions are capable of supporting mixed-ligand [4Fe-4S] clusters. The implication is that two [4Fe-4S] clusters must be present in PsaC to be incorporated into PS I complexes. It is likely that the C51D, C51S, C14D and C14S proteins also have altered structures, resulting in less-than-perfect interactions with PsaA/PsaB. Yet, size and charge considerations are only one possibility. If the iron-sulfur center insertion requires an efficient ligand exchange reaction at the C14 or C51 positions (this is not provided by the Ala mutations and may be altered to some extent in the Ser and Asp changes), then PsaC biogenesis could be suppressed with the resulting phenotype. Consequently, the mutant PsaC proteins may not bind tightly, or they may dissociate easily, or they may be degraded in the cell, leading to a decreased amount of fully-assembled PS I complex.

PsaC Mutations and Electron Transport

The C51D, C51S, C14D and C14S mutant strains demonstrate whole chain oxygen evolution of modest but significant levels along with at least 50% or better wild-type PS I electron transport capacity. Characterization of isolated PS I complexes (Fig. 3.4) demonstrates that electron transport is less efficient when incorporating a modified PsaC subunit. Assuming that the levels of PsaC revealed by Western blots in the isolated PS I complexes of the above four mutants are similar to the wild type, the ΔA_{820} kinetics results imply that the lower rates of electron transport are due to a qualitative functional alteration of PS I. The single-turnover flash data are in an

agreement with the $NADP^+$ reduction data and show that the inefficient electron transfer step occurs between F_X and F_A/F_B regardless of whether the mutation is in cysteine 14, which is associated with the F_B site, or in cysteine 51, which is associated with the F_A site. Particular values of lifetimes and contributions of the ΔA_{820} decay phases vary slightly from preparation to preparation even in the wild type samples. However, analysis of decay kinetics over several orders of time scale provides a rationale to distinguish between the "integral-complex" and "core-type" kinetics signature and detect a decrease in efficiency of electron transport to F_A and F_B (Vassiliev *et al.*, 1995). We have tabulated the overall amplitude of the ΔA_{820} kinetic components with lifetimes longer than 7 ms as an indicator of efficient photoreduction of F_A and F_B. As shown in Table 3.1, electron transfer to F_A/F_B in the serine and aspartate mutants roughly correlates with the rates of ferredoxin-mediated $NADP^+$ photoreduction.

Comparison of some of these mutants (C14S, C51S) with analogous *in vitro* PS I mutants (Jung *et al.*, 1996) indicates that F_A/F_B photoreduction in the *in vivo* mutants samples occurs with a lower apparent quantum efficiency. One possible explanation is that the external thiolate of ß-mercaptoethanol, used in the iron-sulfur insertion protocol, provides the ligand to the [4Fe-4S] cluster. The PsaC conformation would be rendered closer to that of the wild type, which would then confer higher efficiency of forward electron transfer to the PsaC-bound clusters. On the other hand, the higher contribution of the fast kinetic phases (in the μs to ms time domain) in the *in vivo* PS I mutants may occur due partially to a decrease of the amount of PsaC per reaction center, which would not be resolved in the western blots of the PsaC protein. In any event, one important question regarding the functional properties of PsaC in the *in vivo* mutants is whether only one or both of the PsaC-bound [4Fe-4S] clusters are functioning as the electron acceptors. The goal of the next chapter is to probe this question using low-temperature EPR spectroscopy and absorbance difference kinetics

measurements using repetitive flash excitation.

A redox equilibrium between A_1 and F_X has been proposed (Sétif and Brettel, 1993). Based on this proposal, a reasonable rationale for the function of F_A and F_B is to draw the equilibrium completely away from A_1, thereby ensuring a high quantum yield in PS I. The single substitutions with either aspartic acid (C14D, C51D) or serine (C14S, C51S) are sufficiently similar to wild-type PsaC in structure and charge for the mutant PsaC subunit to draw the equilibrium away from A_1. For the Ala substitutions, C14A and C51A, and the double Asp mutant, C14D/C51D, the modified PsaC was not stably incorporated into PS I thylakoids *in vivo*. These mutants also demonstrated greater impairment in whole chain oxygen evolution than the other mutants, with rates similar to the ΔC-RCPT recipient strain that entirely lacks a functional PsaC. PS I electron transport measured in three different assays also displayed baseline activity, indicating that no functional PS I was present.

Decreased amounts of complete PS I complexes and reduced electron transport efficiencies in complete complexes could both lead to reduced PS I activity, making PS I the rate-limiting step in photosynthetic electron transport. The reduced PS I activity apparently causes dramatically different phenotypes in growth of the PsaC mutants by two different mechanisms. Under dim light the reduced PS I activity limits photosynthetic conversion of light energy to the extent that cells cannot grow photoautotrophically; under moderate white light the electron transfer chain between PSII and PSI is over-reduced, resulting in inhibition of growth.

Acknowledgment

The PSI activity measurement and optical spectrocopy were performed by Y.-S. Jung and I. Vassiliev in J. Golbeck lab.

References

Anderson SL, McIntosh L: Light-activated heterotrophic growth of the cyanobacterium *Synechocystis* sp. strain PCC 6803: a blue-light-requiring process. *J Bacteriol* **173**: 2761-2767 (1991a).

Anderson SL, McIntosh L (1991b) Partial conservation of the 5'*ndhE-psaC-ndhD* 3' gene arrangement of chloroplasts in the cyanobacterium *Synechocystis* sp. PCC 6803: implications for NDH-D function in cyanobacteria and chloroplasts. *Plant Mol Biol* **16**: 497-499.

Brettel K and Golbeck JH (1995) Spectral and kinetic characterization of electron acceptor A_1 in a photosystem I core devoid of iron-sulfur centers F_X, F_B, and F_A. *Photosynth. Res.* **45**, 183-193

Chitnis PR, Xu Q, Chitnis VP, and Nechushtai R (1995) Function and organization of photosystem I polypeptides. *Photosynth Res* **44**: 23-40

Chitnis VP and Chitnis PR (1993) PsaL is required for the formation of photosystem I trimers in the cyanobacterium *Synechocystis* sp. PCC 6803. *FEBS Lett.* **336**, 330-334

Golbeck JH (1994) Photosystem I in cyanobacteria. In: The molecular biology of cyanobacteria. Bryant DA, ed. Kluwer Academic Publishers, pp. 319-360

Golbeck JH and Bryant (1991) Photosystem I. *Curr. Topics Bioenerg.* **16**: 83-177

Henry R, Takemoto L, Murphy J, Gallegos G, and Guikema J (1992) Development and use of domain-specific antibodies in a characterization of the large subunits of soybean photosystem I. *Plant Physiol. and Biochem.* **30**, 357-364

Jung Y-S, Yu L, Golbeck JH (1995) Reconstitution of iron-sulfur center F_B results in complete restoration of $NADP^+$ photoreduction in Hg-treated photosystem I complexes from *Synechococcus* sp. PCC 6301. *Photosynth Res* **46**: 249-255

Jung, Y-S., Vassiliev, I.R., Qiao, F., Yang, F., Bryant, D. and Golbeck, J.H. (1996) *J. Biol. Chem.* (In press)

Jung YS, Vassiliev I, Yu J, McIntosh L, and Golbeck JH (1996) Strains of *Synechocystis* sp. PCC 6803 with altered PsaC. II. EPR and optical spectroscopic properties of F_A and F_B in aspartate, serine and alanine replacements of cysteines 14 and 51. *J. Biol. Chem.* (In press)

Li N, Warren PV, Golbeck JH, Frank G, Zuber H, and Bryant DA (1991a) Polypeptide composition of the photosystem I complex and the photosystem I core protein from *Synechococcus* sp. PCC 6301. *Biochim Biophys Acta* **1059**: 215-225.

Li N, Zhao J, Warren PV, Warden JT, Bryant DA, and Golbeck JH (1991b) PsaD is required for the stable binding of PsaC to the photosystem I core protein of *Synechococcus* sp. PCC 6301. *Biochemistry* **30**: 7863-7872.

Lichtenthaler HK (1987) Chlorophylls and carotenoids: pigments of photosynthetic biomembranes. *Methods Enzymol* **148**: 350-382.

Lowry OH, Rosebrough NJ, Farr AL, and Randall RJ (1951) Protein measurement with the folin phenol reagent. *J Biol Chem* **193**: 265-275.

Mannan RM, He W-Z, Metzger S, Whitmarsh J, Malkin R, and Pakrasi HB (1996) Active photosynthesis in cyanobacterial mutants with directed modifications in the ligands for two iron-sulfur clusters in the PsaC protein of photosystem I. *EMBO J* **15**: 1826-1833

Mannan RM, Pakrasi HB, and Sonoike K (1994) The PsaC protein is necessary for the stable association of the PsaD, PsaE, and PsaL proteins in the photosystem I complex: analysis of a cyanobacterial mutant strain. *Arch Biochem Biophys* **315**: 68-73.

Martin AE, Burgess BK, Stout CD, Cash VL, Dean DR, Jensen GM, and Stephens PJ (1990) Site-directed mutagenesis of *Azotobacter vinelandii* ferredoxin I: [Fe-S] cluster-driven protein rearrangement. *Proc. Natl. Acad. Sci. USA* **87**, 598-602

Mehari T, Qiao F, Scott PM, Nellis DF, Zhao J, Bryant DA, and Golbeck JH (1995) Modified ligands to FA and FB in photosystem I. I. Structural constraints for the formation of iron-sulfur clusters in free and rebound PsaC. *J. Biol. Chem.* **270**, 2108-28117

Mühlenhoff U, Kruip J, Bryant DA, Rögner M, Sétif P, and Boekema E (1996a) Characterization of a redox-active cross-linked complex between cyanobacterial photosystem I and its physiological acceptor flavodoxin. *EMBO J.* **15**, 488-497

Mühlenhoff U, Zhao J, and Bryant DA (1996b) Interaction between photosystem I and flavodoxin from the cyanobacterium *Synechococcus* sp. PCC 7002 as revealed by chemical cross-linking. *Eur. J. Biochem.* **235**, 324-331

Ohad N, and Hirschberg J (1992) Mutations in the D1 subunit of photosystem II distinguish between quinone and herbicide binding sites. *Plant Cell* **4**: 272-283

Sambrook J, Fritsch EF, and Maniatis T (1989) Molecular Cloning: A Laboratory Manual. Cold Spring Harbor, New York: Cold Spring Harbor Laboratory Press.

Sétif P and Brettel K (1993) Forward electron transfer from phylloquinone-A_1 to iron sulfur centers in spinach photosystem I. *Biochemistry* **31**, 7846-7854

Shen G, Boussiba S, and Vermaas WFJ (1993) *Synechocystis* sp PCC 6803 strains lacking photosystem I and phycobilisome function. *Plant Cell* **5**: 1853-1863.

Smart LB, Bowlby NR, Anderson SL, Sithole I, and McIntosh L (1994) Genetic manipulation of the cyanobacterium *Synechocystis* sp. PCC 6803: development of strains lacking PSI for the analysis of mutations in PSII. *Plant Physiol.* **104**, 349-354

Smart LB and McIntosh L (1991) Expression of photosysthesis genes in the cyanobacterium *Synechocystis* sp. PCC 6803: *psaA-psaB* and *psbA* transcripts accumulate in dark-grown cells. *Plant Mol Biol* **17**: 959-971

Smart LB, Warren PV, Golbeck JH, and McIntosh L (1993) Mutational analysis of the structure and biogenesis of the photosystem I reaction center in the cyanobacterium *Synechocystis* sp PCC 6803. *Proc Natl Acad Sci USA* **90**: 1132-1136

Steinmüller K (1992) Identification of a second *psaC* gene in the cyanobacterium *Synechocystis* sp PCC 6803. *Plant Mol Biol* **20**: 997-1001.

Taylor LA and Rose RE (1988) A correction in the nucleotide sequence of the Tn903 kanamycin resistance determinant in pUC4K. *Nucl Acids Res* **16**: 358-358

Vassiliev IR, Jung YS, Mamedov MD, Semonoc AY, McIntosh L, and Golbeck JH (1996) Absorbance changes and electrogenic reactions in the μsec-to-sec time domain in photosystem I. *Biophys J* (In press)

Vassiliev IR, Jung YS, Smart LB, Schulz R, McIntosh L, and Golbeck JH (1995) A mixed-ligand iron-sulfur cluster ($C556S_{PsaB}$ or $C565S_{PsaB}$) in the F_X-binding site leads to a decreased quantum efficiency of electron transfer in photosystem I. *Biophys J* **69**: 1544-1553

Vermaas WFJ, Ikeuchi M, and Inoue Y (1988) Protein composition of the photosystem II core complex in genetically engineered mutants of the cyanobacterium *Synechocystis* sp PCC 6803. *Photosynth Res* **17**: 97-113.

Vieira J and Messing J (1982) The pUC plasmids, an M13mp7-derived system for insertion mutagenesis and sequencing with synthetic universal primers. *Gene* **19**: 259-268.

Warren PV, Smart LB, McIntosh L, and Golbeck JH (1993) Site-directed conversion of cysteine-565 to serine in PsaB of photosystem I results in the assembly of [3Fe-4S] and [4Fe-4S] clusters in F_X. A mixed-ligand [4Fe-4S] cluster is capable of electron transfer to F_A and F_B. *Biochemistry* **32**: 4411-4419.

Williams JGK (1988) Construction of specific mutations in photosystem II photosynthetic reaction center by genetic engineering methods in *Synechocystis* 6803. *Meth Enzymol* **167**: 766-778

Yu J, Smart LB, Jung Y-S, Golbeck JH, and McIntosh L (1995) Absence of PsaC subunit allows assembly of photosystem I core but prevents the binding of PsaD and PsaE in *Synechocystis* sp. PCC 6803. *Plant Mol Biol* **29**: 331-342

Yu L, Bryant DA, and Golbeck JH (1995a) Evidence for a mixed-ligand [4Fe-4S] cluster in the C14D mutant of PsaC. Altered reduction potentials and EPR spectral properties of the F_A and F_B clusters on rebinding to the P700-F_X core. *Biochemistry* **34**, 7861-7868

Yu L, Vassiliev IR, Jung YS, Bryant DA, and Golbeck JH (1995b)Modified ligands to FA and FB in photosystem I. II. Characterization of a mixed ligand [4Fe-4S] cluster in the C51D mutant of PsaC upon rebinding to P700-F_X cores. *J. Biol. Chem.* **270**, 28118-28125

Yu L, Zhao J, Lu W, Bryant DA, and Golbeck JH (1993) Characterization of the [3Fe-4S] and [4Fe-4S] clusters in unbound PsaC mutants C14D and C51D. The midpoint potentials of the single [4Fe-4S] clusters are identical of F_A and F_B in bound PsaC of photosystem I. *Biochemistry* **32**: 8251-8258

Chapter 4

STRAINS OF *SYNECHOCYSTIS* SP. PCC 6803 WITH ALTERED PsaC. II. EPR AND OPTICAL SPECTROSCOPIC PROPERTIES OF F_A AND F_B WHEN CYSTEINES 14 AND 51 ARE REPLACED BY ASPARTATE, SERINE AND ALANINE

Introduction

There are several exceptions to the nearly universal occurrence of cysteine thiolate ligands to iron-sulfur clusters in the ferredoxin class of electron transfer proteins (Moulis *et al.*, 1996). Examples include the N-ligands from histidine residues in the Rieske-subclass of iron-sulfur proteins (Davidson *et al.*, 1992; Shergill and Cammack, 1994; Britt *et al.*, 1991), O-ligands from (most likely) aspartate in Fd III from *Desulfovibrio africanus* (Telser *et al.*, 1995), and a proposed O-ligand from serine to the pentacoordinated iron in the P- cluster of nitrogenase (Mouesca *et al.*, 1994). Recently, oxygen ligands have been introduced in lieu of cysteine thiolates by site-directed mutagenesis in proteins which contain [2Fe-2S], [3Fe-4S] and/or [4Fe-4S] clusters. Examples include the introduction of serine for cysteine in the interpolypeptide F_X cluster of PS I (Warren *et al.*, 1993; Vassiliev *et al.*, 1995) and the [4Fe-4S] cluster of *Escherichia coli* fumarate reductase (Kowal *et al.*, 1995). The consequence of these changes include a change in the EPR spectrum and a decreased electron transfer efficiency

in the case of serine- ligated F_X, and a change in the cluster midpoint potential and intercluster spin interaction in the case of *E. coli* fumarate reductase.

One instance of a functional [4Fe-4S] cluster derived from an aspartate-for-cysteine change is the modified PsaC subunit of PS I. In a previous study, mutant PsaC proteins expressed in *Escherichia coli* were reconstituted onto P700-F_X cores, and the assignment of the ligands for the two terminal electron acceptors was determined by EPR spectroscopy (Zhao *et al.*, 1992). The substitution of aspartate for cysteine in position 14 of PsaC led to the retention of an S = ½, [4Fe-4S] cluster at the unmodified site with *g*-values characteristic of F_A. Similarly, the substitution of aspartate for cysteine in position 51 of PsaC led to the retention of an S = ½, [4Fe-4S] cluster at the unmodified site with *g*-values characteristic of F_B. Since the pattern of cysteine ligation in PsaC is expected to be identical to that of ferredoxins with two [4Fe-4S] clusters whose structures have been determined, it follows that F_B is ligated by cysteines 11, 14, 17, and 58 and F_A is ligated by cysteines 21, 48, 51, and 54 (Zhao *et al.*, 1992).

The *in vitro* reconstitution experiments led to several hypotheses regarding alternative ligands to iron-sulfur clusters: 1) unbound PsaC refolds only in the presence of one [3Fe-4S] and one [4Fe-4S], or two [4Fe-4S] clusters when cysteine is replaced in positions 14 and 51 by aspartate, serine and alanine (Yu *et al.*, 1993; Mehari *et al.*, 1995). According to these results, a stable 3-dimensional structure requires the presence of two iron-sulfur clusters, one of which must be a [4Fe-4S] cluster. 2) The failure to observe a [3Fe-4S] cluster in the *in vitro* reconstituted C14X-PS I or C51X-PS I complexes (where X = D, A or S) indicates that the binding of PsaC onto P700-F_X cores requires the presence of two [4Fe-4S] clusters. If rigorously true, it may be difficult to introduce a

[3Fe-4S] cluster motif into PsaC *in vivo*. 3) An oxygen ligand to the [4Fe-4S] cluster in the mutant site of the C14D-PS I and the C51D- PS I complexes leads to a high-spin state (likely S = 3/2).

In this work, these hypotheses were tested through the generation of a series of *in vivo* mutations in F_A and F_B. The choices to replace cysteine residues with aspartic acid, serine and alanine were made because aspartate is known to support [3Fe-4S] and [4Fe-4S] clusters in naturally-occurring ferredoxins (Armstrong *et al.*, 1989; Conover *et al.*, 1990), serine can support [3Fe-4S] and [4Fe-4S] clusters in the F_X binding site of PS I (Warren *et al.*, 1993) and in the *Azotobacter vinelandii* hydrogenase small subunit (McTavish *et al.*, 1995), and alanine, with the absence of a suitable ligand, should support only [3Fe-4S] clusters. This chapter summarizes the EPR spectral characteristics and electron transfer properties of aspartate (C14D, C51D, C14D/C51D) alanine (C14A, C51A) and serine (C14S, C51S) mutations in PsaC in *Synechocystis* sp. PCC 6803. The premise tested is that [4Fe-4S] clusters will only be assembled in those mutants where oxygen ligands are available from the side chains of the replacement amino acids.

Results and Discussion

Summary of results

A *psaC* deletion mutant of the unicellular cyanobacterium *Synechocystis* sp. PCC 6803 was utilized to incorporate site-specific amino acid substitutions in the cysteine residues which ligate the F_A and F_B iron-sulfur clusters in Photosystem I (PS I). Cysteines 14 and 51 of PsaC were changed to aspartic acid (C14D, C51D, C14D/C51D), serine (C14S, C51S) and alanine (C14A, C51A) and the properties of F_A and F_B were

characterized by electron paramagnetic resonance spectroscopy and time-resolved optical spectroscopy. The C14D-PS I and C14S-PS I complexes showed high levels of photoreduction of F_A with *g* values of 2.045, 1.944 and 1.852 after illumination at 15 K, but there was no evidence of reduced F_B in the $g = 2$ region. The C51D-PS I and C51S-PS I complexes showed low levels of photoreduction of F_B with *g* values of 2.067, 1.931 and 1.881 after illumination at 15 K, but there was no evidence of reduced F_A in the $g = 2$ region. The presence of F_B was inferred in C14D-PS I and C14S-PS I and the presence of F_A was inferred in C51D-PS I and C51S-PS I by magnetic interaction in the photoaccumulated spectra and by the equal spin concentration of the irreversible $P700^+$ cation generated by illumination at 77 K. Successive-flash experiments at 298 K in the presence of a fast electron donor indicate that two electron acceptors function after F_X in the four mutant PS I complexes at room temperature.

Number of Electron Acceptors Present in the C14X-PS I and C51X-PS I Mutants

The following generalizations can be made about the C14X-PS I and C51X-PS I mutants (where X = D, S, and A). First, only [4Fe-4S] clusters are found in the *in vivo* mutant PS I complexes, even though the unbound mutant PsaC expressed in *E.coli* contain [3Fe-4S] and mixed-ligand [4Fe-4S] clusters in the altered site (Yu L *et al.*, 1993; Mehari *et al.*, 1995). The PsaC protein does not assemble in the *in vivo* mutants for which cysteines 14 and 51 are substituted with alanine, C14A and C51A, most likely because a [4Fe-4S] cluster cannot assemble in the absence of a suitable ligand. The absence of a suitable oxygen or sulfur ligand from the replacement amino acid, alanine, and the resulting destabilizing effect of a [3Fe-4S] cluster on PsaC binding to the P700-F_X

heterodimer, is apparently the reason for the inability of the C14A and C51A PsaC to bind to PS I. Second, all mutant PS I complexes containing mixed-ligand [4Fe-4S] clusters are capable of electron transfer to F_A and F_B at 15 K. These mutant complexes are also capable of supporting electron throughput to $NADP^+$ at room temperature. This is also true for PS I complexes reconstituted *in vitro* with C14D and C51D (Yu *et al.*, 1995a). Third, the results of the *in vivo* experiments agree with the cysteine ligand assignments to F_A and F_B made using *in vitro* reconstitution of *E. coli* expressed proteins onto P700-F_X cores (Zhao *et al.*, 1992).

It is clear from the optical results that both acceptors are photochemically active in C14D-PS I, C51D-PS I, C14S-PS I and C51S-PS I complexes and that they may operate with lower quantum efficiencies than in the wild type. However, heterogeneity due to incomplete binding of PsaC would give rise to the same kinetics in single turnover experiments as does forward electron transfer inefficiency. To this end, we have taken care to isolate near-homogeneous PS I complexes from the thylakoids based on the different densities of PS I reaction centers with and without PsaC, PsaD, PsaE and PsaL (Chapter 3).

Comparison with in vitro *Reconstituted C14D-PS I and C51D-PS I Mutant Complexes*

The similarities and the differences between the *in vivo* engineered and *in vitro* reconstituted C14D-PSI and C51D-PS I complexes depend on whether the mutation is in the F_A or the F_B site. Under conditions of photoaccumulation, the *in vivo* C51D-PS I complex is similar in spectral appearance to *Escherichia coli*-expressed C51D-PsaC reconstituted *in vitro* onto P700-F_X cores (Yu *et al.*, 1995b). These similarities indicate

that oxygen from aspartate (alternatively, water or OH^-) provide the ligands to F_A in the modified site. The slight differences in the *g*-values between the *in vivo* and *in vitro* PS I complexes may be related to species differences, since the *in vivo* C51D-PS I mutant PS I complexes were derived from *Synechocystis* sp. PCC 6803, whereas the *in vitro* reconstituted PS I complexes were hybrids, composed of a *Synechococcus* sp. PCC 6301 P700-F_X core, PsaC and PsaE derived from *Synechococcus* sp. PCC 7002, and a PsaD protein derived from *Nostoc* sp. PCC 8009 (Li *et al.*, 1991). Under conditions where only one electron was promoted to the acceptor side, only a low spin concentration of the F_B cluster was observed in the *in vivo* mutants and their *in vitro* counterparts; yet the size of the $P700^+$ radical indicates that the majority of the electrons were promoted to the proposed high-spin F_A cluster. However, a very low spin concentration of F_A was also observed after the *in vitro* reconstitution, which may have been derived from a minority population of a S = ½ cluster. One candidate is a sulfur thiolate ligand derived from carryover of the ß-mercaptoethanol used in the reconstitution protocol as suggested in Jung *et al.*(1995).

In contrast, the *in vivo* C14D-PS I complex differs substantially from the *in vitro* reconstituted C14D-PS I complex. In the *in vivo* mutant, the F_B cluster is not observed in the $g = 2$ region, but is inferred from the size of the $P700^+$ radical and the presence of new EPR resonances at very low temperatures which may be derived from intercluster spin interaction between F_A and F_B. The proposal is that the F_B cluster is present as a high-spin system (likely S = 3/2). After the *in vitro* reconstitution, the F_B cluster was observed as a ground state S = ½ spin system with *g*-values of 2.118, 1.911, 1.883. The difference in the *in vivo* engineered and *in vitro* assembled C14D-PS I complexes is that only oxygen

ligands are available in the former whereas sulfur thiolate ligands may also be available in the latter. The ß-mercaptoethanol used in the *in vitro* iron-sulfur reinsertion protocol may have been recruited as a ligand at the mutated site of the *in vitro* complex (Jung *et al.*, 1995). It is likely that sulfur provides a better ligand to an iron-sulfur cluster, replacing some or all of the oxygen- ligated cluster in the *in vitro* experiments. In this *in vitro* reconstituted PSI complex, F_B may be present as a mixed population of sulfur-ligated S= ½ clusters visible in the $g = 2$ region, and oxygen-ligated S = 3/2 clusters invisible in the $g = 2$ region. The fraction of sulfur- and oxygen-ligated clusters may have more to do with steric hindrance or accessibility to solvent than with inherent differences in the C14D and C51D sites of PsaC.

The inability to engineer a PsaC protein with either a missing cluster or a [3Fe-4S] cluster *in vitro* in PsaC from *Synechocystis* sp. PCC 7002 (Mehari *et al.*, 1995) or *in vivo* in *Synechocystis* sp. PCC 6803 (this work) is further evidence that two [4Fe-4S] clusters must be present for PsaC to bind to the PS I core. This result is consistent with *in vitro* reconstitutions of *E. coli*-expressed mutant PsaC proteins, where only those proteins with two intact [4Fe-4S] clusters could be rebound onto P700-F_X cores (Jung *et al.*, 1995).

In conclusion, the studies presented here demonstrate that mixed-ligand [4Fe-4S] clusters can assemble in the PsaC protein of PS I *in vivo*, and that PsaC protein containing such mixed-ligand clusters can bind to PS I core complexes and function in electron transfer reactions from P700 to ferredoxin or flavodoxin. The efficiency of iron-sulfur center insertion into the mutant proteins, or the stability of mutant proteins after cluster insertion, varies depending upon the chemical nature of the side group on the replacement amino acid. Differences observed between the spectroscopic properties of PS I complexes

containing mutant PsaC proteins formed by *in vitro* or *in vivo* methods are most likely due to the chemical nature of the ligands to the [4Fe-4S] clusters. The common denominator is that only those PsaC proteins containing two [4Fe-4S] clusters are capable of assembling onto P700-F_X cores either *in vivo* or *in vitro*.

Note: This chapter is condensed from a manuscript in press in J. Biol. Chem. by Yean-Sung Jung, Ilya R. Vassiliev, Jianping Yu, Lee McIntosh, and John H. Golbeck.

References

Armstrong FA, George SJ, Cammack R, Hatchikian EC, and Thomson AJ (1989) Electrochemical and spectroscopic characterization of the 7Fe form of ferredoxin III from *Desulfovibrio africanus*. *Biochem J* **264**: 265-273

Britt RD, Sauer K, Klein MP, Knaff DB, Kriauciunas A, Yu CA, Yu L, and Malkin R (1991) Electron spin echo envelope modulation spectroscopy supports the suggested coordination of two histidine ligands to the Rieske Fe-S centers of the cytochrome b6f complex of spinach and the cytochrome bc1 complexes of *Rhodospirillun rubrum*, *Rhodobacter sphaeroides* R-26, and bovine heart mitochondria. *Biochemistry* **30**: 1892-1901

Conover PR, Kowal AT, Fu W, Park JB, Aono S, Adams MWW, and Johnson MK (1990) Spectroscopic characterization of the novel iron-sulfur cluster in *Pyrococcus furiosus* ferredoxin. *J Biol Chem* **265**: 8533-8541

Davidson E, Ohnishi T, Attaasafoadjei E, and Daldal F (1992) Potential ligands to the [2Fe-2S] Rieske cluster of the cytochrome bc1 complex of *Rhodobactter capsulatus* probed by site-directed mutagenesis. *Biochemistry* **31**: 3342-3351

Jung Y-S, Yu J, Yu L, Zhao J, Bryant DA, McIntosh L, and Golbeck JH (1995) *In vivo* site-directed mutations of the cysteine ligands to F_A and F_B in *Synechocystis* sp PCC 6803: a comparison with *in vitro* reconstituted PSI complexes. in Photosynthesis: From Light to Biosphere (Mathis, PA ed) Vol II, pp. 127-130. Kluwer Academic Publishers, Dordrecht

Kowal AT, Werth MT, Mandori A, Cecchini G, Schroder I, Gunsalus RP, and Johnson MK (1995) Effect of cysteine to serine mutations on the properties of the [4Fe-4S] center in *Escherichia coli* fumarate reductase. *Biochemistry* **34**: 12284-12293

Li N, Warren PV, Golbeck JH, Frank G, Zuber H, and Bryant BA (1991) Polypeptide composition of the photosystem I complex and the photosystem I core protein from *Synechococcus* sp. PCC 6301. *Biochim Biophys Acta* **1059**: 215-225

McTavish H, Sayavedrasoto LA, and Arp DJ (1995) Substitution of *Azotobacter vinelandii* hydrogenase small-subunit cysteines by serines can create insensitivity to inhibition by O_2 and preferentially damages H_2 oxidation over H_2 evolution. *J Bacteriol* **177**: 3960-3964

Mehari T, Parrett KG, Warren PV, and Golbeck JH (1991) Reconstitution of the iron-sulfur clusters in the isolated F_A/F_B protein: ESR characterization of the same-species and cross-species photosystem I complexes. *Biochim Biophs Acta* **1056**: 139-148

Mehari T, Qiao F, Scott PM, Nellis DF, Zhao J, Bryant DA, and Golbeck JH (1995) Modified ligands to F_A and F_B in photosystem I. I. Structural constraints for the formation

of iron-sulfur clusters in free and rebound PsaC. *J Biol Chem* **270**: 28108-28117

Mouesca JM, Noodleman L, and Case DA (1994) Density functional/Poisson-Boltzmann calculations of redox potentials for iron-sulfur clusters. *Inorg Chem* **33**: 4819-4830

Moulis JM, Davasse V, Golinelli MP, Meyer J, and Quinkal I (1996) The coordination sphere of iron-sulfur clusters: lessons from site-directed mutagenesis experiments. *J Inorg Biol Chem* **1**: 2-14

Shergill JK and Cammack R (1994) ESEEM studies of the iron-sulphur clusters of succinate dehydrogenase in *Arum maculatum* spadix mitochondrial membranes. *Biochim Biophys Acta* **1185**: 35-42

Telser J, Smith ET, Adams MWW, Conover R, Johnson MK, and Hoffman BM (1995) Cyanide binding to the novel 4Fe ferredoxin from *Pyrococcus furiosus*: Investigation by EPR and ENDOR spectroscopy. *J Am Chem Soc* **117**: 5133-5140

Vassiliev I, Jung Y-S, Smart LB, Schulz R, McIntosh L, and Golbeck JH (1995) A mixed-ligand iron-sulfur cluster ($C556S_{PsaB}$ or $C565S_{PsaB}$) in the F_X-binding site leads to a decreased quantum efficiency of electron transfer in photosystem I. *Biophys J* **69**: 1544-1553

Warren PV, Smart LB, McIntosh L, and Golbeck JH (1993) Site-directed conversion of cysteine 565 to serine in PsaB of photosystem I results in the assembly of [3Fe-4S] cluster and [4Fe-4S] clusters in F_X. A mixed-ligand [4Fe-4S] cluster is capable of electron transfer to F_A and F_B. *Biochemistry* **32**: 4411-4419

Yu L, Bryant DA, and Golbeck JH (1995a) Evidence for a mixed-ligand [4Fe-4S] cluster in the C14D mutant of PsaC. Altered reduction potentials and EPR spectral properties of the F_A and F_B clusters on rebinding to the P700-F_X core. *Biochemistry* **34**, 7861-7868

Yu L, Vassiliev IR, Jung YS, Bryant DA, and Golbeck JH (1995b)Modified ligands to F_A and F_B in photosystem I. II. Characterization of a mixed ligand [4Fe-4S] cluster in the C51D mutant of PsaC upon rebinding to P700-F_X cores. *J. Biol. Chem.* **270**, 28118-28125

Yu L, Zhao J, Lu W, Bryant DA, and Golbeck JH (1993) Characterization of the [3Fe-4S] and [4Fe-4S] clusters in unbound PsaC mutants C14D and C51D. The midpoint potentials of the single [4Fe-4S] clusters are identical to F_A abd F_B in bound PsaC of photosystem I. *Biochemistry* **32**: 8251-8258

Zhao J, Li N, Warren P, Golbeck JH, and Bryant DA (1992) Site-directed conversion of a cysteine to an aspartate leads to the assembly of a [3Fe-4S] cluster in PsaC of photosystem I. Photoreduction of F_A is independent of F_B. *Biochemistry* **31**: 5093-5099

Chapter 5

ISOLATION AND GENETIC CHARACTERIZATION OF PSEUDOREVERTANTS FROM SITE-DIRECTED PSI MUTANTS IN *SYNECHOCYSTIS* 6803

Introduction

Reversion of mutation results from a change in DNA that either exactly reverses the original alteration (a true reversion), or compensates for it (a suppressor mutation). Suppressor mutations yield valuable information about other sites and/or other polypeptides that interact with the site altered by the original (primary) mutation. An organism with a suppressor mutation can be called a pseudorevertant. Selection of pseudorevertants can yield an array of suppressor mutations.

Suppressor selection has been applied to *Synechocystis* sp. PCC 6803 for the molecular analysis of the structure, function, and assembly of photosystem I (PSI). This methodology involves the isolation of spontaneous pseudorevertants from site-directed PSI mutants. Suppressor mutations can then be located to a specific gene or operon by complementation and/or identified by DNA sequencing. In this way, specific amino acids and electron carriers may be assigned to a PSI structural model, and insights may be gained into the roles of specific amino acids on the assembly/stability of the complex and on modulating electron transport.

Synechocystis 6803 is a model organism for the study of oxygenic photosynthesis. Its genome (3.57Mb) has recently been sequenced (Kaneko *et al.*, 1996) and it is naturally competent, can be easily transformed. It also has an active homologous recombination mechanism (Williams, 1988). Furthermore, it can grow photoheterotrophically on glucose, which has allowed propagation of PSII mutants that are incapable of photosynthesis (Williams, 1988), and it can grow under light-activated-heterotrophic-growth (LAHG) conditions, permitting isolation of PSI mutants in the absence of PSI function (Anderson *et al.*, 1991). Site-directed mutagenesis has been successfully used in this organism to study structure-function relationships both in PSII (Williams, 1988) and in PSI (Smart *et al.*, 1993; Schulz *et al.*, 1995; Yu *et al.*, submitted).

PSI consists of at least 11 different proteins in cyanobacteria (Chitnis, 1996). All PSI proteins are believed to be present as one copy per P700 reaction center. They vary considerably in their molecular weights, hydrophobicities, and locations with respect to the lipid bilayer. In addition to proteins, the PSI complex contains approximately 100 Chl *a* molecules, two β-carotenes, two phyloquinone molecules, and three [4Fe-4S] clusters. The cofactors of PSI are bound to the PsaA, PsaB, and PsaC proteins. Trimers of PSI have been observed by electron microscopy in the photosynthetic membranes of cyanobacteria and are considered to be *in vivo* functional units (Boekema *et al.*, 1994). On the basis of the electron density maps, a structural model for trimeric PSI from *Synechococcus elongatus* was initially proposed at a resolution of 6 Å (Krauss *et al.*, 1993). From new data, many aspects of this model have been later refined to a resolution of 4.5 Å (Schubert *et al.*, 1995; Fromme *et al.*, 1996). Resolution of PSI structure at the atomic level will require further x-ray diffraction analyses of better crystals of PSI. These

fine structure determinations are being complemented by topological explorations, electron microscopy, and genetic analysis.

Genetic inactivation of the *psaA*, *psaB*, or *psaC* genes in *Synechocystis* 6803 produced mutants that lack PSI function and depend on glucose for growth (Smart *et al.*, 1991; Chapter 2). Photosynthesis-deficient PSI mutants have also been created by site-directed mutagenesis of these genes (Smart *et al.*, 1993; Schulz *et al*, 1995; Chapter 3). An additional phenotype, inhibition of mixotrophic growth by moderate light intensities, has also been observed for some PSI mutants (Smart *et al.*, 1993; Chapter 3). Characterization of these site-directed mutations has yielded valuable information on biogenesis of PSI and on functions of electron carriers. One limitation of the site-directed mutagenesis approach is that it relies on proposed models or predictions. Studies using pseudorevertants will add additional power to the mutagenesis approach and may potentially reveal information about PSI biogenesis and function that may not have been predicted. This chapter describes a procedure for isolating spontaneous pseudorevertants from PSI mutants of *Synechocystis* 6803, localization and identification of the suppressor mutations, and some of the properties of the genetic transformation system in this cyanobacterium.

Isolation and genetic characterization of pseudorevertants from PSI mutants

A flow chart for isolation and genetic characterization of a 'typical' pseudorevertant from a primary PSI mutant in *Synechocystis* 6803 is shown in figure 5. 1.

Primary mutant

↓

Photoautotrophic growth or mixotrophic growth under inhibitory light intensity

↓

Colonies are subject to three or more serial streakings under the selective conditions

↓

PCR amplification of a fragment containing the primary mutation to confirm presence of the primary mutation by restriction analysis and/or sequencing

↓

Transform the primary mutant with total DNA isolated from the revertants to demonstrate presence of suppressor mutations

↓

Locate suppressor mutations by functional complementation

↓

Identify the suppressor mutations by sequencing the cloned or amplified fragments

↓

If necessary, the identified mutation may be introduced into the primary mutation background by site-directed mutagenesis to confirm its function.

Figure 5.1. A flow chart for isolation and genetic characterization of a 'typical' pseudorevertant from a primary PSI mutant.

Isolation of pseudorevertants from PsaC mutants

The PsaC subunit, encoded by *psaC*, provides the ligands for two [4Fe-4S] clusters, F_A and F_B. The proposed cysteine ligands have been studied by a combination of site-directed mutagenesis and *in vitro* reconstitution. Mutant PsaC derived from overexpression in *E. coli* was reconstituted with a biochemical preparation of PSI cores. These experiments showed that Cys 51 in PsaC is a ligand to the F_A cluster, whereas Cys14 is a ligand to the F_B cluster (Zhao *et al.*, 1992). PsaC mutants C51D, C51S, C51A, C14D, C14S, and C14A were introduced into *Synechocystis* 6803, in which a cysteine ligand to F_A or F_B, respectively, is changed to aspartate, serine or alanine by site-directed mutagenesis. Physiological characterization has shown that these mutations have decreased PSI capacity and efficiency, making PSI limiting for whole chain photosynthesis. As a result, these mutants cannot grow photoautotrophically under white light and their mixotrophic growth (in the presence of glucose) is inhibited by white light (22-60 $\mu mol\ m^{-2}\ s^{-1}$; Chapter 3). To isolate pseudorevertants, 10^8 cells from a mid-log phase culture grown under LAHG (Anderson and McIntosh, 1991) conditions were spread onto 90-cm plates with solid BG-11 medium supplemented with gentamycin (glucose is added for mixotrophic growth). The plates were placed at 30°C under 10 $\mu mol\ m^{-2}\ s^{-1}$ white light for two days then transferred to 22 $\mu mol\ m^{-2}\ s^{-1}$ white light for up to forty days. Colonies have been found to appear spontaneously under these selective conditions at frequencies between 10^{-6}-10^{-8} in several tests. Hundreds of the isolates were serially streaked three to four times, with about half of them able to grow on the fourth and successive plates. Why other isolates could appear on the first selective plates but could not grow on the successive plates is not clear. Following the fourth serial plating,

selected isolates were characterized physiologically and genetically, as discussed below.

Photoautotrophic and mixotrophic growth under a light intensity of 22 μmol m^{-2} s^{-1} was used to isolate and characterize pseudorevertants. Isolates obtained from one selective condition were tested for their ability to grow in other conditions by streaking on plates. Three classes of pseudorevertants have been found: those capable of growth under: (1) photoautotrophic conditions, but not mixotrophic conditions; (2) mixotrophic conditions, but not photoautotrophic conditions; (3) both conditions.

Genetic conformation for suppressor mutations

Since there are multiple copies of the genome in each *Synechocystis* cell (Williams, 1988), revertant colonies are serially streaked at least four times on selective medium in order to achieve genetic homogeneity. The presence of the primary mutations was checked using a rapid genetic screening technique developed based on polymerase chain reaction (PCR). Target fragments were directly amplified from cyanobacterial cells using a pair of specific primers (see Materials and Methods for details), then used for complementation tests, restriction analysis, and direct sequencing. Although true reversions have been found in C14S revertants (codon TCT for serine was reverted to TGT for cysteine), most of the revertants of PsaC mutants contained the primary mutations, and no second-site mutations were found elsewhere in psaC. These results suggest that suppressor mutations in other genes may be responsible for growth under the selective conditions. However, the metabolism of cyanobacteria is very flexible. For example, flavodoxin can substitute for ferredoxin under conditions of iron-limitation (Ho and Krogmann, 1982). It is important therefore to demonstrate that the revertants have

come from genetic mutations rather than from physiological acclimation. DNA applied directly to the surface of a lawn of *Synechocystis* 6803 embedded in agar can result in the transformation of these cells (Dzelzkalns and Bogorad, 1988). This observation provides a simple procedure named "dot transformation" for the rapid assay of large numbers of DNA samples that may functionally complement a primary mutation. Dot transformation was used in characterization of revertants in this study. Total DNA was isolated from revertant colonies and was used to transform the primary PSI mutants. An example of such transformation assay is shown in figure 5.2. All the isolates tested so far demonstrated specific DNA modifications.

Suppressor mutations can be localized to other proteins

Mutations in PsaC such as C51D result in unstable assembly of the complex and lower electron transfer efficiency in assembled complexes. Conceivably the defects could be complemented by suppressor mutations in PsaA/PsaB dimer which may restore complex stability and/or electron transfer efficiency. Dot transformation was used to locate suppressor mutations to a particular DNA fragment by functionally complementing primary mutant cells using specific fragments amplified from the revertants. Suppressor mutations in ten pseudorevertant isolates from C51D have been localized to PsaA/PsaB in this way. These pseudorevertants show consistently different growth rates, indicating that the mutant phenotype that results from C51D can be suppressed by several different mutations on PsaA/PsaB. In contrast, no suppressor mutation for C14S has been localized to any tested genes for PSI subunits (psaA-psaB, psaC, psaD, and psaE).

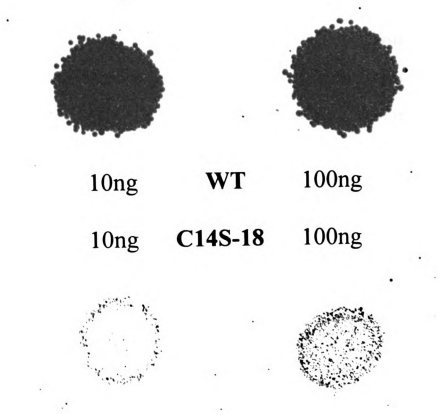

Figure 5.2 *In situ* "dot transformation" demonstrates suppressor mutation. Log phase culture 0.1 ml (OD_{730} 0.3) of a primary PSI mutant C14S was added to 3 ml melted 0.7% Bacto-agar at 50°C, then the mixture was poured onto a 90cm petri dish containing 50 ml BG-11 solid medium supplemented with gentamycin. Total DNA (10 ng and 100 ng) isolated from wild-type and a pseudorevertant C14S-18 was dropped in 5 µl on the lawn at marked areas. The plates were placed under 10 µmol m^{-2} s^{-1} white light for four days before transfer to 22 µmol m^{-2} s^{-1} white light. The plate was photographed 40 days after transformation. In a control experiment total DNA isolated from C14S was dropped on a lawn of C14S cells, and no cluster of colonies appeared at the marked areas in 40 days. Note that some colonies appeared spontaneously outside of transformed areas. The protocol was modified from Dzelzkalns et al. (1988).

Implication for position and function of F_A and F_B

The path of electrons through F_A and F_B is an unresolved area in the electron transfer pathway in PSI (Jung *et al.*, 1995). The electrons may travel in a series: F_X to F_B to F_A to Fd, or F_X to F_A to F_B to Fd . Alternatively, the electrons from F_X may be transferred to F_A or F_B and then one or both of these reduced clusters can donate electrons to Fd. The proposed locations of these redox centers in the x-ray crystallographic structure are at different distances from F_X, thus implying a serial flow of electrons between F_B and F_A (Krauss *et al.*, 1993). As shown in figure 5.3, the most striking feature revealed by the PSI crystal structure is the arrangement of the three Fe-S clusters in the form of an irregular triangle, with one cluster 15.4 Å and the other, 22.2 Å from F_X (Schubert *et al.*, 1995). The crystal structure gives no hint as to which cluster represents F_A and F_B. Selective, specific inactivation of F_B with mercurials such as $HgCl_2$ indicates that photoreduction of F_A is independent of F_B (Jung *et al.*, 1995). In contrast, Fd-mediated electron transfer from PSI requires functional F_B (Jung *et al.*, 1995). Our results with pseudorevertants show that only a mutation at F_A site can be suppressed by mutations in PsaA/PsaB. The results imply that the F_A site has extensive interaction with PsaA/PsaB, while the F_B site is exposed on the stroma side. The combined data are not conclusive but argue that F_A is the proximal cluster to F_X and F_B is the distal cluster, and that electrons travel serially from F_X to F_A to F_B.

Secondary mutation can be at the same site as the primary mutation

The primary photochemical reactions catalyzed by the PSI reaction center occur on a core heterodimer composed of the subunits PsaA and PsaB, and a small subunit

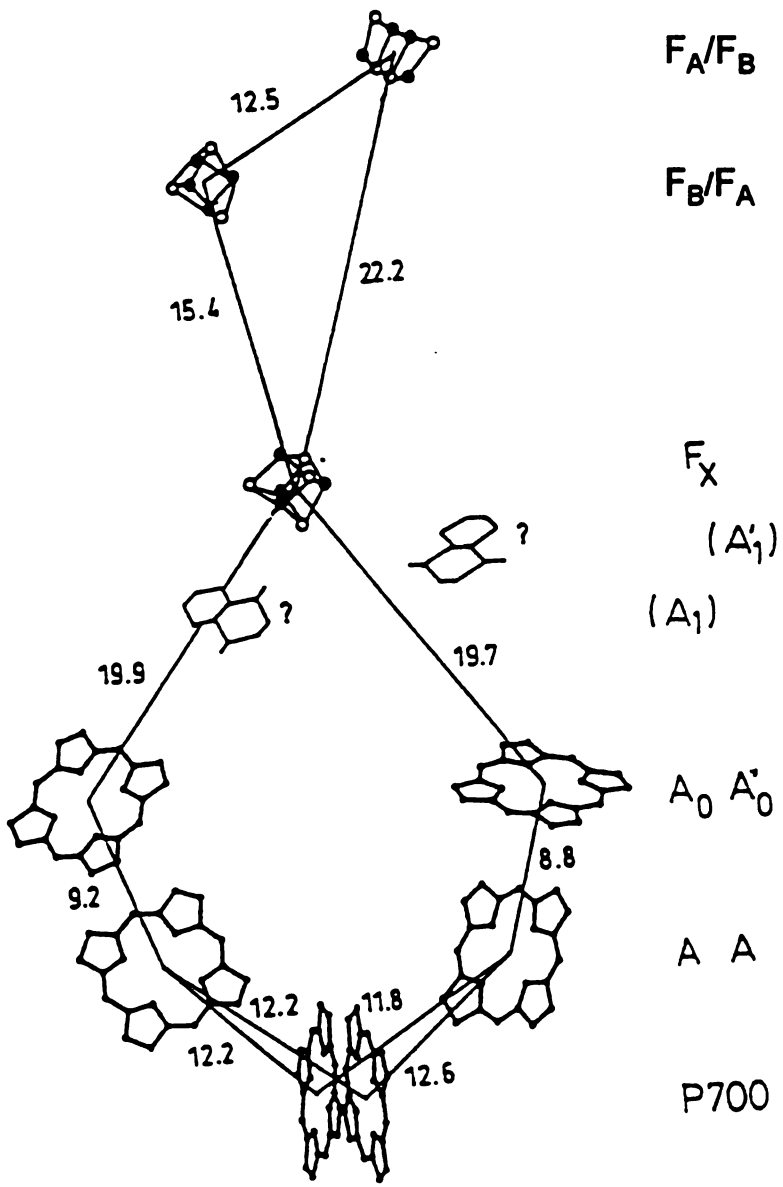

Figure 5.3. Arrangement of the geometrical centers of PSI electron carriers. Distances are in Å. A/B, PsaA/PsaB dimer. C, PsaC. Modified from Schubert *et al.* (1995).

PsaC. The interaction between the PsaC subunit and the core heterodimer has been studied by molecular modeling and it was proposed that the two conserved regions between the cysteine ligands of the F_X cluster on PsaA and PsaB (CDGPRGGTC) are two flexible loops that form a surface-exposed cavity to accommodate the PsaC subunit (Rodday *et al.*, 1993). To test the proposal an arginine residue $R561_{PsaB}$, which may interact with a negatively charged residue on the PsaC subunit in *Synechocystis* 6803, was changed to glutamate by site-directed mutagenesis. The mutant R561E can not grow photoautotrophically due to reduced level of PSI (Schulz *et al.*, 1995). To further understand the role of $R561_{PsaB}$ in assembly/stability of PSI complex, spontaneous revertants have been isolated from R561E at a rate of 4×10^{-7} under photoautotrophic growth conditions. The spontaneous mutations have been localized to the psaA-psaB operon in many revertants by functional complementation. Sequencing of PCR fragments amplified from one of the revertants revealed a secondary mutation at 561_{PsaB} which converts codon GAA for glutamate to AAA for lysine. The reversion restores photoautotrophic growth to a rate comparable to wild type cells. This result strongly suggests a role for a positively charged residue at this site in stable assembly of the PSI complex.

Genetic transformation in *Synechocystis* 6803

Some characteristics of genetic transformation in *Synechocystis* 6803 have been studied previously (Williams, 1988). When dot transformation is used in characterization of pseudorevertants, some colonies grow under selective conditions as a result of transformation, and other colonies appear on the plates spontaneously (see figure 5.2 for

an example). Therefore the success is dependent on a higher transformation frequency over the proportion of cells containing spontaneous mutations. Spontaneous mutations have been found to accumulate in cultures of the primary mutants, making aged cultures unusable for suppression test. To avoid such a problem, a fresh liquid culture should be used for suppression tests. In order to achieve a high transformation frequency, several parameters have been studied: growth conditions of the primary mutants, methods for preparation of transforming DNA, competency of primary PSI mutants, and transformation techniques.

Comparison of growth conditions for primary PSI mutants

Isolation of *Synechocystis* 6803 mutants deficient in PSI function was initially made possible by growing cells under light-activated-heterotrophic-growth (LAHG) conditions (Anderson *et al.*, 1991). The PsaC mutants, including C51D, can grow under LAHG or mixotrophic conditions with dim light (5 μmol m^{-2} s^{-1}; Chapter 3). The frequencies of transformation of C51D cells grown under these conditions was tested using plasmid pCG which contains a 3.5kb insert including a wild-type *psaC* gene (Chapter 3). As shown in table 5.1, mixotrophically grown cells were transformed with frequencies about three times that of LAHG cells. Although the reason for this differential is not known, the LAHG grown cells may have to go through an additional physiological acclimation to continuous light. It should be noted that the transformation frequency for both LAHG and mixotrophically grown PSI mutant cells varies considerably with different transforming DNA molecules, in agreement with a previous report with autotrophically grown wild-type cells (Williams, 1988).

Table 5.1. Comparison of transformation frequencies for LAHG and mixotrophically grown C51D cells.

Growth conditions	pCG amount (ng)	Transformation frequency (10^{-5} cell)
LAHG	2	6
Mixotrophic	2	20
LAHG	20	15
Mixotrophic	20	40

C51D cells (10^7) from LAHG culture (OD_{730} 0.33) and mixotrophic culture (OD_{730} 0.50) were harvested (OD_{730} = 0.25 corresponds to 1 x 10^8 cells ml^{-1}) by centrifugation at 4500 g for 6 min at room temperature. The cell pellet was suspended in 20 µl BG-11 medium with 22 ng or 200 ng of plasmid pCG. The mixture of cells and DNA was incubated for 2 hr in a sterile test tube under 30°C, 12 µmol m^{-2} s^{-1}. Fresh medium was added to final volume of 500 µl then 50 µl diluted mixture (containing 10^6 cells, 2 ng or 20 ng pCG) was spread onto BG-11 agar plates supplemented with 1 µg ml^{-1} gentamycin. The plates were placed under 30°C, 12 µmol m^{-2} s^{-1} for 3 days before transferred to 22 µmol m^{-2} s^{-1} . Colonies were counted 10 days after transformation. No colonies appeared in 10 days in a control experiment from which pCG DNA was omitted.

Comparison of methods for preparation of transforming DNA

To study whether transformation is sensitive to impurities in transforming DNA, wild-type cells were transformed to kanamycin resistance using plasmid pKW1194 (Williams, 1988) prepared in four different ways: (1) direct use of a crude preparation made by ethanol precipitation of *E. coli* cell lysate (Wizard midiprep system, Promega); or further treatment of the crude preparation by the following means: (2) purification using Wizard miniprep system (Promega); (3) purification using QiaExII system (Qiagen); (4) purification by phenol-chloroform extraction. WT-Gm^R is a strain carrying a Gm resistance gene downstream of the *psaC2* but otherwise wild-type (Chapter 3). Cells (3 ml) of this strain grown in BG-11 liquid medium supplemented with 1 μg ml^{-1} gentamycin were pelleted when OD_{730} was 0.41. The cells were resuspended in 3 ml of fresh BG-11. A 300 μl portion was transferred to a 15-ml Corning tube, and was mixed with 30 or 300 ng of plasmid. The mixture was then incubated for 20 hr at 30°C under 22 μmol m^{-2} s^{-1} white light, and was agitated several times to keep the cells suspended. This mixture (100 μl/plate) was then spread onto 9-cm BG-11 plates supplemented with 5 μg ml^{-1} kanamycin and was incubated as before. Colonies were counted nine days after transformation. Transformation frequencies between 3×10^{-3} to 5×10^{-3} were observed for all four DNA preparations when 10 ng plasmid was mixed with 10^6 cells, and transformation frequencies between 5×10^{-3} to 1×10^{-2} was observed for all four DNA preparations when 100 ng plasmid was mixed with 10^6 cells. No colonies appeared in a control experiment from which the plasmid was omitted.

Competency of the PSI mutant cultures at various stages of log phase

Mixotrophically grown C51D cells in early log phase (OD_{730} 0.15), mid log phase (OD_{730} 0.30), and late log phase (OD_{730} 0.65) were plated onto BG11 medium. Total DNA (10 ng in 5 µl) isolated from the wild-type strain was dropped on cell lawns at marked areas, and the plates were put under 5 µmol m^{-2} s^{-1} light for four days before transfer to 22 µmol m^{-2} s^{-1} white light. Some clusters of colonies were observed at the areas on all the plates ten days following transformation. This shows that the PSI mutant cells were competent throughout the log phase. In addition, total DNA (10 ng in 5 µl) isolated from the wild-type strain was dropped on plates containing the mid-log phase cells two days and five hours, respectively, before the plates were transferred to 22 µmol m^{-2} s^{-1} white light. Transformation was observed in ten days, showing the PSI mutant cells stayed competent for at least four days under dim light on plates.

Materials and Methods

Strains and Growth Conditions

Experiments were performed using a glucose-tolerant strain of *Synechocystis* sp. PCC 6803, which was acclimated for growth on solid medium in the dark. PSI mutants were maintained under LAHG conditions (Anderson, 1991). Cultures were grown in BG-11 medium prepared according to Williams (1988) except lab-purified Bacto-agar was used for LAHG (Anderson, 1991) Antibiotics were added in the following concentrations: kanamycin (Km), 5 mg/liter; gentamicin (Gm), 1 mg/liter. Photoautotrophic and mixotrophic growth were on solid media with or without supplemental glucose in a chamber providing continuous light. Cool white fluorescent

bulbs made by General Electric were used. The light intensity was varied by covering plates with layers of cheese cloth and was monitored using a L1-185A photometer (LICOR, Lincoln, NE). Fully grown plates may be wrapped with parafilm and stored in the dark at 4°C for up to six months.

DNA Manipulations

Polymerase Chain Reaction (PCR) was performed using a PTC 200 thermal cycler (MJ research Inc., Watertown, MA) and Taq polymerase (Boehringer Mannheim, Indianapolis, IN). Cells picked from a medium size colony or an equivalent amount of cells collected from liquid culture were washed once with water and used as template. For amplification of long fragments (≥ 3 Kb), total DNA was used as template, and Pwo polymerase (Boehringer Mannheim) was used at 1/5 total polymerase activity in addition to Taq polymerase. Amplification products were checked in agarose gel and may be directly used for dot-transformation. For restriction analysis or sequencing, PCR products were purified using Wizard PCR purification kit (Promega Corporation, Madison, WI) or Ultrafree-MC 30,000 NMWL filter unit (Millipore Corporation, Bedford, MA) which is recommended for long fragments. DNA sequencing was performed using dye-terminator chemistry for fluorescence sequencing at the Plant Biochemistry Facility, Michigan State University. The procedure for preparation of cyanobacterial DNA was adapted from (Ohad, 1992), with two "loopfuls" of cells scraped from plates or cells from 10 ml liquid culture being used to extract DNA. RNA was removed from the preparation by incubation with RNase A, and DNA was recovered by ethanol precipitation.

Acknowledgment

I thank Yong Wang for her contribution in characterization of R561E-derived revertants.

References

Anderson SL, McIntosh L: Light-activated heterotrophic growth of the cyanobacterium *Synechocystis* sp. strain PCC 6803: a blue-light-requiring process. *J Bacteriol* **173**: 2761-2767 (1991).

Boekema EJ, Boonstra AF, Dekker JP, and Rogner M (1994) Electron microscopic structural analysis of photosystem I, photosystem II, and the cytochrome *b6/f* complex from green plants and cyanobacteria. *J Bioenerg Biomembr* **26**: 17-29

Chitnis PR, Xu Q, Chitnis VP, and Nechushtai R (1995) Function and organization of photosystem I polypeptides. *Photosynth Res* **44**: 23-40

Chitnis PR (1996) Photosystem I. *Plant Physiology* **111**: 661-669

Dzelzkalns VA, and Bogorad L (1988) Molecular analysis of a mutant defective in photosynthetic oxygen evolution and isolation of a complementing clone by a novel screening procedure. *EMBO J* 7: 333-338

Fromme P, Witt HT, Schubert W-D, Klukas O, Saenger W, and Krauß N (1996) Structure of photosystem I at 4.5 Å resolution : a short review including evolutionary aspects. *Biochim Biophys Acta* **1275**: 76-83

Ho KK and Krogmann DW (1982) Photosynthesis. In The Biology of Cyanobacteria, Carr NG and Whitton BA, eds. Los Angeles: University of California Press, pp.191-214

Jung Y-S, Yu L, Golbeck JH (1995) Reconstitution of iron-sulfur center F_B results in complete restoration of $NADP^+$ photoreduction in Hg-treated photosystem I complexes from *Synechococcus* sp. PCC 6301. *Photosynth Res* **46**: 249-255

Kaneko T, Sato S, Kotani H, Tanaka A, Asamizu E, Nakamura Y, Miyajima N, Hirosawa M, Sugiura M, Sasamoto S, Kimura T, Hosouch T, Matsuno A, Muraki A, Nakazaki N, Naruo K, Okumura S, Shimpo S, Takeuchi C, Wada T, Watanabe A, Yamada M, Tasuda M, and Tabata S (1996) Sequence analysis of the genome of the unicellular cyanobacterium *Synechocystis* sp. Strain PCC 6803. II. Sequence determination of the entire genome and assignment of potential protein-coding regions. *DNA research* **3**: 109-136

Kless H, Vermaas WFJ, and Edelman M (1992) Photosystem II function and integrity in spite of drastic protein changes in a conserved region of the D2 protein. *Biochemistry* **31**: 11065-11071

Krauß N, Hinrichs W, Witt I, Fromme P, Pritzkow W, Dauter Z, Betzel C, Wilson KS, Witt HT, and Saenger W (1993) Three-dimensional structure of system I of photosynthesis at 6 Å resolution. *Nature* **361**: 326-331

Ohad N, and Hirschberg J (1992) Mutations in the D1 subunit of photosystem II distinguish between quinone and herbicide binding sites. *Plant Cell* **4**: 272-283

Rodday SM, Jun S-S, and Biggins J (1993) Interaction of the F_A-F_B binding subunit with the photosystem I core heterodimer. *Photosynth Res* **36**: 1-9

Schubert WD, Klukas O, Krauss N, Saenger W, Fromme P, Witt HT (1995) Present state of the crystal structure analysis of photosystem I at 4.5 Å resolution. In Mathis P, ed, Photosynthesis: From Light to Biosphere, Vol II. Kluwer Academic, Dordrecht, The Netherlands, pp 3-10

Schulz R, Smart LB, Yu J, and McIntosh L (1995) A new set of site-directed mutations in photosystem I core reaction center from *Synechocystis* sp. PCC 6803. In Mathis P, ed, Photosynthesis: from light to biosphere, vol II. pp. 119-122

Smart LB, Anderson SL, and McIntosh L (1991) Targeted genetic inactivation of the photosystem I reaction center in the cyanobacterium *Synechocystis* sp PCC 6803. *EMBO J* **10**:3289-3296

Smart LB, Warren PV, Golbeck JH, and McIntosh L (1993) Mutational analysis of the structure and biogenesis of the photosystem I reaction center in the cyanobacterium *Synechocystis* sp PCC 6803. *Proc Natl Acad Sci USA* **90**: 1132-1136

Williams JGK (1988) Construction of specific mutations in photosystem II photosynthetic reaction center by genetic engineering methods in *Synechocystis* 6803. *Meth Enzymol* **167**: 766-778

Zhao J, Li N, Warren PV, Golbeck JH, and Bryant DA (1992) Site-directed conversion of a cysteine to aspartate leads to the assembly of a [3Fe-4S] cluster in PsaC of photosystem I. The photoreduction of F_A is independent of F_B. *Biochemistry* **31**:5093-5099

Chapter 6

DISCUSSION AND POTENTIAL FUTURE EXPERIMENTS

My thesis research has accomplished many of the goals established at its inception: identification of the gene for the PsaC subunit in PSI by gene inactivation, elucidating the function of PsaC in PSI biogenesis, and the site-directed mutagenesis of PsaC to study structure-function relationships. An unexpected finding was the isolation of pseudorevertants from the primary PSI mutants. The development of genetic techniques for characterizing PSI pseudorevertants has begun to show potential as a new approach in the study of PSI. However, this new tool brings to the surface new questions that warrant future experimentation. The following is a summary on the study of PsaC mutants, and a brief discussion of some of the new questions and possible experimental approaches to address them.

Summary on the study of the PsaC mutants

Insertional inactivation of the *psaC* gene (Chapter 2) resulted in a photosynthesis-deficient strain. The mutant lacks the PsaC, PsaD and PsaE polypeptides in isolated thylakoid membranes, while the PsaA/PsaB and PsaF subunits were found. The EPR signals attributed to F_A and F_B were absent in the mutant strain, but a reversible F_X signal was present. Addition of PsaC and PsaD proteins to the thylakoids from the PsaC minus

strain gave rise to resonances resembling that of wild-type PSI complex. In room-temperature optical spectroscopic analysis, addition of PsaC and PsaD to the thylakoids also restored a 30-ms kinetic transient which is characteristic of the $P700^{+}[F_A/F_B]^{-}$ backreaction. These results demonstrate that the PsaC polypeptide is necessary for stable assembly of PsaD and PsaE into PSI complex, and that PsaC, PsaD and PsaE are not needed for assembly of the PsaA-PsaB dimer or for electron transport from P700 to F_X.

PsaC provides ligands for two [4Fe-4S] clusters, F_A and F_B, the terminal electron carriers in PS I. The cysteine ligands in positions 14 and 51 to F_B and F_A, respectively, were replaced with aspartate, serine, or alanine in order to probe the function of these two clusters in photosynthetic electron transport (Chapter 3). All mutant strains were unable to grow photoautotrophically and, compared to wild type, mixotrophic growth was inhibited under moderate light intensity. The mutant cell lines supported lower rates of whole-chain photosynthetic electron transport. Thylakoids isolated from the aspartate and serine mutants have lower levels of PsaC, PsaD, and PsaE and lower PS I capacity compared to the wild-type. The alanine and double aspartate mutants have no detectable levels of PsaC, PsaD, and PsaE. In addition, Asp and Ser substitutions decrease PSI quantum efficiency at the F_X -> F_A/F_B electron transfer step. The Ala and double Asp mutants failed to show any F_A/F_B activity. These results indicate that the various mutations of the cysteine 14 and 51 ligands to F_B and F_A affect biogenesis and electron transfer differently depending on the type of substitution, and that the effects of mutations on biogenesis and function can be biochemically separated and analyzed.

Further characterization (Chapter 4) of the mutant PSI complexes shows that a "mixed-ligand" (sulfur ligand and oxygen ligand) [4Fe-4S] cluster is present in the mutant

sites with Asp or Ser, and that it is capable of accepting electrons after F_X. The fourth ligand may be an oxygen from aspartate or serine residues, or alternatively, from water or OH^-. The PSI complexes from Ala mutants and the double Asp mutant show only the photoreduction of F_X, consistent with the absence of PsaC. These results show that only those PsaC proteins containing two [4Fe-4S] clusters are capable of assembling into PSI complexes. However, since neither F_A or F_B was specifically inactivated in the mutants, it could not be determined from these characterizations which of two clusters accepts electrons from F_X, or which one donates electrons to ferredoxin.

Genetic characterization of pseudorevertants has been applied to the study of PSI structure and function in *Synechocystis* 6803 (Chapter 5). Photoautotrophic and mixotrophic growth under moderate light intensity were used to isolate and characterize pseudorevertants from the site-directed PsaC mutants. Three classes of pseudorevertants were found: those capable of growth under: (1) photoautotrophic conditions, but not mixotrophic conditions; (2) mixotrophic conditions, but not photoautotrophic conditions; (3) both conditions. Suppressor mutations in some pseudorevertants have been localized to the PsaA-PsaB dimer by functional complementation. In combination with a previous study on chemical inactivation of F_B (Jung *et al.*, 1995), the current data indicate that F_A is the "proximal" cluster in the X-ray PSI crystal structural model, and that electron transfer proceeds serially from F_X to F_A to F_B.

The mechanisms of suppressor mutations restoring PSI activity

Since the primary PsaC mutations affected both complex assembly and quantum efficiency, suppressor mutations may be expected to restore either one or both, resulting

in partial or complete PSI activity. If a suppressor mutation stabilizes PSI assembly, its effects may be shown by PSI activity measurements and/or western blot analysis of thylakoid membranes isolated from the primary mutant and the pseudorevertant. It is expected that the levels of PsaC, PsaD, and PsaE subunits, and/or the PSI capacity in the pseudorevertant would be higher than that in the primary mutant. If a suppressor mutation restores quantum efficiency, its effects may be shown by kinetic studies using optical spectroscopy. If properties of the Fe-S clusters are changed by a suppressor mutation, the effects may be found by EPR spectroscopy and redox titration. Integration of the findings from physiological, biochemical and biophysical characterizations should help build a better structural model for PSI and further our understanding of its assembly and function.

Light inhibition of PSI mutants

Mutants of *Synechocystis* 6803 that lack PSI are sensitive to continuous white light greater than 3 μmol m^{-2} s^{-1} (Smart *et al.*, 1993). The PsaC mutants with reduced PSI activity are less sensitive yet still cannot grow under white light greater than 22 μmol m^{-2} s^{-1}. Clearly, PSI allows cells to grow mixotrophically under moderate light. How is this accomplished? A possible mechanism for the light inhibition is shown in figure 6.1. In cyanobacteria, part of the respiratory electron transport chain is shared with the photosynthetic electron transport chain (Kallas, 1994). Cytochrome oxidase has been shown to be the rate-limiting step in cyanobacterial respiratory electron transfer chain (Schmetterer, 1994). In PSI mutants, respiratory reactions may be feedback inhibited when the shared components are highly reduced by PSII activity under moderate light.

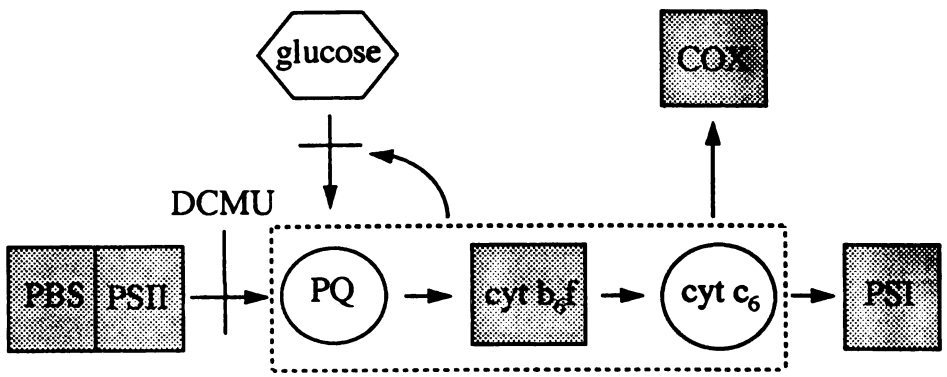

Figure 6.1. Over-reduction of the shared components inhibits growth. In cyanobacteria, part of the respiratory electron transport chain is shared with the photosynthetic electron transport chain. The shared components are shown in the dashed box. In PSI mutants, respiratory electron transfer may be inhibited when the shared components are highly reduced by PSII under white light. PBS, phycobilisome; COX, cytochrome oxidase.

The hypothesis that over-reduction of the electron transfer chain between PSII and PSI inhibits growth is supported by the following observations (Chapter 3): (1) C51D and C14S were found to grow photoheterotrophically under 22 μmol m^{-2} s^{-1} white light in the presence of 5 μmol m^{-2} s^{-1} DCMU, a PS II inhibitor; (2) C51D and C14S were found to grow mixotrophically when 22 or 60 μmol m^{-2} s^{-1} of white light was filtered by a red plastic sheet; and (3) C51D grows photoautotrophically when 60 μmol m^{-2} s^{-1} of white light was filtered by a red plastic sheet. Red light is primarily absorbed by PSI over PSII (Fujita *et al.*, 1994), therefore it does not cause over-reduction of the shared components. In a study with isolated thylakoid membranes from spinach, it was found that DCMU could stimulate cyclic photophosphorylation as measured by ferredoxin-mediated O_2 reduction, and the stimulation was eliminated by the addition of $NADP^+$ (Hosler and Yocum, 1987). Since $NADP^+$ should be present in the PsaC mutants, the presence of DCMU is not likely to affect cyclic phosphorylation. It has also been reported that light inhibition in a PSI-minus mutant is relieved when the assembly of phycobilisomes, which serve preferentially as antennae for PSII, is genetically inactivated (Shen, 1993). The available data indicate that PSI allows mixotrophic growth under moderate light by lowering redox poise of the shared components, thereby allowing respiratory reactions which are essential for growth. The available data also indicate that some suppressor mutations may reduce the activity of PSII, thereby restoring the balance between activities of PSI and PSII at a lower level, or they may alter the properties of certain key enzymes in respiration to relieve feedback inhibition. Identification of such suppressor mutations should broaden our knowledge of metabolism in this cyanobacterium.

Identification of suppressor mutations in the genome of *Synechocystis* 6803

Suppressor mutations have been localized to PSI subunits by genetic complementation using PCR fragments containing genes for these subunits (chapter 5). However, as discussed above, suppressor mutations could also occur outside of PSI. This notion is supported by preliminary results from some of the pseudorevertants. For example, despite demonstration of the presence of a suppressor mutation in C14S-18 (Fig 5.2), the mutation that restored photoautotrophy is not present in *psaA*, *psaB*, or *psaC*, as determined by DNA sequencing. Furthermore, transformation with total DNA and PCR fragments (containing genes for PsaA, PsaB, PsaC, PsaD, PsaE, and *petF* for ferredoxin) from other C14S-derived pseudorevertants also imply there are suppressor mutations on other sites of the genome that eliminate light inhibition. Shotgun cloning strategies, such as the one shown in figure 6.2, will be developed to identify those mutations. An integration vector pJY4 (figure 6.2) has been constructed in which a 3.3-Kb *Synechocystis* 6803 sequence cloned in pUC119 was interrupted by a Km^R cassette. The plasmid transforms wild-type *Synechocystis* cells to kanamycin resistance at frequencies up to 10^{-2} (Yu and McIntosh, unpublished). To clone a DNA fragment containing a suppressor mutation using this vector, total DNA from the pseudorevertant will be partially digested with *Sau*3A and ligated to pJY4 at the unique *Bam*H1 site. Ligation products of appropriate sizes (9-15 Kb) will be purified from an agarose gel and directly used to transform primary mutant cells (cloning in *E. coli* is omitted to avoid potential problem in cloning genes for hydrophobic proteins). The mixture of DNA and cells will be spread onto plates containing Km, in the presence (for mixotrophic growth under moderate light) or absence (for photoautotrophic growth) of glucose. Colonies growing under the

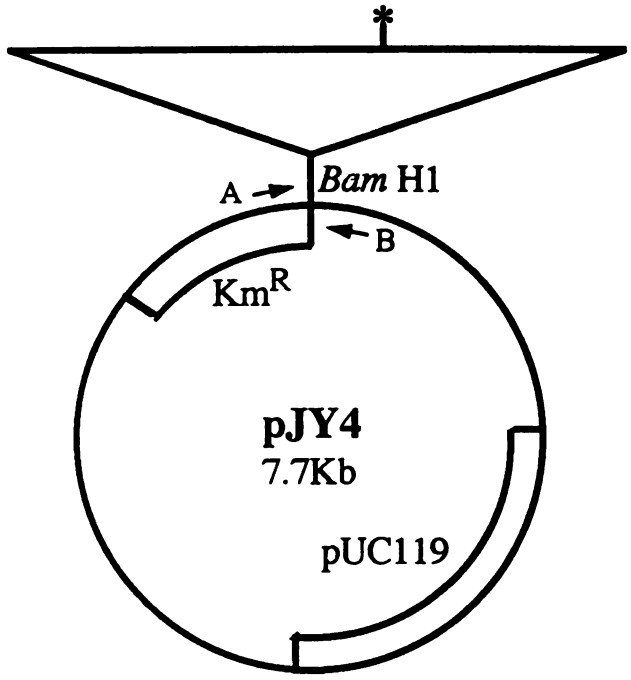

Figure 6.2. A shotgun cloning vector, pJY4. An integration vector pJY4 is shown in which a 3.3-Kb *Synechocystis* 6803 sequence cloned on pUC119 was interrupted by a Km^R cassette. See text for the detailed cloning strategy. Total DNA from a pseudorevertant will be partially digested with *Sau*3A and ligated to pJY4 at the unique *Bam*H1 site. Ligation products will be used to transform the primary mutant cells. A and B, PCR primers near the *Bam*H1 site. The asterisk on the insert indicates a suppressor mutation.

selective conditions will serve as templates for PCR. The inserts ligated onto pJY4 will be amplified using primers near the *Bam*H1 site (Figure 6.2), and will be tested for ability to transform primary mutants using methods described in chapter 5. Other cloning strategies may also be considered. Finally, the recent availability of the complete genome sequence of *Synechocystis* 6803 will undoubtedly simplify genetic studies using this model organism. The development of an efficient complementation-based cloning vector will be critical for the full use of the sequence information.

Combinatorial mutagenesis: Determination of properties and function of Fe-S clusters by protein environment

A major question in protein biochemistry is how primary amino acid sequence leads to specific folding, assembly, stability and function. This question is particularly difficult to address with membrane proteins. For example, the three [4Fe-4S] clusters in PSI have different thermodynamic and electronic properties allowing vectorial electron transfer from F_X to F_A/F_B. Some of the ligands which bind these clusters have been identified by site-directed mutagenesis, and the regions surrounding these ligands are highly conserved. However, until recently (Jung *et al.*, in press), little was known concerning how these sequences determined the properties of the iron-sulfur clusters and facilitated efficient electron transfer. The functional requirements in a short region of a protein can be studied by means of directed molecular evolution, in which a desired or novel function is selected from a pool of randomly arranged sequences of nucleic acids or amino acids. This approach, termed combinatorial mutagenesis, has been used in study of PSII (Kless and Vermaas, 1995), and could be used to further determine functional

requirements for the three Fe-S clusters in PSI. For example, the sequences surrounding a F_A ligand C51 (G50, C51, K52, R53) are conserved in all known PsaC proteins. Using site-directed mutagenesis, C51 has been changed to Asp, Ser, or Ala, and all the mutants lost photoautotrophy. Combinatorial mutagenesis may be applied by two-step PCR (Kless and Vermaas, 1995) to randomize these four amino acids, followed by transformation into a primary PsaC mutant such as C51D. Following positive selection for photoautotrophy, the combinations at these four sites that can support PSI activity will be identified. The contribution of each residue will then be evaluated in relation to assembly of the complex, properties of F_A and efficiency of electron transfer. An appealing possibility for this approach is to generate a series of F_A mutants with a range of mid-point potentials, which would define the relationship between this parameter and electron transfer efficiency, and further our understanding of electron transfer between Fe-S clusters.

References

Fujita Y, Murakami A, Aizawa K, and Ohki K (1994) Short-term and long-term adaptation of the photosynthetic apparatus: homeostatic properties of thylakoids. In: The molecular biology of cyanobacteria. Bryant DA, ed. Kluwer Academic Publishers, pp.677-692

Hosler JP and Yocum CF (1987) Regulation of cyclic photophosphorylation during ferredoxin-mediated electron transport. Effect of DCMU and the NADPH/$NADP^+$ ratio. *Plant Physiol* **83**: 965-969

Jung Y-S, Yu L, and Golbeck JH (1995) Reconstitution of iron-sulfur center F_B results in complete restoration of $NADP^+$ photoreduction in Hg-treated photosystem I complexes from *Synechococcus* sp. PCC 6301. *Photosynth Res* **46**: 249-255

Kallas T (1994) The cytochrome b_6f complex. In: The molecular biology of cyanobacteria. Bryant DA, ed. Kluwer Academic Publishers, pp. 259-317

Kless H, and Vermaas WFJ (1995) Many combinations of amino acid sequences in a conserved region of the D1 protein satisfy photosystem II function. *J Mol Biol* **246**: 120-131

Schmetterer G (1994) Cyanobacterial respiration. In Bryant DA ed, The molecular biology of cyanobacteria. Kluwer Academic Publishers. pp. 409-435

Shen G, Boussiba S, and Vermaas WFJ (1993) *Synechocystis* sp PCC 6803 strains lacking photosystem I and phycobilisome function. *Plant Cell* **5**: 1853-1863.

Smart LB, Warren PV, Golbeck JH, and McIntosh L (1993) Mutational analysis of the structure and biogenesis of the photosystem I reaction center in the cyanobacterium *Synechocystis* sp PCC 6803. *Proc Natl Acad Sci USA* **90**: 1132-1136